Norwegian University
of Life Sciences

The presence of microplastics on the Norwegian Continental Shelf and in Rio Almendares, Havana

Øyvind Lilleeng

Master's in Environmental Science: Limnology and water resources

Submitted 15.05.2018 by:

Øyvind Lilleeng.

Faculty: IMV-MINA

Main Supervisor:
Research Prof. Dr Åsgeir R. Almås (NMBU)

Co-supervisor:
Research Prof. Dr. Hans Peter Arp (Norwegian Geotechnical Institute, NGI and NMBU)

Acknowledgment

Abstract

Microplastics are becoming more frequently detected in all natural environments worldwide as global demand for plastic production continues to rise and studies related to microplastic research are becoming more prevalent. Marine sediments are hypothesized by many researchers to be a major sink for microplastics as they will sink to the ocean floor over time due to size and density modifications in open waters. Microplastic research has become a stimulated topic receiving increasing attention globally. To this date, there is no standard analytical protocol for microplastic quantifications and identification, leading to dissimilarities in methods and less comparability between studies.

This thesis investigates two separate benthic sediments, one being deep-sea sediments from the Norwegian Continental Shelf and the other river sediment from Rio Almendares (Cuba). Sediment samples were investigated for microplastic using density separation, purification, and polymer identifications practicing both visual analysis and FTIR analysis.

Results offer evidence of low-density particles (PS, PE) being present in all analyzed samples; in shallow river sediments and down to ocean depths of 508 meters. Polyethylene (PE) was the most dominant polymer type, being present in 10 out of 11 samples.

On average, the Norwegian Continental Shelf is estimated to hold 64 ± 82 mg MP $_{max}$ per kg of dry sediment (corresponding to $36\ 650 \pm 49\ 980$ MP $_{max}$ items per m^2 sediment surface). The central North Sea had the highest concentration of MP$_{max}$ compared to the northern North Sea and the Barents Sea areas holding 88 ± 99, 32 ± 40 and 32 ± 16 mg MP$_{max}$ per kg dry sediment. Further, the samples with the top five highest concentrations were all found in the central North Sea, representing the shallowest sediments analyzed for microplastic in this study. Not all samples from the Norwegian Continental Shelf were analyzed by an FTIR for particle identified, as they were only visually analyzed. However, sediments from the three deepest and most remote sampling stations were confirmed by an FTIR to contain microplastic, suspecting an omnipresence of microplastic in the entire Norwegian Continental Shelf. A comprehensive FTIR analysis of the whole Norwegian Continental Shelf using the unidentified samples is suggested.

Sediment samples collected from the Rio Almendares contained (on average) 4429 ± 5327 mg MP $_{max}$ /kg dry sediment (corresponding to 8523 ± 13029 MP $_{max}$ items / kg dry sediment). The sediments collected upstream the river had the highest average concentration of microplastics regarding abundance (mg MP $_{max}$/kg dry sediment, MP $_{max}$ items/kg dry sediment and polymer distribution by percentage) compared to the river outlet sediments. However, there is no significant trend in the river system based on the calculations in this study due to too few observations. Additional sampling of river sediments from the Rio Almendares are suggested, especially representing the sediments upstream of the river.

The method precision was expressed as a relative standard deviation of 39 % for a set of replicates from Norwegian Continental Shelf, while a set triplicates from the Rio Almendares had a relative standard deviation of 26% by comparison.

Sammendrag

Mikroplast i naturen blir i økende grad påvist i stadig flere miljøtyper ettersom den globale etterspørselen etter plast fortsetter å stige, og studier relatert til mikroplastforskning blir stadig mer utbredte. Enkelte forskere mener at havbunnen utgjør et reservoar for akkumulert mikroplast. Gjennom biologiske-, kjemiske- og mekaniske prosesser i marine omgivelser vil plastpartikler gjennomgå størrelses- og tetthetsendringer, noe som igjen kan føre til at mikroplast sedimenterer til havbunnen. Forskning på mikroplast er for tiden et høyrelevant tema som i økende grad får oppmerksomhet på et globalt nivå. Per dags dato finnes det ingen standardisert analytisk protokoll for kvantifisering og identifisering av mikroplast i havsedimenter. Store metodiske forskjeller innad i forskningsmiljøene påvirker blant annet sammenlignbarheten av resultatene på tvers av studier, noe som gjør det vanskelig å påvise en signifikante forskjell.

Denne oppgaven undersøker to ulike typer sedimenter; et utvalg av dybhavsliggende sediment fra norsk kontinentalsokkel (NCS) og elvesedimenter fra Rio Almendares (Cuba). Sedimentprøvene ble undersøkt for mikroplast ved bruk av tetthetsseparasjon, kjemisk nedbrytning av organisk materiale og identifisering ved hjelp av både visuell analyse og FTIR-analyse.

Resultater bekrefter tilstedeværelsen av syntetiske polymerer, ofte med lav tetthet (PS, PE) i alle analyserte prøver; fra grunne elvesedimenter og helt ned til 508 meters dyp. Polyetylen (PE) var den mest dominerende typen mikroplast, og var til stede i 10 av 11 prøver.

Beregninger anslår at norsk kontinentalsokkel inneholder 64 ± 82 mg MP $_{maks}$ per kg tørr sediment (tilsvarende $36\,650 \pm 49\,980$ MP $_{maks}$ partikler per m^2 sedimentoverflate). De sentrale delene av Nordsjøen hadde den høyeste konsentrasjon av MP$_{maks}$ i forhold til de nordlige deler av Nordsjøen og Barentshavet (88 ± 99, 32 ± 40 og 32 ± 16 mg MP$_{maks}$ / kg tørr sediment). Fem av de totalt 35 prøvene med høyest innhold av mikroplast (uavhengig av enhet) ble funnet i de sentrale delene av Nordsjøen. Ikke alle prøvene fra den norske kontinentalsokkelen ble identifisert ved hjelp av en FTIR-analyse, men ble heller analysert visuelt ved bruk av optisk mikroskopi. Videre ble prøver fra de mest dypt- og fjerntliggende sedimentene ved hjelp av en FTIR-analyse for å bekrefte funn av mikroplast. Disse resultatene styrker mistanken om tilstedeværelse av mikroplast over hele den norske kontinentalsokkel. En omfattende FTIR-analyse av de gjenstående prøvene vil bekrefte denne mistanken samt utbedre de gjeldende estimatene.

Sedimentprøvene fra *Rio Almendares* inneholdt 4429 ± 5327 mg MP $_{maks}$ / kg tørr sediment (tilsvarende 8523 ± 13029 MP $_{maks}$ partikler / kg tørr sediment). Sedimentene som ble samlet oppstrøms i elven hadde de høyeste konsentrasjonene av mikroplast (mg MP $_{maks}$ / kg tørr sediment, MP $_{maks}$ gjenstander / kg tørr sediment og basert på fordeling av mikroplast) sammenlignet med sedimenter tatt i utløpet av elven. Det er primært på grunn av et fåtall observasjoner at datagrunnlaget i dette studiet ikke kan fastslå en signifikant trend innad i elvesystemet, med tanke på mikroplast. Ytterligere uttak av sedimentprøver oppstrøms i elven er foreslått.

Presisjonen i metoden ble uttrykt med et relativ standardavvik på 39% (basert på ét sett *replikater)* fra den norske kontinentalsokkel, hvorav (et sett med *triplikater)* fra Rio Almendares hadde et relativ standardavvik på 26% til sammenligning.

Table of Content

1. Introduction

1.1 - Background

The invention of synthetic polymers and plastics have undeniably had a massive impact on human lifestyle throughout the last century. Beneficial properties such as durability, lightweight, chemical stability, thermal insulation and low-cost have resulted in social, medical and technological advances. Today, plastic is anchored in every possible part of the society, either being the main component or partly present in all modern sectors, such as building & construction, electronics, agriculture, healthcare, energy, and transport. For instance, plastic packaging reduces food waste by increasing shelf life and lowers transport costs by bringing packaging weight down (Ellen MacArthur Foundation, 2016).

Throughout the last six decades, there has been close to an exponential growth in plastic production globally, resulting in an all-time-high production of 335 million tons plastic in 2017 (PlasticsEurope, 2017). Globally, more than one-third of all plastic production is intended for packaging purposes often designed for immediate disposal (PlasticsEurope, 2017). Since the early 1950s, it is estimated that a total of 8300 million metric tons of plastics have been produced worldwide. Despite an increasing plastic recycling rate of +79% the recent decade (PlasticsEurope, 2017), only 9% of all generated plastics in 2015 were recycled (Geyer et al., 2017). Best estimates suggest that in total over 150 million tons of plastic has found its way into the world's oceans (Ellen MacArthur Foundation, 2016). According to Jambeck et al. (2015), eight million metric tons of plastic waste entered the ocean in 2010 where it can grow to be a planetary problem through ocean current transport and accumulation in ocean gyres (Lebreton et al., 2012; Ryan et al., 2009).

The increasing amount of marine litter costs tax-payers millions of dollars in clean-up program, e.g., in Australia, where the tax-payers pays billions of dollars annually (Willis et al., 2017). In addition to being an aesthetic problem, the presence of plastics in marine environments are unconditionally destructive for all marine biota in the long term. Marine animals are subject to entanglement, ingestion, smothering, ghost fishing, fatal injuries, starvation and general exhaustion (Derraik, 2002; Gregory, 2009; Jambeck et al., 2015). Also, other studies have investigated the properties of smaller plastic particles acting as transporters of environmental contaminants due to their charge balance; finding up to 10^7 times the concentration of many POPs (*Persistent Organic Pollutants*) attached on plastic pellets compared to seawater (Holmes et al., 2012; Koelmans et al., 2016). Some experts conclude that plastic waste fulfills two of the three requirements for a pollution to pose as a planetary boundary threat (Jahnke et al., 2017; Villarrubia-Gómez et al., 2017). Others (Rochman et al., 2013) have suggested defining plastic as hazardous waste to reduce the ongoing accumulation of plastic in all natural environments.

The floating behavior and buoyancy of plastics have proven to be linked to the size, shape, and density of the plastic particles in the aquatic environment (Filella, 2015; MEPEX, 2014). The definition *microplastic* (MP) is a frequently used term to describe the smaller (micro) fractions of plastic particles, but the applied size range may differ somewhat among different researchers. An upper limit of 5 mm is generally agreed upon, but some researchers also use 0.5 or 1 mm to differentiate between the micro and the macro fractions (Andrady, 2011; Cole et al., 2011). An argument for using the upper limit of 5 mm is to include conventional virgin plastic pellets with 1 – 5 mm in diameter. There are two sources of microplastic; *primary* and *secondary sources*

(MEPEX, 2014). Primary sources of microplastics are plastics that are *directly* released into the environment as micro-sized particles. Examples are virgin pellets specifically designed for the cosmetic industry and raw granulates. Also, all sources deriving from land-based sources such as synthetic fabrics in domestic wastewater, paints, and car tire particles are generally considered to be of primary origin. *Secondary sources*, however, are plastic particles subject to *polymer degradation* in the marine environment (MEPEX, 2014).

1.2 - Introducing the problem

Rivers are an important pathway for plastic debris from the land to the sea and are estimated to transport between 1.15 - 12.7 million tons of plastic annually (Lebreton et al., 2017; Schmidt et al., 2017). Plastic wastes from land-based sources contribute to 80 % of all plastics in marine environments and are consequently correlated to population density and industrial activity (Jambeck et al., 2015; MEPEX, 2014). Today, traces of plastics are found in all aquatic environments including; lakes (Eriksen et al., 2013; Free et al., 2014), rivers (Lebreton et al., 2017; Siegfried et al., 2017), coastal regions (Browne et al., 2011; Fok & Cheung, 2015; Zhang, 2017) ocean surfaces (Eriksen et al., 2014; Goldstein et al., 2012; Law et al., 2010), throughout the water column (Cole et al., 2011; Lattin et al., 2004) and in sediments (Hurley et al., 2018). Microplastic has been identified in all investigated locations on earth (Baztan et al., 2017); even at ocean depths of 4844 meters (Van Cauwenberghe et al., 2013) and in arctic regions (Obbard et al., 2014; Peeken et al., 2018; Waller et al., 2017; Zarfl & Matthies, 2010).

Global estimates of plastic debris transported by rivers to the ocean are becoming increasingly documented (Lebreton et al., 2017; Schmidt et al., 2017; Siegfried et al., 2017), yet estimates suggest that expected amounts of plastic debris accumulated in surface water are tens of thousands of tons less than first predicted (Cózar et al., 2014). Also, historical time series of plastic concentrations in open waters do not seem to differ significantly over the three last decades at the California Currents nor the Eastern Tropical Pacific despite increasing plastic production globally (Gilfillan et al., 2009; Goldstein et al., 2012); opening the discussion of the *missing plastic* at sea. There are two lesser explored areas of the sea which potentially could contain large quantities of *the missing plastic*: sediment beds and suspended in the water column.

Whether plastic particles will sink to the seabed or stay afloat in open water being carried away far from their sources, depends entirely on the particle density, shape and size. Instead of going through complete mineralization macro plastic debris may break down into smaller pieces altering the chemical properties of the plastic particles, and thus also the fate in marine environments (Filella, 2015). The smallest microplastics, *the colloidal fraction* (< 1 µm but potentially larger) will by definition not sink, and particles larger than colloids will sink very slowly as they are sensitive to motion. In general, microplastics with a density higher than seawater (~1.03), such as polyethylene terephthalate (PET), polyvinyl chloride (PVC) and synthetic textiles (polyester resin) will be moving downwards in the water column. Lighter plastic products, e.g., polypropylene (PP) and polyethylene (PE) have a lower density, thus, floating in seawater (Scientific Polymer Inc, 2013; Statista, 2016). However, regardless of these buoyant attributes plastics may undergo attribute modifications by chemical-, biological- and physical weathering (Singh & Nisha Sharma, 2008).

The rate of fragmentation into smaller particles depends on the strength of the polymer material, but despite superior chemical stability polymer degradation is inevitable. Such physical alterations are led by an accelerating chain-reaction of thermal degradation, photo-oxidative degradation, ozone-induced degradation, mechanochemical degradation, catalytic degradation, and biodegradation. Abiotical hydrolysis, photo-oxidation, and physical fragmentation may

also promote further biodegradation, or *biocolonization* by marine microorganisms (Singh & Nisha Sharma, 2008).

Another process altering plastic attributes are *Biofouling,* which is known to be a *density-manipulative* process occurring when marine microbes form biofilm onto the surface of the plastic and facilitate sinking of plastic items (Andrady, 2011; Woodall et al., 2014; Ye & Andrady, 1991). During algal blooms in Spring/early Summer, microplastic can accumulate on the seafloor through various aggregating processes collectively known as *marine snow*. Smaller aggregates containing clay particles, detritus, and living organisms may form larger macroscopic aggregates which become accessible for large particle feeders or becoming captured in sediment. The formation of aggregates can be produced directly by living plants and animals or by physical aggregation of smaller particles *enhanced* by marine biology (Alldredge & Silver, 1988; Cole et al., 2016). All processes above are influencing the movement of plastic particles throughout the water column affecting the fate of plastics, primarily low-density plastic polymer. Given the immenseness of the ocean and the ubiquity of microplastics throughout the environment, the deep-sea sediment bed seems to give a fitting response to the question—what might be the ultimate sink for the missing plastic?

On the 23rd of April 2018, the keyword *microplastic* generated 326 search hits on sciencedirect.com (Figure 1), being a scientific topic increasingly reported all over the world. General growing concern regarding the possible ecological impact that marine debris might represent has recently stimulated microplastic research tremendously. However, studies concerning microplastic research are far from fully uncovering all mechanisms involved in the transport, behavior, and fate of microplastics. Like many other pollutants, microplastic distribution and occurrence are highly variable, being subject to temporal and spatial variations. Microplastic concentrations in sediments have been found to range from eleven particles per kg sediment in the Taihu Lake (Su et al., 2016) to up to 621.000 particles per kg sediment in beaches of the East Frisian islands (Liebezeit & Dubaish, 2012).

Maybe more importantly, to this date much needed standardized operation protocols in the scientific communities are still missing; meaning that there is no approved method for sampling, microplastic-sediment separation, purification, identification nor quality control for microplastic analysis.

Figure 1: The number of search results containing the keyword "microplastic" from 2010 to 2018 (data retrieved from www.sciencedirect.com, 23.04.2018).

Minor differences in methods or the absence of sufficient validity of the analysis result in microplastic studies often being incomparable or at worst unreliable. Even a standard *particles size range* is so far not yet recognized by microplastic researchers (Vollertsen, n.d.). Having a standardized protocol for microplastic quantifications and identifications in sediments could be highly beneficial for mapping exact microplastic hotspots, but also for variations among diverse types of aquatic sediments, such as freshwater, estuarine and marine systems.
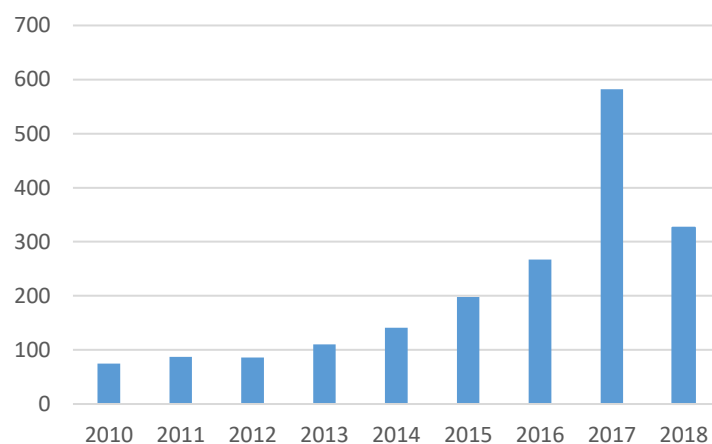
1.3 - Introducing the areas of interest

This thesis uses findings from two areas of the world separated by distance, yet mutually connected by *the Gulf Stream*. The *first part* of the thesis focuses on deep-sea sediments (66 - 508 m) collected at the Norwegian Continental Shelf, while the *second part* is devoted to urban river sediments (< 15 m) from Rio Almendares in Havana, Cuba. River sediments form Rio Almendares, and surrounding coastal sediments are considered a hotspot for microplastics and are for the first time investigated in these waters. This study hopes to give a deeper understanding of the microplastic pathway and sedimentation process along a river network before inevitably entering the ocean. Also, until now, only a few microplastic studies have been conducted in in deep-sea sediments, especially the Norwegian Continental Shelf. Density modification of macroplastic and microplastic particles are believed to be a significant mechanism to cause plastic accumulation in all aquatic sediments, even low-density plastic polymers. Standardized knowledge addressing the fate of microplastics may also be of good use in the ongoing debate about the ocean being the ultimate sink for the missing plastics.

Ever since the *Norwegian oil age* started in 1971 on the Ekofisk oil field, a total of 107 fields have been developed on the *Norwegian Continental Shelf*. The Norwegian petroleum industry has played an essential role for the Norwegian economy and welfare (Ryggvik & Smith-Solbakken, 2018; The Norwegian Petroleum Directorate, 2018b). The Norwegian Continental Shelf covers 2 039 951 km^2 of the sea, being 6.5 times larger than the Mainland Norway, Svalbard and Jan Mayen (The Norwegian Petroleum Directorate, 2018a). Every specific group of oil fields is obliged to have reference stations (here defined as regional stations) located outside the area of influence. The purpose of these stations is to annually monitor chemical parameters to document the physical, chemical and biological responses of the nearby oil activities (Department of Climate and Industry, 2011). To date, there are no ongoing monitoring programs specifically purposed to map microplastic concentrations in these regions. An existing regional offshore sediment monitoring program provided *DNV-GL* (Norwegian: *Det Norske Veritas* and *Germanischer Lloyd*) with additional sediment samples for microplastic analysis on request by the Norwegian Environment Agency.

The *Rio Almendares* is a 47 km long river network which runs through the most populated city in the Caribbean, Havana (World Population Review, 2018). Rio Almendares empties into the Straits of Florida, and the Almendares River watershed is one of the most important in Cuba with a total area of 40.2 km^2. As much as 47% of the city's drinking water is derived from groundwater underneath this basin, providing over 500.000 inhabitants with freshwater daily (Olivares-Rieumont et al., 2005). Consequences of overpopulation, soil erosion, and unsustainable water management and deforestation are currently affecting the water quality in the river system, impacting economic, social and recreational interests. Also, ungoverned contaminants and pollutants from industry and urban areas are polluting the river at increasing rates, with more than 70 identified point source pollutants (Olivares-Rieumont et al., 2005). Additionally, growing interest for tourism and improved social standards generate tremendous amounts of waste, somewhere between 1200 and 1500 tons of solid waste daily. (Colantonio & B. Potter, 2006; Gorry, 2017). Due to lack of general environmental concerns among the Cuban population and improper governmental garbage management, wastes accumulate in either open-cast landfills or on the streets, eventually entering the ocean during periodic floods.

1.4 - Aim and objectives

The aim of this study is to investigate all benthic sediment samples collected on the Norwegian Continental Shelf and along, and at the outlet of the River Almendares, Cuba. Microplastic quantification and identifications are performed by using a well-documented approach for separation, purification, quantification, and identification. The outcome of the analysis will be used to determine the presence and distribution of microplastic in the two different benthic sediments.

Three hypotheses are tested in this study:

i.   Microplastics are present in all investigated locations; at the Norwegian Continental Shelf and in Cuba (Rio Almendares).

ii.   Microplastic concentrations found at the Norwegian Continental Shelf are higher in the shallower parts of the oceans compared to greater depths.

iii.   Microplastic concentrations are higher at the outlet of the Rio Almendares compared to sampling sites upstream of the river due to river transport and sedimentation of microplastics in the outlet.

To validate the aim, two sets of objectives are followed in this study.

The <u>first set of objectives</u> are:

i.   To quantify microplastic concentrations (mg/kg) in 35 different deep-sea sediments on the Norwegian Coastal Shelf (NCS) using; density separation, chemical digestion, and visual analysis,
ii.   use these data to look for regional trends,
iii.   moreover, estimate the number of plastic particles per square meter seabed (items/m^2) for each of the three regions.

The <u>second set of objectives</u> are:

iv.   To quantify microplastic concentrations (mg/kg) at five locations along the *Rio Almendares* and one location near the cruise terminal using; density separation, chemical digestion, and FTIR analysis,
v.   use these data to interpret the distribution of microplastics along, and at the outlet the Rio Almendares compared to a seemingly polluted cruise terminal,
vi.   and use results from FTIR analysis to compare the distribution of low-density and high-density plastic particles in riverine sediments.

2. Methods and materials

2.1 - Sampling locations

2.1.1 - The Norwegian Continental Shelf (Norway)

In total, 35 sediment samples were sent to NGI (Norwegian Geotechnical Institute) for microplastic analysis (31.08.2017). The sediment samples originated from three regions on the Norwegian Continental Shelf (NCS), covering the central North Sea (CNS), the northern North Sea (NNS) and the Barents Sea (BS) (Figure 2). The top 0-1 cm of the surface sediment was collected using Van Veen Grab samplers. The surface areas of the Van Veen samplers were 0.15 m^2, but for one sample in the northern North Sea (Eko-14) the surface area of the sampler was 0.10 m^2. All sediment samples were stored in glass jars and conserved with 5% formaldehyde before they were sent to NGI, Oslo. Samples were kept in cold storage (2-4 ^{o}C) until analysis.
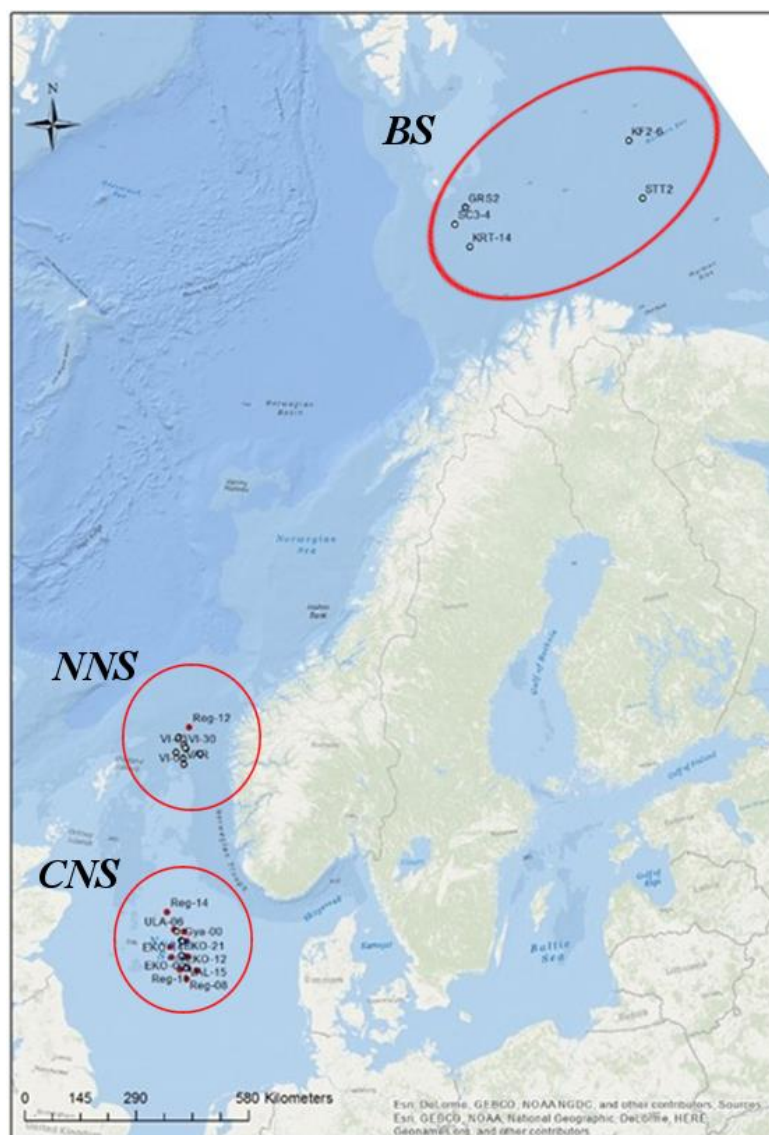
Figure 2: Overview of all sampling locations in the three regions, beginning with the southern region: the central North Sea (CNS), the northern North Sea (NNS) and the Barents Sea (BS). Illustration is borrowed from Møskeland et al. (2018) (Figure 5-1) and modified for explanatory purposes

20 sediment samples (Table 1) were collected between 56 and 57-degree longitude in the region defined as *the central North Sea*. The region is relatively shallow (66-80 meters depth), and the sediment is mainly composed of fine sand (0.125-0.25 millimeter). This region is subdivided into the northern (Table 3) and southern (Table 4) parts of the central North Sea (CNS). Ten sediment samples collected from the following oil fields: Ekofisk (EKO), Gyda (GYDA), Valhall (VAL) and Ula (ULA) field, whereas the samples defined as "*Reg*" were all *regional stations* (Table1).

Figure 3: Geographic illustration is presenting the sampling stations in of the southern part of the central North Sea (CNS). A total of seven samples were collected in this sub-region Illustration is borrowed from Møskeland et al. (2018) (Figure 5-3).

Figure 4: Geographic illustration is presenting the sampling stations in the northern part the central North Sea. A total of 13 samples were collected in this sub-region. Illustration is borrowed from Møskeland et al. (2018) (Figure 5-3).

Table 1: List of the different sampling station in the central North Sea with their respective oilfields, sediment characterization, and depths.

Sample name	Oilfield	Sediment characterization*	Depths* (m)
Reg-01	Regional	Fine Sand	73
Reg-02	Regional	Fine Sand	68
Reg-03	Regional	Fine Sand	68
Reg-04	Regional	Fine Sand	71
Reg-06	Regional	Fine Sand	72
Reg-07	Regional	Fine Sand	73
Reg-08	Regional	Fine Sand	70
Reg-09	Regional	Fine Sand	66
Reg-11	Regional	Fine Sand	71
Reg-14	Regional	Fine Sand	80
EKO-12	Ekofisk	No data	78
EKO-14	Ekofisk	Very fine sand	76
EKO-21	Ekofisk	No data	71
VAL-02	Valhall	Fine Sand	76
VAL-04	Valhall	No data	62
VAL-05	Valhall	No data	70
VAL-15	Valhall	Fine Sand	76
GYDA-18	Gyda	Silt and clay	67
GYDA-21	Gyda	No data	67
ULA-06	Ula	Fine Sand	71

*Measured depths and sediment characterization was done by DNV-GL and are retrieved from report: 2018-0050, Rev. 01., Miljødirektoratet (Møskeland et al., 2018) (Table 5-1).

The Northern North Sea

Ten sediment samples (Table 2) were sampled in the northern North Sea (Figure 5). Five stations were regional, while the last five originated from Kvitebjørn- (KV) and the Visund (VI) field. The sediment samples were sampled from regional stations located between 137-400 meters depth. The sediment composition varied in the different samples, but was mainly composed of silt and clay (<0.002 millimetres).

Figure 5: Locations of the sampling sites in the northern North Sea. A total of 10 samples were collected in this region. Illustration is borrowed from Møskeland et al. (2018) (Figure 5-4).

Table 2: List of the different sampling station in the northern North Sea with their respective oilfields, sediment characterization, and depths.

Sample name	Oil field	Sediment characterization*	Depths* (m)
SNB-16R	Snorre B ref/regional	Silt and clay	342
Reg-12	Regional	Silt and clay	400
Vega-R	Vega	Silt and clay	380
VI-RB	Visund ref/regional	Silt and clay	330
VI-01	Visund	Silt and clay	330
VI-03	Visund	Silt and clay	330
VI-30	Visund	Silt and clay	316
STC-06R	Statfjord C ref/regional	Medium Sand	137
KV-14	Kvitebjørn	Fine Sand	187
KV-02	Kvitebjørn	Fine Sand	185

*Measured depths and sediment characterization was done by DNV-GL and are retrieved from report: 2018-0050, Rev. 01., Miljødirektoratet; (Møskeland et al., 2018)(Table 5-2).

Five sediment samples were collected in the Barents Sea region (Table 3). The samples were spread over a large area with considerable variations in depth among the five stations (Figure 6), ranging from 251 to 508 meters. Silt and clay dominated all of the sediments.

The sampling stations are named Stangnestind (STT), Korpfjell (KF2), Scarecrow3 (SC3), Kråketind (KRT), and Gråspett (GRS) (Table 3). Korpfjell and Stangnestind are found on the same longitude (72°), while the three remaining stations are located at 73° longitude.
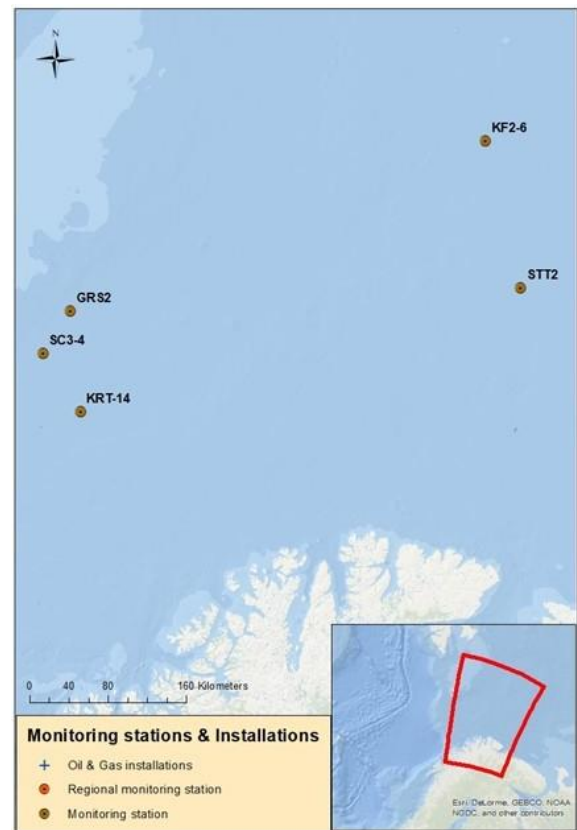
Figure 6: Locations of the sampling sites in the Barents Sea. A total of 1five samples were collected in this region. Illustration is borrowed from Møskeland et al. (2018) (Figure 5-5).

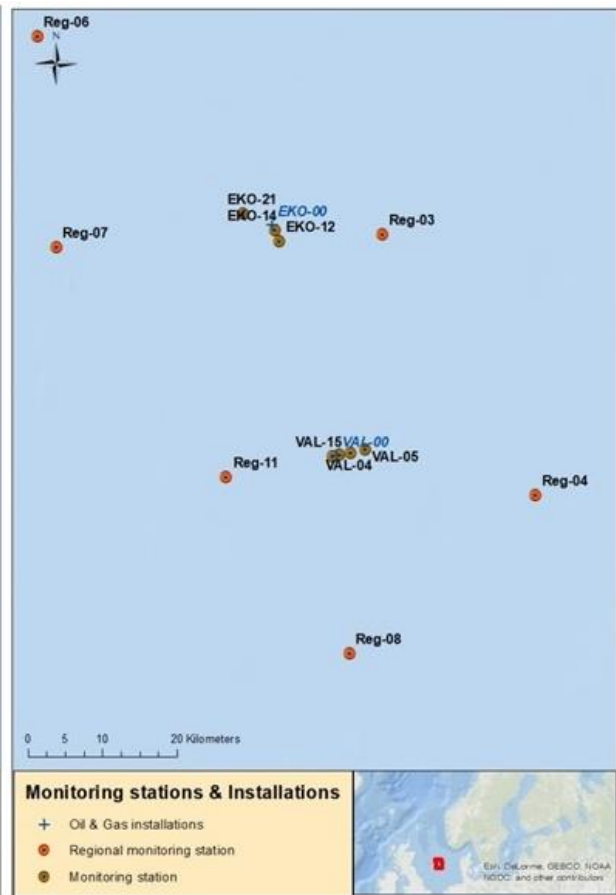*Table 3: List of the different sampling station in the Barents Sea with their respective oilfields, sediment characterization, and depths.*

Sample name	Oil field	Sediment characterization*	Depths* (m)
STT-2	Stangnestind	Silt and clay	251
KF2-6	Korpefjell	Silt and clay	242
SC3-4	Scarecrow3	Silt and clay	461
KRT-14	Kråketind	Silt and clay	440
GRS-2	Gråspett	Silt and clay	508

*Measured depths and sediment characterization was done by DNV-GL and are retrieved from report: 2018-0050, Rev. 01., Miljødirektoratet (Møskeland et al., 2018)(Table 5-3).

2.1.2 - Rio Almendares, Havana (Cuba)

This second part of the study was done in collaboration with WEATHER-MIC, CEAC (Center for Environmental Studies of Cienfuegos) and the Race for Water Foundation, as a part of the environmental clean-up program called *Race for Water Odyssey 2017-2021*. The author himself sampled sediments from Cuba with assistance from Linn Merethe Olsen (NGI) and co-supervisor Hans Peter Arp (NGI). Strategies for sampling and choice of location were made in cooperation with the boat crew and local Cuban scientists. In total, ten sampling locations were initially targeted, but sediment extraction was not successful for all locations as rocky seabed dominated certain spots. These conditions were documented by lowering a GoPro camera attached to a rope into the water. Video can be provided on request. Additionally, samples from 36 kilometers of manta trawling, and 23 water samples at different depths were collected during the period from the 3rd to 6th of August 2017. These samples were not analyzed any further due to time restrictions. The Ships' log was provided by the captain containing dates, coordinates, and other sampling data (Appendix-A2-1).

In total, nine sediment samples were collected at four locations on the 3rd and 6th of August 2017 (Figure 7). Seven samples were taken using a *Van Veen Grab* sampler (0.26 cm^2) from the rear deck of the catamaran (LOC-10 and LOC-1). Two more samples were collected further upstream of the Rio Almendars using only a clean metal garden shovel. The contents were transferred to 300 ml glass sampling jars and stored collectively in aluminum cases. Eight of these samples were analyzed for microplastic content. A set of triplicate samples collected at location 10B were analyzed for microplastic and represent the *river outlet* sediments in further calculations. These sediments do not originate from one single Van Veen Grab extraction but were sequentially collected during a short time-span. These samples had similar characteristics and are assumed to be one sample.
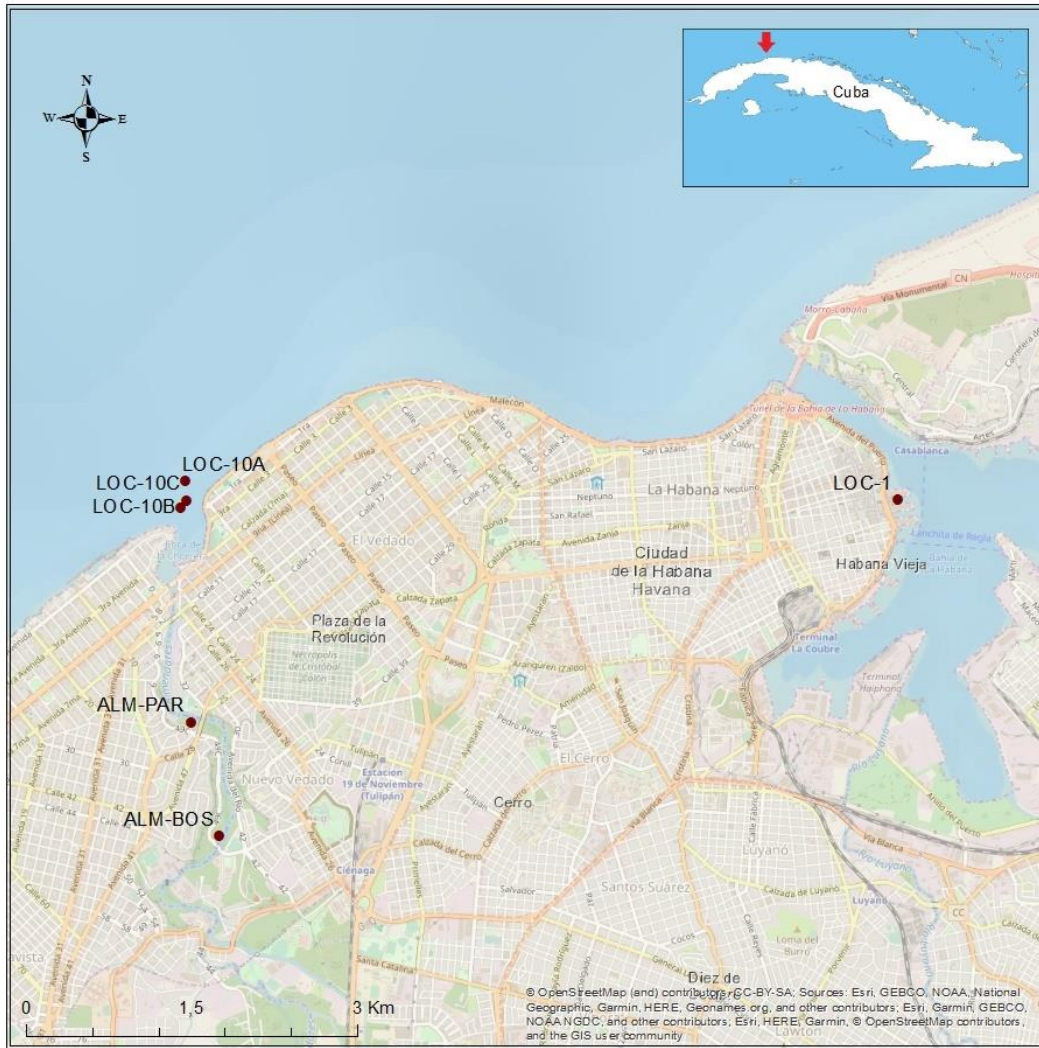
Figure 7: A geographical map showing the sampling sites of the Almendares River and Havana Harbour (Cuba). Six sites include ALM-BOS (Bosque de la Habana), ALM-PAR (Parque Almendares), LOC-10 (river outlet) and LOC-1 (cruise terminal).

Location 1 - Cruise terminal (LOC-1)

Location 1 was situated at the docking site where the boat was anchored in Havana during the Race for Water Odyssey. The ship terminal was frequently visited by international cruise ships also docking nearby. Floating objects (plastic bottles, aluminum cans, twigs, plastic bags) were observed all around sampling site, and the smell of oil was intensive. The sample from this location was collected using a Van Veen Grab, on the 6th of August. The sampling provided 402 grams of sediment sample (Appendix A2-3).

Location 10 – River outlet (LOC-10)

Samples from location 10, outside the river outlet of Rio Almendares, were collected the 3rd of August 2018 by boat. Wind and water turbulence from the river created some difficulties when using the Van Veen Grab as we drifted around the outflow of Rio Almendares. Some sediment extractions were less complicated, giving *six* samples: LOC-10A, LOC-10A2, LOC-B1, LOC-10B2, LOC-10B3, and LOC-10C. The first sample (LOC-10A) consisted of a mixture of small rocks, sand, and shellfish, making up 305 g of raw sediment sample (Appendix A2-3). Three sediment samples from location 10B were described as fine-grained black sediment smelling

of oil residues and tar (327 ± 15 g raw sediment sample). The last sample LOC-10C was a small (53 g), but a biologically rich sample. Sample *20170803-LOC-10A* and *20170803-LOC10C* are only included in this study to provide polymer abundance and accompanying site characteristics. All sediment samples were collected at depths deeper than 15 meters (Appendix A2-1 or Table 4).

Parque Almendares (ALM-PAR) – Recreational Park

This sampling site was located inside a park offering recreational services on the west side of Rio Almendares, near the bridge of the 23rd Avenue. The sample was dug out at the outskirts of the park (Figure 8 and Figure 9) using a simple garden shovel. The sample was collected approximately 10 cm below the depth of the water level. The river seemed wholly polluted, and macroplastics were observed all around the site. The sample appeared black in color and organic matter- rich.

Figure 8: Photo was taken from the site "Parque Almendares".The sampling location is dominated by recreational services, especially water sports such as kayak paddling.

Figure 9: Photo from exact sampling position (ALM-PAR). The sample was dug out 10 cm under water table using a small shovel. The site was polluted by microplastic and other floating objects.

Bosque de la Habana (ALM-BOS) – ruins (Parque Metropolitano)

The sample site farthest upstream was also located on the western riverbank of Rio Almendares (Figure 10 and Figure 11). This area is a popular site for both local Cubans and tourists. This part of the river appeared to be of high religious importance; as voodoo practitioners and ritual items were observed all over the riverbank. The sampling location was rocky and shallow, and the collected sample seemed to be rich in organic matter content.

Figure 10: Photo from sample site "Bosque de la Habana" (ALM-BOS). This part of the river was rocky and shallow. The photo is taken upstream the river (southwards).

Figure 11: Photo also from the west side of the river banks, direction downstream (north). This part of the river was rocky and shallow.

See Appendix A2-3 for more details regarding the sediment samples from Cuba.

Table 4: List of all sampling sites investigated for microplastic in Cuba with a short site description.

Location	Depth	Site and sediment characterization
Location 1	~ 5 m	Docking point. Black and oily sediments.
Location 10 (A)	11 m	River outlet. Mixed rocks, sand, and shell-fish
Location 10 (B)	15 m	River outlet. Fine-grained black sediments
Location 10 (C)	13 m	River outlet. Biological rich sample (grasses etc). Small.
Parque Almendares	< 1 m	Recreational park. Biological rich sample.
Bosque de la Habana	< 1 m	Most southward site. Ruins and ritual grounds. Biological rich sample

2.2 - Experimental design and materials

2.2.1 - The Bauta Microplastic-Sediment Separator

This study uses the *Bauta Microplastic-Sediment Separator* to separate microplastics (≤45µm) from benthic sediments. This concept is based on the same idea as the *Munich Plastic Sediment Separator* (MPSS) by Imhof Hannes et al. (2012). Conceptual designs may differ somewhat for these techniques, but standard for both methods is that they use *density separation* to isolate microplastics from sediments. The design of the BMSS was developed by NGI (Norwegian Geotechnical Institute) in Oslo, and the method was further optimized by Mahat (2017). NGI currently own three functional units used for density separation

The high-density brine solution, being $ZnCl_2$: $CaCl_2$ (ρ=1.51) was used to promote density separation of introduced sediments. A dense particle, such as small rocks, sand, and clay will sink in the solution, while particles with a density lower than 1.51 will float on top of the solution. The sample material was extracted from the top of the *Bauta* when sufficient separation is achieved.

Figure 12: Schematic of Bauta Microplastic-Sediment Separator unit. Dense particles settle at the bottom of the $ZnCl_2$:$CaCl_2$, while less dense particles float on top. Illustrations is borrowed from Mahat (2017)(Figure 4).

The BMSS consist of four separable components (Figure 12), starting from the bottom: *the base unit*, *the sediment chamber*, a *glass column* and lastly *the separation chamber*.

Base unit

The bottom part of the BMSS involves a stationary base unit made from stainless-steel. The units were fitted with frequency-controlled propellers. The three units all have a max speed of 4000 rounds per minute but differ somewhat by having individual gear ratios: 5:1, 10:1 and 50:1. The bases were fitted with an inlet and outlet valve.

Sediment chamber

The sediment chamber is a 126-millimetre tall cylinder made of stainless-steel which fits on top of the base. The cylinder has an additional outlet valve for draining the $ZnCl_2$: $CaCl_2$-solution above the level of the sediments. The sediment chamber is fastened to the base unit by clamps.

Glass column

The column is a transparent glass cylinder with a height of 650 millimetres, providing sufficient column length for efficient separation. The column has an inner diameter of 90 mm while the top of the column is narrowed down to 65 mm to fit the separation chamber.
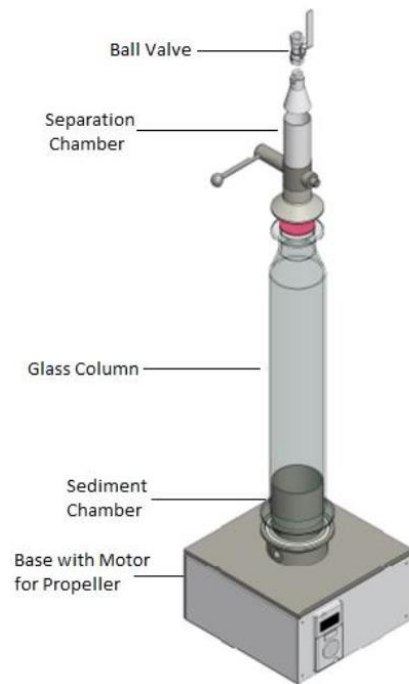
Separation chamber

The separation chamber is made of stainless steel and is used to collect the sample from the top of the glass column by raising the level of the solution. The separation chamber was fitted with a ½ inch ball valve and a shut-off valve in both ends. The unit is also equipped with a depressurizing valve below the shut-off valve to lower the solution level when both the ball valve and the shut-off valve were shut.

Each component is fitted with O-rings between each joint to prevent leakage and loss of solution.

2.2.2 - Preparation, adjustment and recycling of $ZnCl_2$:$CaCl_2$-solution

$ZnCl_2$:$CaCl_2$ (aq) is a highly corrosive solution with high-density properties. One successful microplastic-sediment separation requires approximately 7 liters of filtered $ZnCl_2$:$CaCl_2$. Safety equipment such as eyewear, lab coat, and nitrile gloves was used when handling the solution.

Newly-made batches of $ZnCl_2$:$CaCl_2$ solution were prepared in carboys (composed of high-density polyethylene) by mixing analytical $ZnCl_2$ saturated salts (VWR International, Germany), analytical $CaCl_2$ saturated salts (VWR International, Germany) and ultrapure Milli-Q water in ratio by weight: 4.4:2:3.6 (H_2O: $ZnCl_2$:$CaCl_2$) (Hudgins, 1964). Instructions for solution preparation by Imhof et al. (2012) were followed carefully. All exothermic reactions during preparation were controlled by putting the carboy in ice baths under a fume hood until the reaction reaches equilibrium. Finally, salt crystal formation and impurities were removed by centrifugal separation at 4000 rpm for 10 minutes and then filtration through a Whatman GF/C (pore size: 1.2 μm) glass fiber filter using a 2.12l high-pressure (N2-gas) filtration system (producer). The preparation of $ZnCl_2CaCl_2$-solution process takes approximately 2 days. The carboys and the canisters were regularly washed and rinsed with deionized (DI) water to remove the build-up of crystal from the solution. The densities of the $ZnCl_2$:$CaCl_2$-solutions were tested after preparation, between filtration, and when mixing two solutions with different densities together. The density was calculated using Equation 1 below:

$$Density\ (\rho) = \frac{g}{cm^3} = \frac{\left(m_{V.f\,(g)} + m_{ZnCl_2:CaCl_2(g)}\right) - m_{V.f.\,(g)}}{V_{V.f\,(cm^3)}} \qquad \textit{Equation 1}$$

where $m_{V.f.}$ is the weight of the volumetric flask, $m_{ZnCl2:CaCl2}$ is the weight of the solution and $V_{V.f.}$ is the volume of the volumetric flask.

Adjusting the brine solution was necessary when the density dropped below 1.5 g/cm^3. To correct for this, the old batch was mixed with a newly made high-density solution and shaking for 15 minutes and filtered through a Whatman GF/C glass-fibre filter.

Recycling of $ZnCl_2CaCl_2$-solution is highly recommended as $ZnCl_2CaCl_2$:H_2O is considered hazardous to aquatic environments and should be handled and disposed of properly. In additions, the making of $ZnCl_2CaCl_2$-solution is also a very time-consuming (2 days) and expensive procedure making reuse an appealing option. To detect possible microplastic cross-contamination of microplastic associated with the reusing, method blanks were run through the standard protocol. In addition, all used glass fiber filters and expired $ZnCl_2CaCl_2$-solution was collected and properly taken care of following standard laboratory protocol at NGI.

2.3 - Microplastic extraction and analysis

2.3.1 - Cleaning and assembly of Bauta

The assembly of the Bauta prior to the microplastic-sediment separation was conducted in a specific order following protocols carefully. First, the base was flushed and washed with DI water and then wiped with delicate task wipers. O-rings were controlled for damage before the sedimentation chamber was fitted to the base unit and secured with adjustable clamps. The glass columns were hand-washed with industrial soap and warm water, before being rinsed thoroughly with DI water. Once the glass column was fitted and sealed to the sedimentation chamber, a small amount of $ZnCl_2:CaCl_2$ solution was used to flush the system including the silicon tubes. The glass column was filled up with the solution to just below the narrowed neck, and all valves were shut off before sediment sample was introduced.

Between each sediment sample, the Bauta microplastic-sediment separator was disassembled in the exact opposite order of assembly. Most components and tools that fit the washing machine, such as the separation- and sedimentation chambers, were washed with a pre-set program for 35 minutes using *neodisher LaboClean A8* soap. Whenever the Bauta was left unattended, regardless if it contained sediment or not, all components exposed to the atmosphere were covered with aluminum foil to prevent contamination. All parts were rinsed and dried with DI water prior reassembly.

2.3.2 - Pre-treatment and introduction of sediment sample to BMSS

The samples from the Norwegian Continental Shelf arrived at NGI on 31.08.2017, and the Cuban samples arrived 11.08.2017. Samples from the Norwegian Continental Shelf were stored in cold storage (2-4 °C) at NGI until analysis. Samples from Cuba were frozen at -20° C and unfrozen on 31.01.2018. All samples were kept in cold storage when not being analyzed.

The sediment samples from the Norwegian Continental Shelf were preserved with 5 % formaldehyde at arrival, which needed to be decanted before further processing. The removal of formaldehyde was handled in a fume hood wearing hand protection. A clean 150x150 mm steel mesh filters (45 µm) were placed over the opening of the glass jar and tightened with an over-sized hose clamp so that the formaldehyde could be poured off. Sediments stuck to the filter were transferred back to the jars by best effort with a clean metal spoon. This step was not needed for the sediment samples from Rio Almendares since they were not preserved with formaldehyde.

All sediment content from the glass jar were scooped into disposable pre-weighed aluminum trays. Homogenization was done with a metal spoon until the texture of the slurry appeared homogeneous. Dry weights were obtained by scooping out some of the homogenized sediments into pre-weighed aluminum cups using a metal spoon and dried for >2 days at 60°C before being re-weighed. The moisture content was calculated based on weights before and after drying (section 2.4.6, eq. 12-14). On average, 120 g (NCS) and 30 g (Rio Almendares) of homogenized sediments were used in the soil moisture corrections. The precision for acquiring this data was expressed in a triplicate test for location 10B (Cuba).

The weights of the sediments were noted, and sediments were made into a slurry by adding 100 ml $ZnCl_2:CaCl_2$ and re-weighed. Well-homogenized sediment samples were spoon-fed gradually from the top of the Bauta under full stirring by the propeller. A 500-mL Nalgene wash bottle filled with filtered $ZnCl_2:CaCl_2$-solution was used to wash out any remaining sediment from the aluminum trays to the Bauta. When empty, the weight of the aluminum tray was noted

to correct for any loss of sediments. Finally, the top was sealed with an aluminum cap and left over-night (15 hours) for density separation.

Also, some fine-grained sediment samples experienced lower rates of organic matter and particles in the top of the glass column after separation. These sediments were identified by having a creamy consistency and therefore 10 ml of 0.1% sodium dodecyl sulphate soap (SDS) was added to reduce cohesive forces and facilitate proper mixing.

The amount of sample being introduced to the Bauta sometimes depended on the total available sample, ranging from 51 to 1040 g of wet sediment. If glass jars contained large quantities of sample, some sediments were scooped back into their original glass jar as a backup. Back-ups were not possible for the Cuban samples due to low quantities of collected sediments.

2.3.3 - Sample extraction and filtration

When microplastic-sediment separation was achieved, the separation chamber was placed on top of the glass column and the level of $ZnCl_2$:$CaCl_2$-solution was raised over the shut-off valve. When all sample material was transferred to the separations chamber by slowly raising the level of the solution, both the ball valve and shut-off valve were closed and the level of $ZnCl_2$:$CaCl_2$-solution was lowered from the lower outlet valve fitted the base unit. Once the level of the solution was below the neck of the glass column, the separation chamber was removed and placed onto a rack in an inverted position. A vacuum filtration system (Figure 13) was used to collect the sample from underneath the separation chamber onto pre-weighed steel mesh filters. The separation chamber was flushed with clean $ZnCl_2$:$CaCl_2$ solution using the wash bottle between each filtration, and after repeating the filtration process three times both the separation chamber and the glass funnel was rinsed thoroughly with milli-Q water. After filtration, the vacuum filtration system was disassembled, and the steel mesh filters were folded like an envelope (Figure 14), and finally secured

Figure 13: Photo of filtration setup. Extracted sample was filtered onto steel-mesh filters by using a vacuum filtration system. Filter is placed between the filtering cup and the filtering head.

with a steel wire. Some samples with a high content of organic matter had to be divided into two steel mesh filters and merged after digestion. The top of the glass column was always covered with aluminum foil between filtrations.

Some of the samples from the Norwegian Continental Shelf experienced rust formations on the steel mesh filters. Therefore, all folded filters containing sample were put in glass jars filled with Milli-Q water and radiated in an ultrasonic bath for 2x15 min. Finally, the samples were rinsed and dried over-night at 60ºC. The next morning samples were left for an hour at room temperature before weighing, avoiding false or doubtful values during weighing due to thermal convection inside the enclosed scale cabinet.
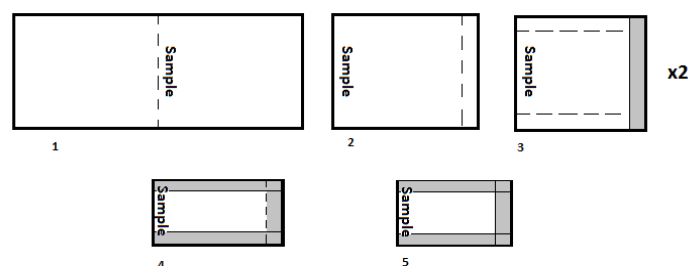
Figure 14: Illustrations demonstrate the folding technique used for the steel-mesh filters. First, the filters were folded at the centre, then at the free ends twice, at the sides twice and one last time at the tip.

2.3.4 - Chemical digestion

Chemical digestion, sometimes referred to as sample purification is a treatment with the aim to remove any unwanted substances other than microplastics. The unwanted substances are primarily labile organic compounds such as leaves, twigs, and detritus. Organic matter may also obstruct the visual analysis and disturb signals transmitted by the Fourier transformed infrared (FTIR) when identifying different polymers. Purification of samples containing microplastic is to this date not standardized. The general requirement is a sensitive treatment which will not damage the plastic polymers present in the sample during the process.

The approach for sample purification in this study is based on previous work by Olsen et al. (*In preparation*) and ensures an efficient and sensitive reduction of organic material. The treatment is a two-step process taking up to two days to completing *one* round of digestion.

The first step involves dissolving of organic compounds using a Sodium hydroxide: Urea: Thiourea [NaOH: CO(NH2)2: CH_4N_2S]-solution (Figure 15 and Table 5). Samples were soaked with 80 ml of NaOH: $CO(NH_2)_2$: CH_4N_2S per 2 gram of dried sample material and stored in -20 °C in glass jars. The samples were stirred up every 15 minutes to prevent crystallization of the solution while in the freezer. After 45 minutes, all samples were taken out and stirred by magnetic stir bars until they reached room temperature ($\approx$2 h). All samples were rinsed at least 15 times with Milli-Q water and left submerged in Milli-Q water for 15 minutes for every fifth wash.

In the second step, all samples are oxidized using 60 ml of 30% Hydrogen Peroxide (H_2O_2) per 2 gram of sample (Figure 16 and Table 5). Additionally, 1.5 ml of 10M NaOH was mixed in to function as a catalyst. The chemical reaction is known to be quite exothermic, so all samples were kept in enclosed glass jars only ventilated by steel mesh (45µm) for depressurizing. These jars were placed in tall plastic containers to control the boil-up from overflowing the fume hood created by the reaction. The samples were stirred by magnetic stir bars in a fume hood until the exothermic reaction occurred, or a minimum of 3 hours. Lastly, all samples were rinsed at least 10 times and left submerged with Milli-Q water for every fifth wash and dried at 60°C overnight.

Figure 15: The photo shows seven samples are set to reach room temperature under continuous stirring. This photo was taken right after the first digestion step.

Figure 16: The photo shows the second part of the chemical digestion. Samples are kept in a partily open container under a fume hood due to the exothermic reactions. The samples are placed on magnetic stirrers.

The maximum number of digestions depends on total organic matter content and the overall chemical resistance of the compounds in the samples. The amount of sample was calculated by subtracting the total weight of the filter containing the sample by the pre-weight steel mesh filter and steel wire. See equation 2 below.

$$w_{Calc.\ sample\ weight\ for\ digestion} = m_{total\ sample} - (m_{filter} + m_{wire}) \quad Equation\ 2$$

When preparing the chemical solutions used in the digestion treatment, the accuracy of the pipettes was controlled between each step in the process along with replacing the pipette tips. Recovery- and method blanks were only chemically digested once, or at maximum twice as low amounts of organic material were expected.

Table 5: Complete list of chemicals used in the study. Calcium Chloride and Zinc Chloride was used in making the $ZnCl_2$:$CaCl_2$ solution, the H_2O_2, $CO(NH_2)_2$, CH_4N_2S and NaOH were used for digestion. Lastly, $CH_3CH_211OSO_3Na$ is the SDS soap. The respective chemicals are listed with molecular formulas, manufacturers, and the chemical purity.

Chemicals	Molecular formula	Manufacturer/ Distributor	Purity (%)
Calcium Chloride	$CaCl_2$	VWR International	90-98
Zinc Chloride	$ZnCl_2$	VWR International	97
Hydrogen peroxide	30 % H_2O_2	VWR International	Analytical grade
Urea	$CO(NH_2)_2$	Sigma Aldrich	≥ 98
Thiourea	CH_4N_2S	Merck K GaA	≥ 98
Sodium hydroxide	NaOH	Merck K GaA	99 – 100
Sodium dodecyl sulphate	$CH_3(CH_2)_{11}OSO_3Na$	Sigma Aldrich	≥ 99 (Chromatography)

2.4 – Quality control and data processing

When quantifying microplastics in the lab, there is a risk of contamination whenever handling the sample. In order to achieve reliable results, it is important to follow protocols strictly. However, avoiding microplastic contamination entirely is practically inevitable. Therefore, proper documentation that can validate the quality of the contamination control is necessary. Possible impurities were corrected for by doing method blanks, the precision was tested by conducting replicate experiments, and the accuracy of the method was expressed through numerous recovery tests.

2.4.1 - Instrument- and sample handling protocol

Reliable measurements from weight scales are a necessity when the study relies on the weight of microplastics in the sample. Therefore, all digital weighing scales were controlled prior this study. Both the enclosed analytical balance and open precision scale electronic were calibrated the 31st of August 2017 by METTLER TOLEDO. The precision of the enclosed high-sensitivity scale was expressed by the final re-weighing of the steel wires used to secure the folded mesh filters for the Cuban samples (Appendix A2-6). Additionally, the final re-weighing of the samples are also documenting the chemical stability of the steel wires. Lastly, the steel wires can also function as an ID for each respective sample, lowering the possibility of sample mix-ups during digestion.

2.4.2 - Method blanks

The complete process of microplastic-sediment separations involves many steps which all could be potential sources of external microplastic contamination. Method blanks are used to indicate the purity throughout the study; reflecting lab conditions, cleaning protocols and quality of chemicals including recycled $ZnCl_2:CaCl_2$-solution.

Data from the method blanks were reported by weight, by microscopy, and by FTIR analysis. The procedure of collecting method blanks ($m_{Method\ blank}$) are identical to microplastic-sediment separation protocol but involves no sediment samples. A total of 13 method blanks were sampled during the study, and the mass of impurities ($m_{impurities}$) was calculated as shown in Equation 3:

$$m_{Impurities} = m_{Method\ blank} - (m_{filter} + m_{wire})\ Equation\ 3$$

where m_{filter} is the mass of the steel mesh filter, and m_{wire} is the mass of the steel wire.

All method blanks from the Norwegian Continental Shelf (n=11) were weighed and visually inspected by microscopy, except sample *20171123-blank (NCS)* and two blanks from Cuba (20180102–Blank 1 and 20180102–Blank 2). See Appendix A3-1 for details.

Three method blanks were conducted to control the quality of the FTIR analysis. Washed filters were treated as indifferent as possible compared to the FTIR handling protocol. The FTIR protocol is described in section 2.4.5.

2.4.3 - Recovery blanks

Ten recovery tests were performed to determine the accuracy of the microplastic-sediment separator. Selected sediments which already had been analyzed for microplastics were added a known amount of the following plastic types; micropowders, microfibres and granulates (Table 6).

The recovery tests were carried out by draining $ZnCl_2:CaCl_2$-solution from the upper outlet valve and transferring sediments to pre-weighed aluminum trays by best effort using metal spoons. The sediment was then spiked with a fixed amount of microplastic ($m_{spiking\ material}$) then re-introduced and filtered following the standard sample protocol. The recovery blanks ($m_{Recovery\ blank}$) were sampled identically to other samples, and the recovery rate (%) was calculated as shown in *Equation 4*.

$$Recovery\ rate_{\%} = \frac{m_{Recovery\ blank} - (m_{filter} + m_{wire})}{m_{spiking\ material}} \qquad Equation\ 4$$

Doing digestion for the recovery samples was considered necessary to remove any residual organic matter since the previous filtrations. This could add additional weight to the recovery blanks, leading to too high recovery rates. Recovered sediments from the sediment sample *20171127-KRT-14* (NCS) were split into two recovery blanks: *20171127KRT-14-Blank #1* and *20171127KRT-14-Blank #2* (Table 11). Sediments from sample *20171113-SNB-16R#1* and *20171113-SNB-16R#2* were a set of replicates which were spiked to determine the method precision and were spiked immediately after the previous sediment samples were treated for density separation (Appendix A1-3).

Table 6: List of spiking material used in the recovery test. The list also includes type, manufacturer, and polymer properties.

Form	Type	Manufacturer/ Distributor	Properties
Powder	Polyester (PET, PETP)	Goodfellow Cambridge Ltd. (UK) Catalog nr. ES306030	Density 1.40 g/cm3 Diameter 75 – 300 µm
Fiber	Polyethylene (LDPE)	Goodfellow Cambridge Ltd. (UK) Catalog nr. ET315710	Density: 0.92 g/cm3 Length 5 – 10 mm
Granulate	Polyester (PET)	Goodfellow Cambridge Ltd. (UK) Catalogue nr. ES306312	Density =1.40 g/cm3 Nominal size range 3 – 5 mm.

2.4.4 - Visual inspection by microscopy and extrapolation of microplastic items

Visual identification offers significant limitations and is associated with either an overestimate or underestimate compared to FTIR, Raman or Pyrolysis GC-MS analysis. Visual Inspection by Microscopy (Nikon Eclipse E40) was only practice on the samples from the Norwegian Continental Shelf due to the absence of an FTIR instrument.

Figure 17: Photo of sample 20171124 – GRS2 locked in place with two acrylic plates. The transparent grid system were attached to the top of the sample.
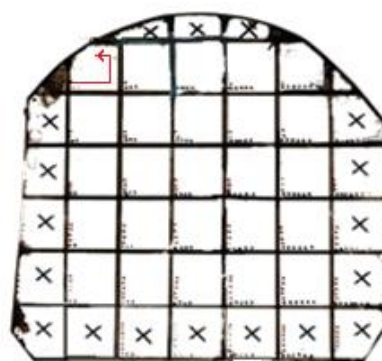
Figure 18: Illustrations of the 5x5 grid system used for counting microplastics. Red arrouw indicate the direction for systematic counting used in the study.

Some samples potentially containing microplastics were visually inspected using a microscope after sufficient digestion. Samples were dried and weighed before being unfolded and placed between two transparent 10 x 10 cm acryl plates and finally sealed with scotch tape along the two edges. Then, a transparent 5x5 grid system was centrally fixed on top of each sample (Figure 17).

The counting of particles was conducted by a total of three persons strictly following the *MERI - Guide to Microplastic Identification protocol* (MERI, 2015). The samples were systematically investigated using both x10 and x40 optics; starting at bottom left moving right, up and then left, as illustrated in Figure 18. Each counted particle was categorized based on shape (fiber, layer or granule), color and size (Table 7Table 7). Due to the acryl plates covering the samples, the hot-needle test could not be used in this study.

In total nine microplastic samples were visually counted: *20171103-GYDA-18, 20171117-Reg-09, 20171117-Reg-12, 20171113-SNB-16R, 20171117-VI-RB, 20171121-STC-06R, 20171120-VI-03, 20171116-Vega-R,* and 20171127-KRT-14". However, only four of these samples were used to estimate the number of particles per gram of sample (Appendix D1-2).

Table 7: Template for categorization and counting microplastic during visual analysis. Particles were sorted based on size (see A, B, C, and D), color (Red, blue, etc.) and shape (1- dimensional: fiber, 2- dimensional: layer or 3—dimensional: granule).

Colour	Fibre 1D				Layer 2D				Granule 3D			
	A	B	C	D	A	B	C	D	A	B	C	D
Clear/white												
Light brown												
Dark brown												
Black	≥ 45 to < 100 m	100-300 µm	300 - 1000 µm	1 -5 mm								
Blue												
Red												
Green												
Orange												
Yellow												

Estimates and extrapolations of microplastic *items* per kilo sediment and area were calculated based on the findings from the visual analysis. First, counted particles were corrected for by subtracting the number of particles found on method blanks within each group, as seen in Equation 5 and 6.

$$n_{mMP\ type} = n_{mMP\ type\ in\ sample} - n_{mMP\ type\ in\ Method\ Blank} \qquad \textit{Equation 5}$$

$$n_{mMP\ sample} = \sum n_{mMP\ type} \qquad \textit{Equation 6}$$

where:

- $n_{mMP,}$ = MP$_{max}$ items within an individual group in the sample
- $n_{mMPmax\ type\ in\ sample}$ = average MP$_{max}$ items (within an individual group) counted in the sample
- $n_{mMP\ type\ in\ Method\ Blank}$ = average number of items (within an individual group) counted in the method blanks
- $n_{mMP\ sample}$ = blank corrected MP$_{max}$ items in the sample

Some samples could not have the exact number of particles determined because individual particles were not distinguishable. These samples were extrapolated for the number of items based on the samples that were determined ($n_{mMP\ sample}$) with their corresponding mMP weights (m_{mMP}), given that the mass of the samples were above the LOD (limit of detection), by using *Equation 7* stated:

$$f_e = \frac{n_{mMP\ sample}}{m_{mMP}} \hspace{4cm} \textit{Equation 7}$$

Where:

- f_e = the extrapolation factor
- $n_{mMPmax\ sample}$ = average maximum number of MP items in the sediment samples
- m_{MPmax} = average maximum weight of MP in the sediment samples (Formula 5)

In this way, the estimated number of MP$_{max}$ items was calculated by multiplying the extrapolation factor with the dry weight of sample material after digestion (m_{mMP}).

In order to make comparisons to similar studies, results should be reported in units of items/kg dry sediment and items/m^2 sediment surface, using the equations listed below:

Max weight concentration:

$$c_{microplastic\ d.w.}\left(\frac{items}{kg_{d.w.}}\right) = \frac{n_{mMP\ sample}}{m_{bauta\ sed.d.w.}} \hspace{3cm} \textit{Equation 8}$$

Max area concentration:

$$c_{microplastic\ area}\left(\frac{items}{m^2}\right) = \frac{n_{mMP\ sample}*\frac{m_{bauta\ sed.w.w.}}{m_{sed.w.w.}}}{A_{grab}} \hspace{2cm} \textit{Equation 9}$$

The area of the Van Veen Grab was 0.15 m^2 for all samples except one. See section 2.1.1. The approach for visual analysis is identical to the approach described in Møskeland et al. (2018). Also, see Appendix D1-1 for method blanks results and D1-2 for the extrapolation factor.

2.4.5 - FTIR analysis and extrapolation of microplastic items

An FTIR instrument detects functional groups of polymers using infrared spectroscopy, allowing fast and precise identification. A Perkin Elmer FTIR Microscope Spotlight 200i instrument was purchased by NGI at the beginning of 2018, allowing all samples from Rio Almendares to be analyzed with this instrument, but not all of the samples from the Norwegian Continental Shelf. However, a few samples from the NCS were analyzed at a later point of the study. Full FTIR reports are sent on request.

Before the FTIR scan, sample material (0.0065 ± 0.0012 g) was divided into three pre-punched steel-mesh filters (Ø=13mm). These circular filters were obtained by punching holes in the same steel mesh sheet used throughout this study. See Figure 19. The punched filters were treated with 0.1 % SDS soap in UV bath for 20 minutes and rinsed multiple times before being dried at 100°C over-night. When preparing the sub-samples, particularly exciting particles were manually transferred to the 13 mm filters together with a pinch of random sample material carefully scattered over the filters. All samples were covered with a glass slide when not being analyzed.

Figure 19: To the right, a hole puncher used for making steel mesh filter fitting the black platform slide (to the right). The diameter of the punched steel mesh filters is 13 mm. The holes in the slide are 10 mm.

Three sub-samples per sediment sample were analyzed by a transmittance beam (wavenumber: $4000 - 650$ cm^{-1}, 4 cm^{-1} accumulations, and 4 cm^{-1} resolution). The lower size limit of the FTIR was 0.1 µm, but the minimum size is limited to a greater extent by the ability of the software to recognize particles. The aperture was set to 10 mm mapping a 10.000 µm x 10.000 µm survey image for each subsample (Figure 20). Then, particles were detected with the auto-detection function and missed out particles were manually added. All markers were corrected by the background spectrum *before* the marker were scanned and analyzed by the library provided by PerkinElmer (Spectrum IR). The best hit chosen by the software was set to represent the identified markers. Each identified marker was saved with its position (µm (X), µm (Y)), analysis quality and polymer type. Scan results from the sub-samples were exported, merged and sorted based on their location in Excel. On average, 148 ± 94 particles (markers) were analyzed per sample. Only markers with a search score above 0.6 were included in the final results, being 32 ± 17 % of all markers analyzed. All identified markers were categorized as either plastic, paint, rubber, petro-pyro, organic, inorganic, unknown or air (Table 8). *Plastic, rubber, paint, and petro-pyro* were categorized collectively as anthropogenic (from now referred to as "anthropogenic") sources throughout this study. *Petro-pyro* includes all petroleum-based particles other than plastics, such as in principle coal, soots, tars, etc., but in practice were generally based on FTIR matches of Hydrocarbon resins and petroleum residues Plasticisers, copolymers, adhesives, and additives, as identified by the FTIR, are categorized as *various* under *plastic*.

FTIR analysis:		Sorted after search score:		Categories:		Sub-categories
Total markers		- Identified markers:		Organic		
(148±94)	→	above 0.6 (47±53)	→	Inorganic		
				Unknown		
				Air		**Plastic**
				Anthropogenic	→	Paint
		- Identified markers:				Rubber
		under 0.6 (100±70)				Petro-pyro

Figure 20: Image view of sample 20171124-GRS-2 on the circular steel mesh filter
Image to the right show the same sample with particles marked for analysis by the auto-detect
function. The diameter of the filter is 10 mm.

Estimates for items per kg dry sediment were made exclusively for the triplicate set of samples (LOC-10B) and samples 20170806-ALM-PAR and 20170806-ALM-BOS. These samples appeared to be the most fit to represent the *river outlet sediments* and *upstream sediments* when looking at polymer distribution (review section 2.1.2). The weights of the analyzed sample material were noted before and after FTIR identification to assure no loss of particle when handling the sub-samples. The formula for estimated particles per kg dry sediments is described in *Equation 10*, are based on the mass of the marked particles:

$$\frac{Items\ MP_{max}}{kg_{dry\ sediment}} = \frac{items_{total\ markers}}{m_{sub-samples\ (g)}} * \frac{items_{identifed\ polymers}}{items_{total\ markers}} * mg\ MP_{max}\ concentration\ \left(\frac{g}{kg}\right)$$

(Equation 10)

where the factor $\frac{items_{total\ markers}}{m_{sub-samples\ (g)}}$ represent the number of particles per gram sample material and $\frac{items_{identifed\ polymers}}{items_{total\ markers}}$ is the fractions of plastic polymers with a search score over 0.6.

Additionally, some *macroplastics* were analyzed separately by the FTIR instrument due to too large particle size. Also, overview photos were taken from each sample during pre-treatment (Appendix C2). ALM-PAR #1 and #2 were combined into one single sample (ALM-PAR #1*) before FTIR scan. The mass of the particles was recorded for all samples at location 10B.

Some samples from the NCS (20171124-GRS-2, 20171122-SC3-4, and 20171127-KRT-14) were analyzed with FTIR the 3rd of May 2018. These samples were initially sealed with acryl plates and were uncovered prior analysis. The FTIR instrument analyzed the acrylic material to determine whether there has been contamination to the sample by these plates. As the FTIR reports are massive in size, all reports are provided upon request, including the reference for the acrylic plastic plates.

2.4.6 - Correction of Data

Multiple corrections were made during the study to improve the quality of the final data, involving correction for any remaining organic matter (exponential reduction-model based on chemical digestion), possible foreign contaminants (method blanks), the efficiency of microplastic-sediment separation (recovery test) and the water content in the analysed sediments (dry matter and dry-weight)

Chemical digestion

Some samples which were observed with excessive amounts of organic matter were treated up to six rounds of chemical digestion. However, after repeated attempts to remove all organic matter some plastics, such as fibers which are a bit fragile, may also be removed as well. It is also noteworthy that the chemical process requires amounts of chemicals (20 mL per 0.1 g dry weight) and is a time-consuming process (each step takes 2 hours person time, and overnight to complete).

Some of the samples from Cuba needed additional rounds of digestion compared to the samples from the Norwegian Continental Shelf (NCS). Due to generally higher contents of organic matter, repeated rounds of digesting for these samples resulted in a comprehensive dataset of reduction in mass per round of digestion. This data was used to construct a theoretical model based on a reduction in the sample mass since the last digestion step. Equation 9 shows the basic calculation of reduction in mass. Also, see Appendix-A2-5.

$$m_{reduction}(\%) = \left(1 - \frac{m_{after\ digestion} - m_{prior\ digestion}}{m_{original}} \right) * 100\% \qquad \text{Equation 9}$$

When the mass reduction (dry weight) after a digestion step was less than 4% of the original weight, it was assumed that no substantial mass loss would occur through further digestion. In this case, the weight after digestion would be considered m_{maxMP} (i.e., the maximum MP weight).

From there, the weight of digestible organic matter (m_{OM}) was inferred as

$$m_{OM} = m_{\text{original}} - m_{maxMP}, \qquad \textit{Equation 10}$$

To see how consistent the loss in organic matter was between samples, to extrapolate for other samples, the m_{OM} data was modeled assuming a first-order decay, dependant on the number of digestion steps:

$$m_{OM} = e^{-k(digestion\ step)} \qquad \textit{Equation 11}$$

Or

$$\ln(m_{OM}) = -k(digestion\ step) \qquad \textit{Equation 12}$$

This was calculated by taking the slope of the linear regression of $\ln(m_{OM})$ vs. the digestion step for all samples in which there was an $m_{reduction}$ of 4 (5 samples, namely 10A, 10B-1, 10C, ALM-BOS, ALM-PAR2). The resulting correlation coeffients (r^2) ranged from 0.90 to 1.0, with the average k being 0.80 ± 0.18. This k value was used to extrapolated $m_{maxMP,}$. The final measured and extrapolated m_{MaxMP} is found in Table 9. Note the general good comparison between measured and extrapolated m_{MaxMP}, when measured data was available.

Table 9: List of measured and extrapolated values for mg MP max/kg dry sediment before any further corrections were made to final MP max.

Sample ID	m original	m MPmax (measured)	m MP max (extrapolated)	final m max MP
LOC-10A	0.017421	0.0117	0.0122	0.012
LOC-10B-1	0.104506	0.1554	0.1559	0.16
LOC-10B-2	0.082759	unknown	0.0894	0.089
LOC-10B-3	0.144813	unknown	0.1104	0.11
LOC-10C	0.027515	0.0205	0.0198	0.020
ALM-BOS	0.368444	0.1611	0.1535	0.16
ALM-PAR #1	1.048535	unknown	0.5521	0.55
ALM-PAR #2	0.668866	0.3458	0.3864	0.35
LOC-1	0.379256	unknown	1.1348	1.13

Any foreign contaminants were corrected for merely by subtracting each filtered sample by the average of all method blanks (n=13)(Equation 13). Such correction was done twice if a sample had mass divided over two steel-mesh filters during the filtration procedure.

$$m_{microplastic\ (corrected)} = m_{microplastic} - \frac{\sum m_{method\ blanks}}{n_{total}}$$ *Equation 13*

where $m_{microplastic}$ is the weight of the sample, $m_{method\ blanks}$ is the weight of the method blanks subtracted by the steel wire and the steel filter after digestion and n_{total} is the total number of method blanks.

Recovery blanks

The accuracy of the method was corrected for by dividing the weight of the microplastic by the spiked *recovery rate* (Equation 14):

$$m_{microplastic\ (corrected)} = \frac{m_{microplastic}}{\%\ recovery}$$ *Equation 14*

where $\%_{recovery}$ is the mean recovery rate based on ten recovery blanks spiked with micropowder and microfibers. The mean recovery rate (*the recovery correction factor*) used for correction (n=10) was 79 %.

Dry matter and dry-weight of sediments

Lastly, the dry-weight of sampled sediments were corrected for so that a concentration of microplastic could be defined. Approach for measuring soil water content is described in section 2.3.2. The dry matter of each sediment was calculated using the following formula:

$$\text{Dry Matter (\%)} = \frac{m_{\ dried\ sediment\ (g)}}{m_{\ wet\ sediment\ (g)}} * 100\%$$ *Equation 15*

where $W_{dried\ sediment\ (g)}$ is the weight of the dried sediments subtracted by the weight of the aluminium tray and $W_{wet\ sediment\ (g)}$ is the weight of the wet sediments subtracted by the weight of the aluminium tray. The dry matter percentage (*Equation 15*) was further used in the correction of total dry-weight (*Equation 16*). Total dry-weight also takes the added $ZnCl_2$:$CaCl_2$-solution during sediment preparation into consideration.

$$\text{Dry-weight (g)} = \frac{m_{wet\,sediments\,(g)}}{m_{ZnCl_2:CaCl_2:+sediments}(g)} * m_{sediments\,(g)} * DM_\% \qquad \textit{Equation } 16$$

The concentration of microplastic is corrected for ($C_{microplastic}$) by dividing the mass of each microplastic sample ($m_{microplastic\,(mg)}$) by the corresponding dry-weight. Notice that the dry-weight were expressed as kg.

$$C_{microplastic}\left(\frac{mg}{kg}\right) = \frac{m_{microplastic\,(mg)}}{Dry-weight\,(kg)} \qquad \textit{Equation } 17$$

Maximum microplastic concentration

It is important to point out that all concentrations presented in this thesis are defined as maximum microplastic concentrations (mg MP $_{max}$ concentrations). These concentrations include all matter extracted from sediments which make it through density separation and chemical digestion. Small organic fractions might remain in sample despite numerous rounds of digestion as some organic compounds are resistant to chemical treatment, e.g., coal, shells.

3. Results

3.1 - Case 1: Microplastic in deep-sea sediments from the Norwegian Continental Shelf

In this section the microplastic concentrations from the NCS are presented as mg MP_{max} /kg dry sediment, mg MP_{max} /m², MP_{max} items /kg dry sediments and MP_{max} items /m². There are only a few available data on polymer identifications done by an FTIR instrument in this section. Some results from FTIR analysis are provided with search scores in parentheses, i.e. (0.95) indication an IR spectrum with a match of 95%.

Only short sample names are presented in the figures throughout this section (Figure 21-24). Full sample names are available in the Appendix B1-[1-3].

3.1.1 - Maximum concentration of microplastic per kg dry sediment and m²

The average MP_{max} concentrations of all samples at the NCS were 64 ± 82 mg MP_{max} /kg dry sediment. The different regions; central Northern Sea, northern North Sea, and the Barents Sea had mean values of 88 ± 99, 32 ± 40 and 32 ± 16 mg MP_{max} /kg dry sediment, respectively.

Sample *20171019-ULA-06* (Figure 21) had the highest MP_{max} concentration of all samples containing 410 mg MP_{max} /kg dry sediment. the following samples *20171002-Reg-14*, *20171117-Reg-12*, *20171113-SNB-16R*, *20171117-VI-RB*, and *20171116-Vega-R* had MP_{max} concentrations below the limit of detection (Figure 21).

A duplicate test was conducted for sample *20170926-Reg-06* (Figure 21). The first replicate contained 110 mg $_{max}$ MP/kg dry sediment, and the second 190 mg MP_{max} /kg dry sediment. The standard deviation for these two samples was 56 mg MP_{max} /kg dry sediment or a relative standard deviation of 39 %.

Figure 21: Maximum microplastics (mg) per kg dry sediment for the 35 sampling sites (x-axis) on the Norwegian Continental Shelf. Samples are collected within the three different regions; the central North Sea, the northern North Sea and the Barents Sea. Detailed lists are available in Appendix B1-[1-3].

When doing the extrapolation of the ocean floor based on the available data, the average MP_{max} concentration for all samples (n=35) was 476 ± 650 mg MP $_{max}$ /m^2. Based on their region; the central Northern Sea, the northern North Sea, and the Barents Sea had following MP $_{max}$ concentrations 704 ± 773, 208 ± 241 and 97 ± 33 mg MP $_{max}$ / m^2. These concentrations ranged from <LOD to 3200 mg MP $_{max}$ / m^2 (Figure 22).

The extrapolation of mg MP max/m^2 (Figure 22) followed the same trend as the data in Figure 21 as they are interconnected by the unit *mg MP $_{max}$*.Figure 21 Sample *20171019-ULA-06* had the highest concentration (3 200 mg MP $_{max}$ /m^{2,}), and samples *20171002-Reg-14, 20171117-Reg-12, 20171113-SNB-16R, 20171117-VI-RB,* and *20171116-Vega-R* were below the limit of detection (Figure 22).
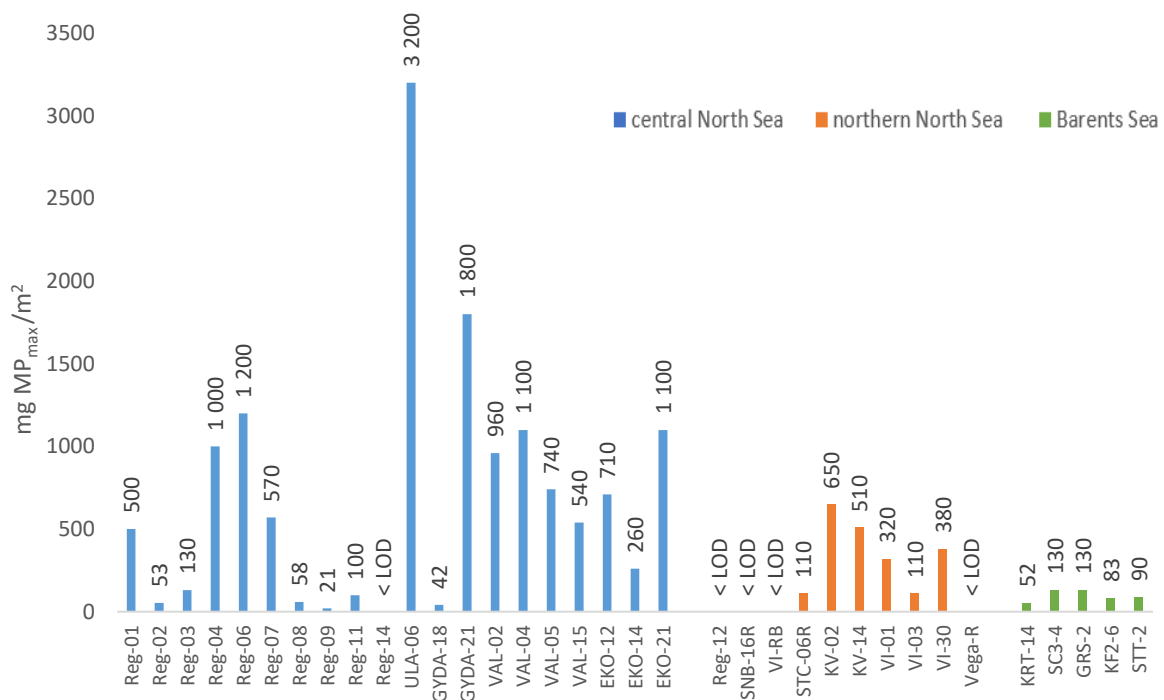
Figure 22: Maximum microplastics (mg) corrected for 1/m^2 for the 35 sampling sites (x-axis) on the Norwegian Continental Shelf. Samples are collected within the three different regions; the central North Sea, the northern North Sea and the Barents Sea. Detailed lists are available in Appendix B1-[1-3].

3.1.2 - FTIR analysis

Sediment samples collected from the deepest stations on the Norwegian Continental Shelf (20171124-GRS-2, 20171122-SC3-4, and 20171127-KRT-14) were analyzed by the FTIR to confirm the presence of plastic polymers. All samples contained particles identified as synthetic polymers, having *Ethylene-propylene copolymers* and *oxidized polyethylene* present in all samples (min. search score 0.72). Also, the early commercial synthetic polymer *Bakelite* was identified in samples 20171124-GRS-2 and 20171122-SC3-4 (average search score = 0.71).

No traces of the acrylic plates (*poly-methyl methacrylate*) were detected when performing an FTIR analysis of the method blanks, but two non-plastic particles were detected with low spectral matches.

3.1.3 - Visual analysis and the estimated number of MP $_{max}$ items/ kg dry sediment and m^2

The average number of particles per mg/kg for the following samples: *20171117-VI-RB* (NNC), *20171127-KRT-14* (BS), *20171117-Reg-09* (CNS) and *20171103-GYDA-18* (CNS) was 76326 (± 56340, RSD = 74%), also known as the extrapolation factor (Appendix D1-2). The average number of particles per visually analyzed sample was 141 + 72 MP $_{max}$ items (n=9). Unfortunately, only the four samples *20171117-VI-RB*, *20171127-KRT-14*, *20171117-Reg-09*, and *20171103-GYDA-18* had mg MP above the limit of detection.

The average extrapolated value for the entire Norwegian Continental Shelf was 4880 ± 6152 MP $_{max}$ items /kg dry sediment. These values ranged from 180 to 31000 MP $_{max}$ items /kg dry sediment (Figure 23).

Based on items/kg within each region; the central North Sea, the northern North Sea, and the Barents Sea had 6707 ± 7432, 2464 ± 2891 and 2406 ± 1269 MP $_{max}$ items /kg dry sediment.

When doing visual analysis, many transparent particles were passively observed. No effort was put in counting these particles as they were *too many to count* (TMTC). See Appendix C1-3, C1-5, C1-6, and C1-7. See also Appendix D1.

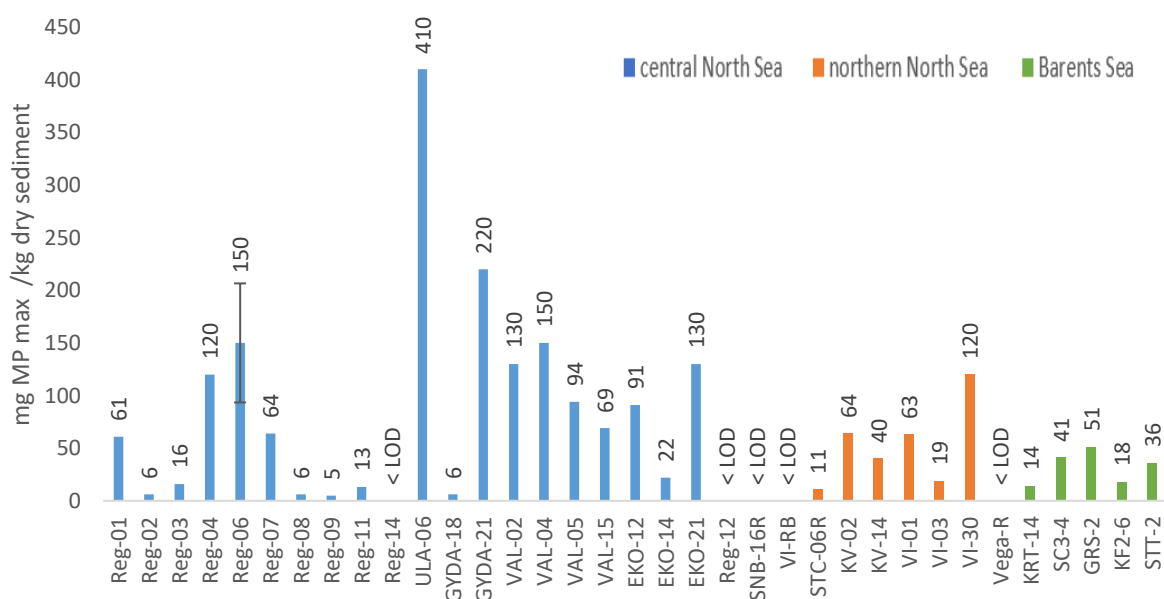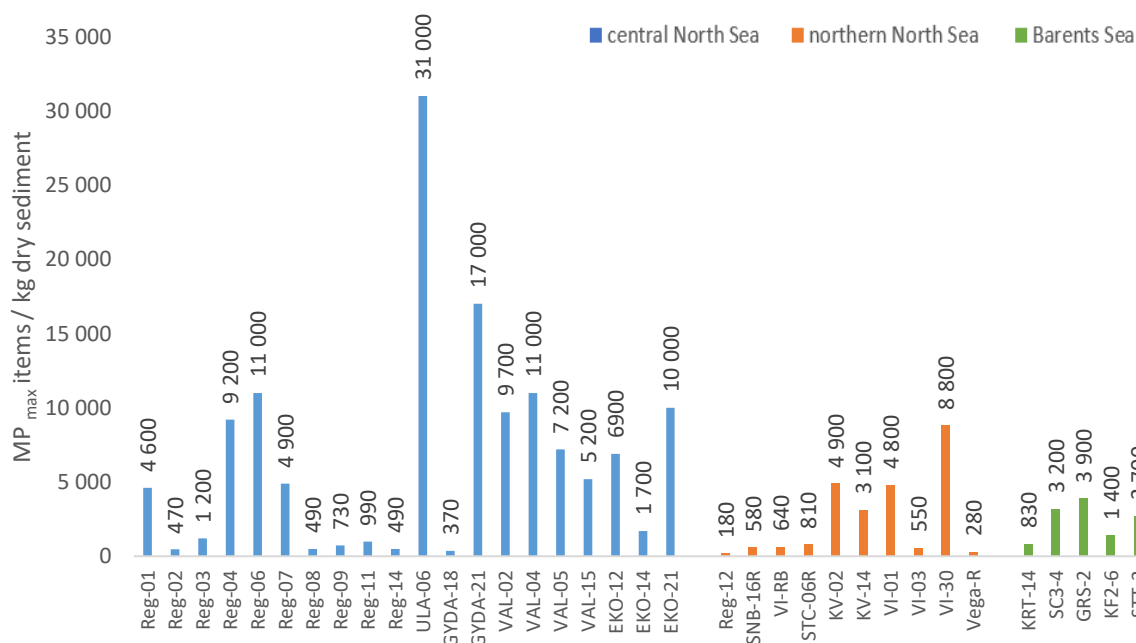*Figure 23: Estimated microplastic particles (MP $_{max}$ Items) per kg dry sediment for the 35 sampling sites (x-axis) on the Norwegian Continental Shelf. Samples are collected within the three different regions; the central North Sea, the northern North Sea and the Barents Sea. Detailed lists are available in Appendix B1-[1-3].*

Regarding the number of MP $_{max}$ items per m^2, the average value for all locations (n=35) was 36650 ± 49980 MP $_{max}$ items /m^2. Based on the regions; 81280 ± 89108, 15938 ± 18354 and 7140 ± 2809 MP $_{max}$ items /m^2 for the central North Sea, northern North Sea, and the Barents Sea. The concentrations ranged from 700 - 370 000 MP $_{max}$ items /m^2 (Figure 24).

Based on each sampling location, the Central North Sea region experienced the highest abundance of maximum microplastic items, MP$_{max}$ items / m^2 (Figure 24).
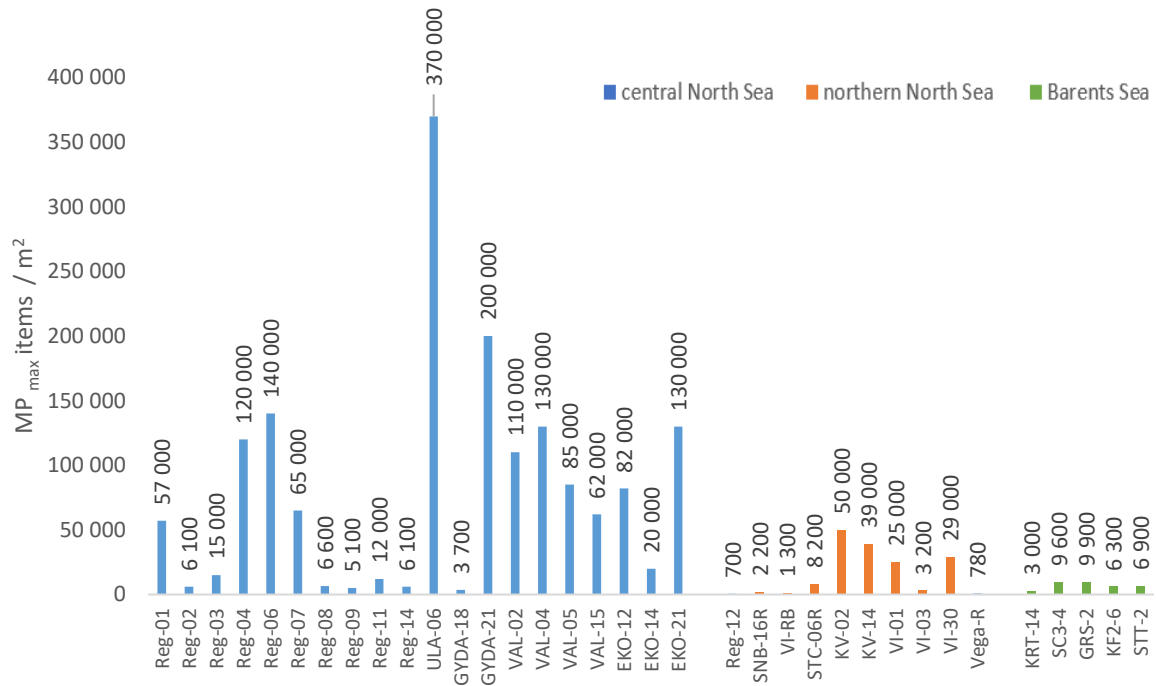
Figure 24: Estimated microplastic particles (MP $_{max}$ Items) per m^2 for the 35 sampling sites (x-axis) on the Norwegian Continental Shelf. Samples are collected within the three different regions; the central North Sea, the northern North Sea and the Barents Sea. Detailed lists are available in Appendix B1-[1-3].

Detailed sketches and particle count logs concerning the systematic counting of particles are presented in Appendix D1.

3.1.4 - Sediment characterization

The average dry matter (%) for all samples from the NCS was 67 ± 14%. Based on region, the central North Sea, northern North Sea, and the Barents Sea had a dry matter content of 76 ± 6, 61 ± 13 and 44 ± 6 %. Highest was *20171002-Reg-14* (CNS) with 80% dry matter content, and lowest was sample *20171116-Vega-R* (NNS) with only 36% dry matter content.

The average weight of dry sediments was 466 ± 206 g for the whole NCS (n=35). The average weight of dry sediments for the central North Sea, the northern North Sea and the Barents Sea region was 605 ± 134, 315 ± 138 and 215 ± 31 g, respectively.

See Appendix-A1-2 for dry matter (%) and Appendix A1-3 for total dry weights.

3.2 - Case 2: Microplastic in river sediments from Rio Almendares (Cuba)

In this section, the microplastic concentrations from the Rio Almendares are presented in mg $_{max}$ MP/kg dry sediment (Figure 25) and MP $_{max}$ items/kg (Figure 27). The polymer distribution based on the locations are also presented in this section (Figure 26).

Some results from the FTIR analysis are provided with search scores in parentheses.

3.2.1 - Maximum concentration of microplastic per kg dry sediment

The average MP $_{max}$ concentration for all eight sediments collected from Rio Almendares (Cuba) was 4429 ± 5327 mg MP $_{max}$ /kg dry sediment. Sample 20170806-LOC-1 had the most sample by weight (Figure 24). Overview photos taken when opening the sample reveal that most of the sample by mass are chunky black particles (Appendix-C2-1).

The mean concentration for all sediment collected at locations 10 (n=5) was 1675 ± 1720 mg MP $_{max}$/kg, while the set of triplicates representing the *river outlet* (LOC-10B) gave an average concentration of 1235 ± 316 mg MP $_{max}$ /kg dry sediment (Figure 25). These samples had a relative standard deviation of 26%. Sample *20170803-LOC-10A* had the lowest mg maximum microplastics concentration per kilo of dry sediments, while *20170803-LOC-10C* had the highest MP$_{max}$ concentration (Figure 25). There is a possibility that sample *20170803-LOC-10C* are overestimated regarding microplastics present in the sample as it only represents 5.2 g of dry sediment sample (Appendix A2-3). The concentration could become misleading as the mass per kg would increase by a factor of x200 when correcting for the soil moisture content (Appendix A2-5).

The two samples collected in the urban residential and recreational areas (sample *20170806-ALM-PAR* and *20170806-ALM-BOS)* had an average concentration of 6897 ± 7669 mg MP $_{max}$ / kg dry sediment. Sample *20170806-ALM-PAR* had the most sample material by weight, but after a quick visual inspection, a minimum of 0.8897 g of the total sample material was made up of seashells.
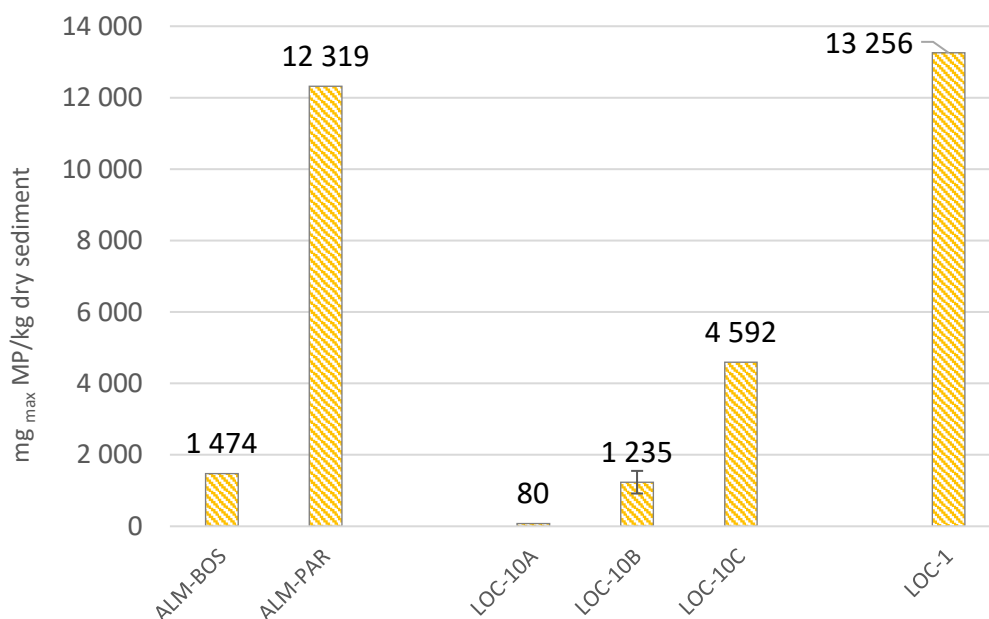
Figure 25: The average concentrations expressed as maximum microplastics per kilo dry sediment in Rio Almendares, Havana. Location ALM-PAR and ALM-BOS were sampled on-land, LOC-1 at the cruise terminal and LOC-10 at the outlet of the river. See Appendix B2-1.

3.2.2 - FTIR Analysis and extrapolation of microplastic items per kilo dry sediment

Anthropogenic particles (rubber, paint, plastic, and petro-pyro) were dominant in all samples (n=8), making up 69 ± 14 % of total identified particles (Appendix D2-3). This was also the case for plastic polymers, accounting for 25 % of total identified particles in all samples. The six most abundant polymer types were polyethylene (PE, 20 %), followed by polypropylene (PP, 19%), polystyrene (PS, 13 %), polyvinyl chloride (PVC, 10 %), polyethylene terephthalate (PET, 4 %) and polyurethane (PUR, 4 %) (Appendix D2-1). PP was found in 7 out of 8 samples (not *20170806-LOC-10C*), while PS was detected in 6 out of 8 samples. PE was present in all samples except for *20170806-LOC-1*. Low-density particles (PE and PP) were present in every investigated location and added up to 24% of all identified polymer types. Polytetrafluoroethylene (PTFE) was only present in one sample (*20170806-ALM-BOS*). Sample *20170806-ALM-PAR* had the highest number of detected polymers (19%) opposed to sample *20170803-LOC-10A* which had the lowest amount of identified plastic particles (5%) (Appendix D2-2 and D2-3).

A wide range of polymer-derived particles (*various*) was also observed (Appendix-D2-1). Copolymers, additives, adhesives, and plasticizers (*various*) were detected in 6 out of 8 samples accounting for 13 % of all plastics. Sample *20170803-LOC-10B1* had the highest number of particles in the category, including the chemical substance *dibutylphthalate* which is a conventional plasticizer.

The distribution of anthropogenic particles among some locations varied significantly (Figure 26). Sample *20170806-LOC-1* were uniquely dominated by *petro-pyro* particles, sharing a resemblance to coal and crystalized tar (Appendix C2-1). The FTIR analysis reveals that sample *20170806-LOC-1* were dominated by "HYDROCARBON RESIN, MAINLY AROM. FILM//CSI" (search score 0.8). These particles were also identified in all samples at location 10B but to a much lesser degree (Appendix C2-3, C2-4, and C2-5).

The set of triplicate samples for location LOC10-B (*river outlet*) were all analyzed using an FTIR, having an average plastic fraction of 32 ± 3% (Figure 26). The average fraction of plastic particles per sample for the *upstream river sediments* (n=2) was 55 ± 6 %.

Lastly, the category *organic* adds up to 30% of total identified markers. Sample *20170806-LOC-1* had the highest number of particles identified as organic, while 20170803-LOC-10C had none markers identified as *organic*. Markers identified as *air* (Figure 26), was identified as N_2O-gas, H_2-gas, CO_2-gas, etc.
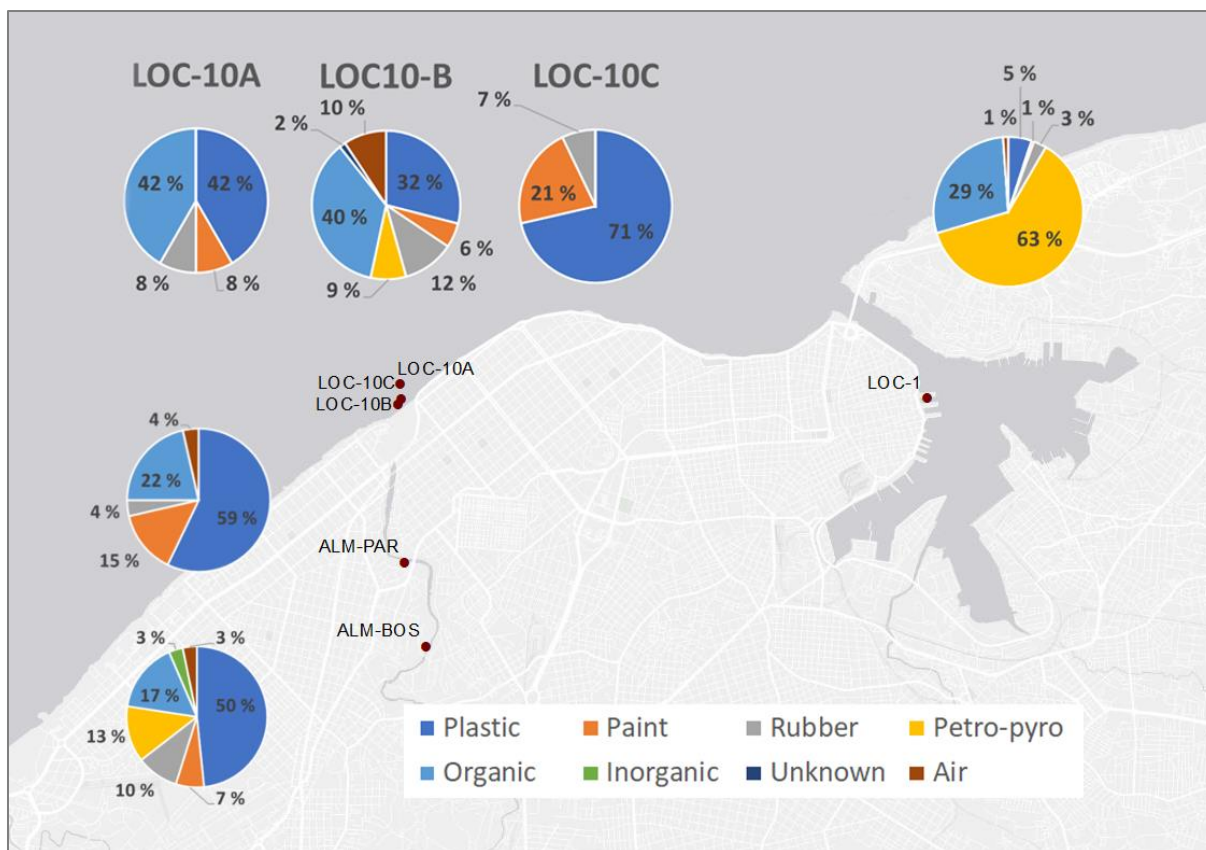
Figure 26: The % distribution of identified particles (>0.6) in samples from the different sampling sites, Havana (Cuba).

A few macroplastics were found in samples *20170806-LOC-1 and 20170806-ALM-PAR*. A single seemingly unfractioned pellet (3.2 (h) x 2.2 millimeters (Ø)) was found in *20170806-LOC-1*(Appendix C2-1), and the FTIR scan indicated that this was a PS particle (0.95). An elastic rubber-looking granulate 15 (l) x 5.5 (w) x 2.5 (h) millimetres was detected in sample *20170806-ALM-PAR* (see Appendix C2-7). This particle was identified as a plasticizer (0.70). Also, samples *20170806-ALM-BOS* and *20170806-ALM-PAR* experienced high concentrations of seashell ranging from 1 mm – 10 mm. See Appendix C2-7 and C2-8. Since there currently is no protocol for such circumstances, the final results were not corrected for larger objects inferred to be non-plastic objects.

The average estimate of plastic items per kg dry sediments was 8523 ± 13029 for the selected samples (n=5). The mean concentration for the set of triplicates (*river outlet sediments* or LOC-10B*)* was 2750 ± 1019 MP $_{max}$ items/kg dry sediment (Figure 27), having a relative standard deviation of 37%. The *upstream sediments* (ALM-PAR and ALM-BOS) had a mean concentration of 17182 ± 20663 MP $_{max}$ items/kg dry sediment (Figure 27). See Appendix D2-2 for more details.
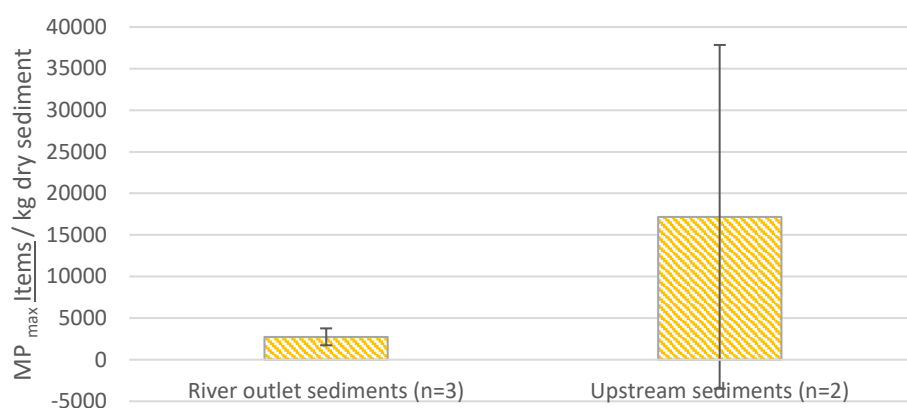
Figure 27: Estimated microplastic particles (items) per kg dry sediment for the river outlet (LOC10B[1-3] and the upstream sediments (ALM-PAR and ALM-BOS). The following categories paint, rubber or petro-pyro are not included in these estimates. Details are provided in Appendix D2-2.

3.2.3 - Sediment characterization

The dry matter percentage for all sediment samples was 56 ± 15 %, ranging from 37% (LOC-1) to 85% (LOC10B-1) (Appendix A2-2). Average dry matter for samples at location 10 (n=5) was 60 ± 22%, while the triplicate samples for location 10B gave a dry matter content of 54 (± 0.23) %. Inland samples (ALM-BOS and ALM-PAR) had a higher mean dry matter content (61 ± 14 %) than the outlet of the river (58 ± 16 %).

The mean total dry-weight of sediments from all sampled locations was 110 ± 48 g. Sediments extracted from location 10C were originally a small sample, as only 5.44 g of dry sample was left for MP analysis after correcting for dry weight. See Appendix A2-2 and A2-3 for more details concerning total sediments and dry matter contents.

3.3 - Quality control

3.3.1 - Method blanks

All collected method blanks in this study had impurities detectable by weight prior chemical digestion. These impurities were significantly reduced by chemical treatment, as samples *20171019-Blank (NCS)*, *20180201-Blank (RA)* and *20180131-Blank (RA)* had their impurities reduced by more than 100% (Table 10). Such reduction in mass could be caused by corrosion (Figure 28-D) or uncertainty related to the scale. Blank *20171123-Blank* were not weighed due to human error but was instead counted as part of the visual analysis (Table 10).

The limit of detection (LOD) and limit of quantification (LOQ) are were calculated as three times the standard deviation and ten times the standard deviation respectively. The LOD was set to be 0.001 g, being the average weight of the impurities (m $_{impurities}$) of the 13 Method blanks. The limit of quantification was set to three times the LOD.

Even after digestion $ZnCl_2:CaCl_2$-crystals were observed during visual analysis and particle count (Figure 28-C). Also, white granulates and fibers particles were observed in almost all samples. Blue fibers (Figure 28-A) were detected in 6 out of 8 method blanks (Appendix D1-1). These are assumed to originate from the blue cotton lab coats worn during analysis.

Three circular mesh filter (Ø=13 mm) were also controlled for foreign contaminations. These filters, acting as method blanks were analyzed by FTIR finding only two non-plastic particles divided over the three filters.

Table 10: List of all method blanks with the corresponding weight of "impurities" before and after digestion. Method blanks from case 1 are listed as "NCS" and blanks from case 2 as "RA". See below the table for details.

Method Blank-ID	Density of $ZnCl_2:CaCl_2$ (g/mL)	Weight of collected impurities		Reduction
		Before chemical digestion (g)	After chemical digestion (g)	
20170922-Blank 1 (NCS)	1.54	0.0059	0.0001	98 %
20170922-Blank 2 (NCS)	1.57	0.0023	0.0003	87 %
20170922-Blank 3 (NCS)	1.55	0.0046	0.0015	67 %
20171019-Blank (NCS)	1.51	0.0126	-0.0002	102 %
20171109-Blank 5:1 (NCS)	1.51	0.0196	0.0026	87 %
20171123-Blank (NCS)*	1.50	-	-	-
20171121-Blank (NCS)	1.48	0.0119	0.0005	96 %
20171129-Blank 1 (NCS)	1.47	0.0038	0.0008	79 %
20171129-Blank 2 (NCS)	1.52	0.0027	0.0001	96 %
20171206-Test 1 (NCS)	1.53	0.0108	0.0013	88 %
20171213-Test 2 (NCS)	1.51	0.0136	0.0031	77 %
20180131-Blank (RA)	1.51	0.0003	-0.0006	300 %
20180201-Blank (RA)	1.50	0.0002	-0.0005	350 %
MEAN ± SD	1.52 ± 0.03	0.0074 ± 0.0062	0.0008 ± 0.0012	-

*No weights available. Only visual analysis.
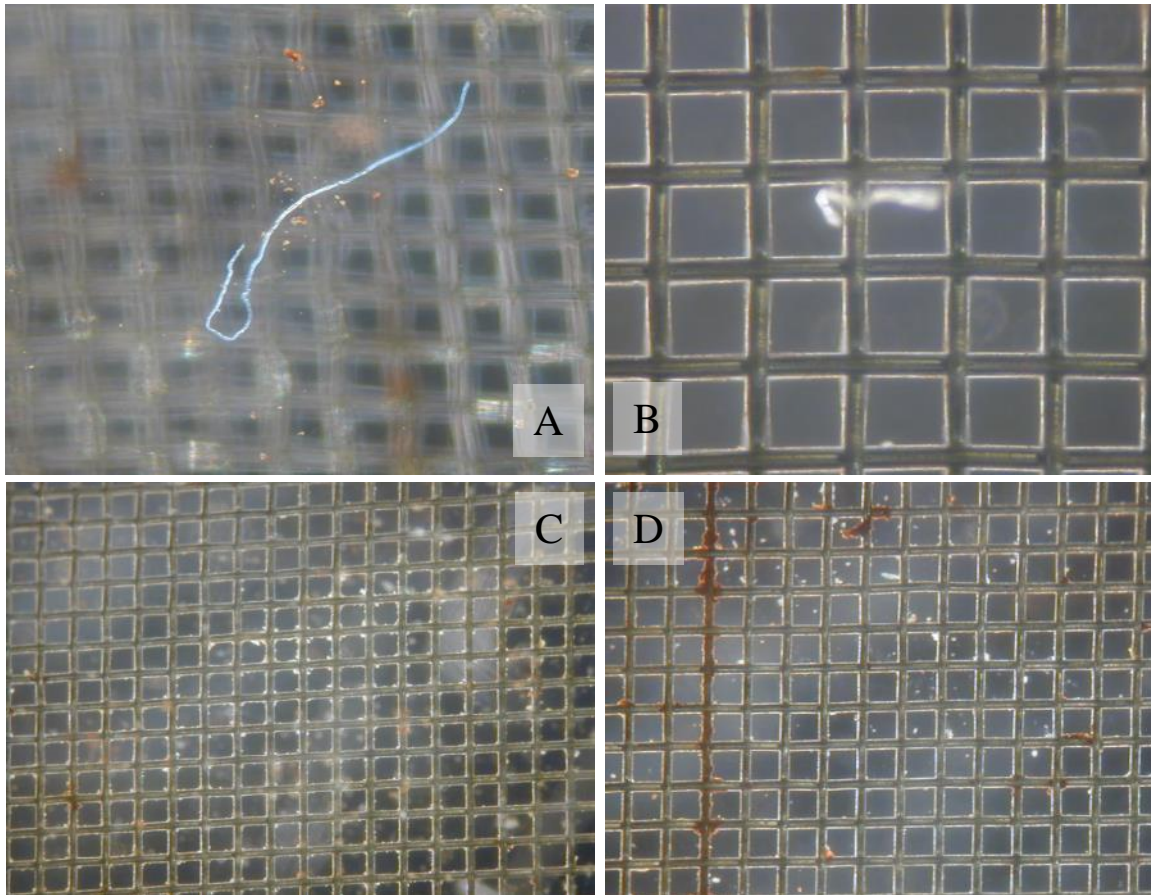
Figure 28: Pictures taken while conducting a visual analysis of method blanks. All photos show impurities on method blanks: Blue fiber (A), unknown white fiber (B) $ZnCl_2$:$CaCl_2$ formation (C) and rust formation (D). Pore-size = 45µm.

3.3.2 - Recovery blanks

In total ten recovery blanks were collected from spiking of eight sediments. Samples *20171005-Reg-09-Blank* and *20171009-Reg-01-Blank* were spiked with both fibers and pellets, all having high recovery rates. The mean recovery rate for all spiked samples was 83 ± 18 %. The BMSS had recovery rates of 92 ± 6 % for LDPE microfibers, 65 ± 16 % for PET micropowder and 100 % for PET granulates (Table 11Table 11).

The PET pellets had a 100 % recovery (n=2). However, the average recovery rates for PET pellets were not included in the correction factor, but rather to illustrate recovery rates on larger PET microplastics. Sediments spiked with microplastic powder showed significantly lower recovery rates than fiber, having a higher standard deviation yet the same number of blanks (n=5).

The "low" average recovery rates were interconnected with the number of steps in the method, reflecting the potential of losing or gaining sample whenever handling the sample material. One of many steps during the approach that is sensitive to loss of sample is: improper separation from sediment, remaining microplastic left in the BMSS or loss of material during filtration, digestion, and drying.

Table 11: Complete list of recovery blanks conducted throughout the study. Recovery blanks from case 1 are listed as "NCS" and blanks from case 2 as "RA". Further details concerning the table are provided below the table.

Recovery Blank - ID	Density of $ZnCl_2:CaCL_2$ (g/mL)	Recovery rate after digestion (%)		
		PET powder	PE fiber	PET pellets
20171002-R1-11-Blank (NCS)	1.51	43		
20171004-Reg-03-Blank (NCS)	1.51	70		
20171005-Reg-09-Blank (NCS)	1.51		95	100
20171009-Reg-01-Blank (NCS)	1.52		97	100
20171114-SNB-16R-Blank 1* (NCS)	1.55		83	
20171114-SNB-16R-Blank 2* (NCS)	1.57	56		
20171130-KRT-14-Blank 1** (NCS)	1.48		89	
20171130-KRT-14-Blank 2** (NCS)	1.47	84		
20180202-LOC-10-B3 (RA)	1.51	74		
20180208-LOC-10-B1 (RA)	1.49		99	
Mean ± SD	1.51 ± 0.03	65 ± 16	92 ± 6	100 ± 0

* - Blanks from sample "20171113-**SNB-16R**#1" and "20171113-**SNB-16R**#2" are based on a set of replicates.
** - Recovered sediments from sample 20171127-KRT-14 were split into two separate blanks.

3.3.3 - Density of $ZnCl_2:CaCl_2$-solution

The properties of the brine solution remained constant throughout the study (Table 12). Also, for detailed lists see Appendix A3-3 to A3-6.

Table 12: Overview of all samples with their respective mean density. The table is sorted based on the type of sample.

Samples from	Mean densities	Deviations	(n =)
NCS	1.531	0.020	35
RA	1.501	0.007	8
Method blanks	1.520	0.030	13
Recovery blanks	1.511	0.030	10
Mean	1.516	0.022	

4. Discussion

This study brings forth new findings regarding microplastic contaminations in deep-sea sediments on the Norwegian Continental Shelf and in river sediments from the assumed microplastic hotspot, the Rio Almendares, Cuba. Herein the results will be discussed in terms of how they addressed the hypotheses of the study.

4.1 - Addressing the study's hypotheses

"Microplastics are present in all investigated location; at the Norwegian Continental Shelf and in Cuba (Rio Almendares)."

In total, sediments from 43 samples were density separated, purified, quantified and finally identified for microplastics using visual or FTIR analysis. Only 11 out of 43 samples were analyzed by an FTIR instrument to hold synthetic polymers, with the remaining to be done at a later time. Eight of these samples were from the study in Havana, and three samples from the Norwegian Continental Shelf. However, all samples (n=11) that *were* analyzed by an FTIR instrument contained microplastics. Multiple low-density plastic particles (PE, PP) were present in the analyzed sediments, including at 508 meters depth on the Norwegian Continental Shelf. High-density plastics like PET and PVC, on the other hand, were only present in four out of eight samples. A possible explanation for the relatively higher abundance of low-density microplastics could be linked to weathering processes occurring in the marine environment. Previous studies have shown that the accumulation of biofilm or algae accumulation affects the sinking behavior of microplastic, in addition to the effects of UV-light (Andrady, 2011; Singh & Nisha Sharma, 2008; Woodall et al., 2014). Whether the high abundance of low-density particles is related to the polymer composition in the sediments or by segregation of some high-density particles due to a low density of the solution remain an open question.

Eight out of 35 samples from the Norwegian Continental Shelf were visually analyzed using only an optical microscope, systematic identification protocol (FTIR), and human intuitions. In total, 24 samples from the Norwegian Continental Shelf remains unidentified, with no visual or FTIR analysis, though visual microscopic images were taken of these samples (and many suspected plastics are seen within these images). Therefore, to improve all estimates regarding microplastics concentrations on the Norwegian Continental Shelf, it is suggested to do a comprehensive FTIR analysis of the remaining samples. Complete mapping of polymer distribution over the whole region could help in understanding the potential mechanisms that influence the transport of plastic particles in deep waters, especially the distribution of high-density and low-density particles at greater depths. Finding reliable *microplastic hotspots* on the Norwegian Continental Shelf could also reveal what effects the ocean currents might have on microplastic transport and deposition. How these might change over time (stratification or temporal analysis) would be the ultimate goal to investigate.

"Microplastic concentrations found at the Norwegian Continental Shelf are higher in the shallower parts of the oceans compared to greater depths."

In general, the central North Sea has the lowest average sampling depth (71 meters) followed by the northern North Sea (294 meters) and the Barents Sea (380 meters), based on the samples collected. One could roughly say that the sampling depths increase as one go north. According to the data, the central North Sea region had the leading five samples with the highest microplastic concentrations, regardless of the estimated units (Figure 21-24). The central North Sea had twice the average concentrations compared to the northern North Sea and the Barents Sea. Also, the central North Sea had only one sample with concentrations lower than the limit of detection, as for the northern North Sea had four out of 10 samples under the limit of detection. It is doubtful that samples below the limit of detection contain a higher number of plastic particles per sample, compared to the other samples with higher mass. Small black particles (here believed to be coal) should be just as sensitive to water movements as microplastics, meaning that the sediment samples rich in the sample material (e.g., ULA-06) are either more exposed to anthropogenic pollutions, or the water conditions allow a higher rate of sedimentation. These terms are perhaps not equal, but somehow relevant. Also, whether or not the occurrence of the small coal particles (<5 mm) in the top 1 cm of the sediments is natural is worth giving some thoughts.

Though, as these observations are based on maximum possible concentrations for microplastic without any representative FTIR identification (or other form identification) to confirm the identities and the total particle distribution in the sample material, there is not enough evidence to confirm that there are higher concentrations of microplastic in the shallower parts of the Norwegian Continental Shelf compared to the deeper parts. However, samples from the three deepest parts of the Norwegian Continental Shelf (GRS-2, SC3-4, and KRT-14) were all analyzed and proven by an FTIR to contain ethylene/propylene copolymers, meaning that the most remote sediments collected from the Norwegian Continental Shelf are verified to hold microplastics.

Another interesting polymer detected in sediments from the Norwegian Continental Shelf was Bakelite, a formerly mass-produced synthetic polymer first used in the early 20th century. This particle could potentially originate all the way back to 1910 (Britannica, 2009). Regardless of its age, the presence of Bakelite is proof of incomplete mineralization due to the excellent chemical resistance of the polymer material.

If it is assumed that the mg MP $_{max}$ / kg dry sediment *is* the actual concentrations of microplastic in the samples from Cuba, then, the samples representing the *upstream river sediments* (n=2) would have a higher average microplastic concentration per kg dry sediment compared to the *river outlet* (n=5). This would conflict with the current hypothesis. When estimating the maximum number of microplastic items per kilo dry sediment for the set of triplicates from LOC-10B (*the outlet sediments*), the data reflect a relatively good precision for the current locations, and could be suited to represent the *river outlet* (1235 ± 316 mg $_{MP\ max}$ /kg, 2750 ± 1019 items $_{MP\ max}$ / kg dry sediment and 32 ± 3 % plastic). The mean number of items also appears to be realistic compared to other studies, e.g., Bergmann et al. (2017); Vianello et al. (2013). On the other hand; the two samples representing *the upstream river sediments* shares very few correlations besides having similar polymer distribution by percentage. The samples collected upstream the river is few (n=2) and varies considerably within the localities (17182 ± 20663 items $_{MP\ max}$).

Once again, it is essential to acknowledge that not all sample material consists of microplastics. For instance, seashells were observed in sample *20170206-ALM-PAR,* and by collecting and weighing this macro debris, the following objects would add up a minimum of 0.8897 g of the total sample material. Encounters with larger seashells are somewhat new to this approach having no developed protocol for removing larger macro-objects. The most favorable approach would be to develop a protocol to correcting for larger macro-objects which are identified non-plastics.

However, all sediment samples collected in, and at the outlet of the river were verified to contain microplastic by the FTIR. Neither the microplastic distribution (being independent of concentration by weight) did find any significant difference in the two different river sediments as there were too few observations. If luggage capacity were not an issue, bringing more sediments from Cuba would be highly beneficial. Additional samples from multiple locations upstream the Rio Almendares are necessary to determine any significant difference in microplastic abundance in the river system. Based on the present data, it appears that microplastic concentration in the river and outlet are quite heterogeneous.

4.2 - Literature comparison and review

Microplastic concentrations are generally higher in this study compared to similar studies (Table 13). The only studies using a similar method was conducted by Mahat (2017) and Bergmann et al. (2017). Mahat (2017) used an analytical approach identical to this study, including the same procedure for sediment preparation, sample filtrations, and chemical digestion. However, Mahat (2017) lacks estimates for items/kg and items/m^2. Bergmann et al. (2017) also used a high-density solution (ZnCl) for separations, capable of separation plastic polymers with a higher density than this study.

Most studies focus on the number of plastic items (Table 13), either as per kg dry sediment or m^2. Concentrations in forms of mg/kg are rarely presented, and if so, they are generally lower than data presented here. Variations in concentrations amongst the specified studies can be explained by spatial variations (both local and regional), but the deviation between analytical approaches could also describe some of these dissimilarities. For instance, the particle size range varies considerably (Table 13). The lower limit for microplastic quantifications varies from 0.7 up to 300 µm. By using a Raman microspectroscopy, Imhof et al. (2016) found a substantial increase in the occurrence of microplastic when analyzing particles below 500 µm. Bergmann et al. (2017) detected considerable amounts of microplastic particles smaller than 25 µm while using a µFTIR instrument. Studies using 300 µm as the lower size limit are possibly losing significant amounts of microplastics before analysis.

Also, by using an alternative brine solution (NaCl or NaI) with a lower overall density would not only limit the recovery rate but also neglect certain polymer types (e.g., PVC, PET, Polyamide) from being density separated. As PVS and PET, being naturally high-dense particles, account for 17 % of all produced plastics globally, segregation of these particles would give a significant underestimate of the actual amounts of polymers present in sediments (PlasticsEurope, 2017). This would naturally yield much lower microplastic concentrations in sediments by using density separation.

There are to date very few microplastic studies conducted on deep-sea sediments. Van Cauwenberghe et al. (2013) presented in their study only a simple estimate of microplastic concentrations (items/m^2), as they were mainly focusing on uncovering the presence and size distribution of microplastics in ocean depths down to 4843 meters. Woodall et al. (2014) investigated deep-sea sediments from the Atlantic Ocean, the Mediterranean Sea and the Indian Ocean at 300-2200 meters depths, only to present their data in items/l. Jensen and Cramer (2017) looked at microplastic concentrations in deep-sea sediment down to 1963 meters depths along the coast of Norway. However, only two of 10 samples were confirmed by using a Raman spectroscopy to contain microplastics, whereas the remaining samples were only visual analyzed using the same MERI protocol as this thesis. Also, this study only provides items/kg.

Bergmann et al. (2017) investigated deep-sea sediments at the HAUSGARTEN area for microplastics providing estimates for items per kg dry sediments and m^2. Both estimates (items/kg dry and items/m^2) associated with the NCS samples were slightly higher compared to the estimates from Bergmann et al. (2017), but many samples had concentrations within the same magnitude of 1. Beside from doing *undisturbed sampling*, Bergmann et al. (2017) had similar strategies when it comes to filtration, digestion and FTIR identification. Especially the results from the FTIR identifications are worthy of comparison, looking at polymer composition in all analyzed samples. For instance, this thesis identified 12 plastic particles per 148 markers

(8.1%) on average (RA), whereas Bergmann et al. (2017) identified 31 out of 177 (17.5%) particles as plastic polymers. Bergmann et al. (2017) did also experience local variations in concentrations among samples, ranging from 41 to 6594 items (>500 µm) per kg. Also, numerous black particles were commonly characterized as coals in multiple locations. These particles were represented in samples with high abundance of microplastic per kg just like some samples in this thesis.

Table 13: List of relevant studies including particle size range, separation technique and concentration range. Modified from Møskeland et al. (2018) (Table 7-7).

Location	Location specification	Particle size range	Separation technique	Measured concentration	Reference
Brazil	Beach	2 – 5 mm	Sieving only	60 items/kg	Santos et al. (2009)
Chile	Beach	1 - 4.75 mm	Sieving only	<1-805 items/m^2	Hidalgo-Ruz and Thiel (2013)
India	Ship-breaking yard	1.6µm – 5 mm	Sieving and density separation: NaCl (30%)	81.4 mg/kg	Reddy et al. (2006)
India	Beach	1 – 5 mm	Sieving then density separation: NaCl (1.40 g /l)	10 – 180 items/m^2	Jayasiri et al. (2013)
Singapore	Mangrove	1.6 µm – 5 mm	Density separation: NaCl (1.18 g/l)	36.8 items/kg	Nor and Obbard (2014)
NW Pacific	Deep sea trench	300 µm – 5 mm	Sieving	60 – 2 020 items/m^2	Fischer et al. (2015)
South Korea	Beach	50 µm – 5 mm	Sieving and density separation: NaCl (2.16 g/cm^{-3})	56 – 285 673 items/m^2	Kim et al. (2015)
Belgium	Continental Shelf	38 µm – 1 mm	Unknown	97.2 items/kg	Claessens et al. (2011)
Italy	Subtidal	0.7 µm – 1 mm	Density: NaCl (1.2 g/mL)	672 – 2 175 items/kg	Vianello et al. (2013)
Worldwide	Deep sea	5 µm – 1 mm	Sieving and density separation: NaI (1.6 g cm^{-3})	50 items/m^2	Van Cauwenberghe et al. (2013)
Slovenia	Beach	0.25 – 5 mm	Density separation (1.2 kg/l) and sieving	177.8 items/kg	Laglbauer et al. (2014)
Arctic	Deep sea	10 µm – 5mm	Density separations: ZnCl (1.7 −1.8 g cm^{-3})	42 - 6 595 items/kg dry 3200 – 247 400 items /m^2	Bergmann et al. (2017)
China	River sediments	100 µm – 5mm	Density separation: NaCl (1.2g/mL)	11 - 234.6 items/kg dry	Su et al. (2016)
Norway	Oslo beach	45 µm – 5 mm plus fibers	Density separation: ZnCl$_2$:CaCl$_2$ (1.57 g/mL)	500 – 9800 mg/kg	Mahat (2017)
Norway	Oslo sediment	45 µm – 5 mm plus fibers	Density separation: ZnCl$_2$:CaCl$_2$ (1.57 g/mL)	20 – 90 mg/kg	Mahat (2017)
Norway	Reference areas in the Norwegian coastal shelf	5 µm -1 mm	Density separation NaI (~1.6 g/mL)	23 – 391 items/kg	Jensen and Cramer (2017) (MAREANO)
Norway	Norwegian Continental Shelf	45 µm – 5 mm plus fibers	Density separation: ZnCl$_2$:CaCl$_2$ (1.53 g/mL)	< LOD – ≤ 410 (60) max mg /kg < LOD – ≤ 3 200 (480) max mg /m^2 ≤ 180 – ≤ 31000 (4 900) max items/kg ≤ 700 – ≤ 250000 (37 000) max items/m^2	Møskeland et al. (2018)/ This thesis
Cuba	River sediment	45 µm – 5 (15) mm plus fibres	Density separation: ZnCl$_2$:CaCl$_2$ (1.51 g/mL)	80 – 15256 (4429) max mg / kg 1 576 – 31 793 (8523) max items/kg	This thesis

4.3 – Method assessment and future implications

Like any other method concerning microplastic research, this approach has limits regarding isolation and quantification of microplastics in benthic sediments. This section will evaluate all parts of the method that needs to be discussed. Some implementations are also described in their respective section. This section also includes suggestions for future studies.

4.3.1 - Sampling, separation and filtration

There are many practical advantages regarding sampling of benthic sediment using a Van Veen Grab. However, the main disadvantage associated with the Van Veen Grab is the extraction of a *disturbed sediment sample*. If undisturbed sampling is obtainable, it is possible to investigate the concentration and stratification of microplastic particles in sediments at various depths. This is of course even more time consuming than just investigating the top layer, thus requires significant optimization of the method. Another critical matter concerning sampling is collecting sufficient amounts of sediments for back-ups and running triplicates. Difficult sampling conditions can be a factor for retrieving few samples. A practical example; Locations 10C (RA) gave off only small amounts of sediments (5.4 g dry sediments) as the heterogeneous conditions at the bottom troubled the sampling process greatly. Sample *20170803-LOC-10A and 20170803-LOC-10C* were neglecting in the estimates (items/kg) in favor of the triplicates. The set of triplicates were considered more valuable due to method precision. Also, finding the optimal amount of sediment to add to the Bauta was a consideration during the research, and the 200 g of wet sediments per sample is considered the optimal ratio per 7 liters of $ZnCl_2$:$CaCl_2$. This is reflected in the deviation among total sediment being added to the Bauta in case 1 (Appendix A1-3). Also, mixing of sediments by a propeller is found to be somewhat unfavorable as mechanical parts are weakened by corrosion and grinding of fine sediments over time, which may lead to leakage and loss of sample. Fine bubble aeration from below is suggested in this study as a future design improvement.

Maintaining the high-density properties in the brine solution is crucial for proper microplastic-sediment separation. The density remained constant throughout this study, being a result of periodic maintenance and disposal when necessary. Theoretically speaking, if the density dropped below 1.4 g/mL, various high-density plastic polymers would not be successfully separated. Bergmann et al. (2017) used a ZnCl solution with a density of 1.7-1.8 g/cm^3, providing enhanced microplastic-sediment separations with respect to certain polymer types. This solution option could be implemented to the method used in this study without too many adjustments.

An experiment involving a shorter version of the glass column named *the baby Bauta* was also tried out. This column is only 30 cm tall and turned out to not provide enough column length for sufficient separation. However, the thought of minimalizing the use of $ZnCl_2$:$CaCl_2$-solution could potentially save considerable amounts of time spent on recycling solution. Such optimization allows more samples to be separated, doing triplicates or depths profiling. If for some reason high volumes of brine solution are necessary for density separation, one should consider automatizing the filtration process as performed by Lorenze (2014).

Lastly, the lower size limit for MP quantifications depends entirely on the mesh filter size. The 45µm steel mesh filters are preferred as they are inexpensive and chemical resistant against the currently practiced chemical digestion. The steel mesh filter has also proven to be suitable for

FTIR analysis when using transmittance beam. However, with new FTIR instrument available smaller pore-sized filters are a natural implementation to consider in the future.

Concerning the method in this thesis, there are some general improvements that could be implemented. The importance of contamination control cannot be emphasized enough. Additionally, airborne contaminants could be further investigated by applying dustboxes as in the study by Bergmann et al. (2017) or damp filter papers.

4.3.2 - Digestion

The chemical digestion used in this study is somewhat unique compared to other studies. The digestion process is proven to be effective, yet a sensitive way to remove labile organic matter (Olsen et al., *In preparation*). 70 % of total sample by weight were removed in sample *20170806-ALM-PAR* (see Appendix A2-5). However, repeatedly steps of digestion were necessary (up to 6 rounds) for satisfactory sample reduction. Today, this process is very time-consuming (one round = two days), but this could potentially be automatized if the method is ever to considered to be used for mass production.

Figure 29: Sample 20170806-ALM-PAR before (left) and after digestion (right). The sample was treated with six rounds of digestion, losing 70 % of the total matter by weight.

As briefly mentioned in section 4.1, a protocol to correct for larger presumably non-plastic objects is the next implementation for future microplastic quantification. Seashell (Chitin) and coal (hydrocarbons) were abundant in most digested sediment samples and persisted in samples even after six rounds of digestion. One could develop specially engineered post-digestion treatments to cope with the resistant organic matter in the sample, or alternatively a careful rinse-and-remove technique. The latter protocol may consist of rinsing the objects carefully in a way that collects microplastics stuck to the objects, and then confirm the identities of the non-plastics using the FTIR. If chemical treatment is considering, the chemical must have no visible influence on the plastic polymers.

4.3.3 - Visual analysis and FTIR

FTIR analysis is superior for polymer identification compared to visual analysis using microscopy. Once again, it is important to point out that no FTIR instruments were available during analysis of case 1. However, the visual analysis was carried out by best effort, and all regions were represented in the counted samples. Nevertheless, manual polymer identification

is an extremely time-consuming and uncertain approach, and not even a highly experienced person is assured to separate all potential microplastic particles from chitin or diatom pieces. Lenz et al. (2015) stated that only 68 % of all visually counted particles were spectroscopically confirmed as plastic polymers using a Ramen micro-spectroscopy. Also, the hot needle test was not possible as acrylic plates were covering the samples. The argument for using acrylic plates was that they were considered more practical beneficial regarding contamination and loss of sample during analysis than doing the hot needle test.

As for case 2, the FTIR provided both qualitative and quantitative data. Method blanks for the FTIR identified no foreign polymers on the recycled steel filters, meaning that the results reflect only the sample material. There are, however, some disagreement among microplastic researchers regarding the lower limit of the search score when using FTIRs. Some studies having set the lower limit to 0.7 (70%) (Bergmann et al., 2017; Scheurer & Bigalke, 2018), while others can accept search hits matching reference spectra more than 60 % (Suaria et al., 2016; Woodall et al., 2014; Yang et al., 2015). However, it is not necessarily a common practiced to specifying the lowest acceptable spectra match. Some studies even avoid pre-existing spectral library intentionally, claiming that "… relying solely on automated library searches and statistical methods can lead to inaccurate identifications" (Jung et al., 2018). The search score in this study was set to 0.6 to maximize the dataset as few particles per sample were analyzed. Instead, markers identified as plastic were exclusively included in the estimation of MP $_{max}$ items /kg dry sediment, meaning all potential plastic components among the anthropogenic sources are left out. This generates an underestimate of particles per kilo of sediment, which is considered a countermeasure for the relatively low search score acceptance.

A general issue for all FTIR instruments is the giving poor discrimination and poor reproducibility of rubber particles deriving from car tires (Sarkissian et al., 2004; Vollertsen, n.d.). The transmittance beam struggles to pass through the non-transparent particles and the overall transmissivity yields low scores. This could be the case for the material in sample 20170806-LOC-1. A Pyrolysis-GCMS analysis of the sample could help answer these questions.

4.3.4 - Quality control
The risk of microplastic contaminations was kept at a minimum by strictly following the protocol. Any chance of accidental contamination were carefully documented and corrected for. To avoid atmospheric contamination, the exposure time was kept to a minimal and any airborne contaminants would be identified on method blanks. For every third sediment sample, there was conducted a method blank. All change in mass, either by collecting impurities or corrosion on the filter, was expressed through the doing of method blanks. Blue fibers were detected when visually inspecting the NCS samples and are likely originating from the lab coat. An FTIR analysis of these fibers would remove any doubt.

Spiking with both PET granulates and micropowders, both with a density = 1.40 g/cm3, was giving the methods recovery rate proper testing. The *BMSS* proves to be an efficient method to separate microplastic from sediment; with a combined recovery rate of 79 % for all spiking materials. However, the micropowders used in the study were significantly harder to completely extract out from the *BMSS* as up to 57 % of the powders could remain in the system (20171002-R1-11-Blank). A small loss of sample material was associated with the glass column and the separations chamber potentially affecting the general recovery rate. This was observed when

spiking sediments with micropowders. By experience, the bottleneck of the glass column is a hotspot for these fine plastic particles unless the neck is properly cleaned. This cleaning, however, can be a bit subtle as plastic brushes must be avoided due to possible contamination.

Recovery rates from other studies vary greatly. Nuelle et al. (2014) had recovery rates between 91 % for PET and 99 % for PE. On the other hand, low dense EPS (expanded polystyrene) foam had a much lower recovery rate of 68 %. Another study (Gray et al., 2018) similar to this study used 165 µm microbeads as spiking material. These researchers achieved a recovery rate of 87 %. However, the spiking material was low-density PE which is significantly easier to separate and extract, thus reflected in the high recovery rate.

The method precision was expressed as a relative standard deviation of 39 % for a set of replicates from Norwegian Continental Shelf, while a set triplicates from the Rio Almendares had a relative standard deviation of 26% by comparison. The difference expressed in the two relative standard deviations could be explained by differences in sediment characteristics, insufficient sample homogenization or the total amount of sediment sample being analyzed for microplastic.

4.3.5 - Future fields of studies

The need for a comprehensive FTIR analysis of the remaining samples from the Norwegian Continental Shelf is mentioned earlier in the discussion. The further investigation should, however, follow the same protocol developed in this study to reduce the chance of incomparability.

What is also earlier mentioned (in section 2.1.2), is the additional types of microplastic samples not yet analyzed due to the limited time provided for this MSc-thesis. In order to understand how microplastics are distributed in the deep-sea sediments, microplastic research conducted in the open surface waters cannot be neglected. Manta net samples containing plastic down to 300 µm was laboriously collected along the coast of Havana, but also a long-distance trawl of 17 kilometers towards the Gulf Stream between Havana and Key West (Florida) was accomplished. While doing the manta net sampling, multiple water samples from different depths using a Nansen bottle were also done. By developing protocols, and proper analyzing all these samples one could potentially gain increased knowledge on the topic of global plastic transportation in the surface regions of the Gulf Stream. By also analyzing the water samples taken from different depths, new evidence could potentially bring new knowledge to microplastic size distribution in the water column expressed as a length gradient moving towards the Gulf Stream.

5. Conclusion

The Bauta Microplastic-Sediment Separator, combined with an FTIR instrument, has proven to be a useful tool in quantifying and identifying microplastics on the Norwegian Continental Shelf and in the river sediments of Rio Almendares. Microplastics were identified in all samples analyzed by the FTIR instrument, with the most common microplastic being the low-density polymer *polyethylene* in its pure state, or in the form of a copolymer. As the total sample material seemingly contained other substances than only microplastics, all specified concentrations in this thesis were defined as *maximum microplastic concentration* (MP_{max}).

On average, the Norwegian Continental Shelf is estimated to hold 64 ± 82 mg MP_{max} per kg of dry sediment (corresponding to $36\,650 \pm 49\,980$ MP_{max} items per m^2 sediment surface). The central North Sea had the highest concentration of MP_{max} /kg dry sediment. Further, the samples with the top five highest concentrations were all found in the central North Sea, representing the shallowest sediments analyzed for microplastics in this thesis. Not all samples from the Norwegian Continental Shelf were analyzed by an FTIR to confirm the polymer identities, as most samples were only visually analyzed. However, sediment from the deepest and most remote sampling stations was verified by an FTIR to contain microplastic. A comprehensive FTIR analysis of the whole Norwegian Continental Shelf using the so-far unidentified samples is suggested.

Sediment samples collected from the *Rio Almendares* contained (on average) 4429 ± 5327 mg MP_{max} /kg dry sediment (corresponding to 8523 ± 13029 MP_{max} items / kg dry sediment). All sediment samples from Rio Almendares held microplastic particles, also here being low-density polymers (PS and PE). The sediments collected upstream the river had the highest average concentrations of MP_{max}, (mg MP_{max}/kg dry sediment, MP_{max} items/kg dry sediment and polymer distribution by percentage) compared to the river outlet sediments. However, no significant spatial trend could be determined within the river system as there were too few observations. Additional sediment sampling from the Rio Almendares is suggested, especially representing the sediments upstream of the river.

The method precision was expressed as a relative standard deviation of 39 % for a set of replicates from Norwegian Continental Shelf, while a set triplicates from the Rio Almendares had a relative standard deviation of 26% by comparison. The difference expressed in the two relative standard deviations could be explained by differences in sediment characteristics, insufficient sample homogenization or the total amount of sediment sample being analyzed for microplastics.

It is acknowledged that the applied method in this study has some uncertainties associated with the final result, not unlike other methods, being a complicated and protracted process prone to human errors and mechanical failure. Also, reliable analytical protocols for microplastic quantification and identification is much needed in the microplastic research communities; as proper contamination controls, and equivalent units of microplastic concentrations seem to vary significantly among studies.

The behavior, and the ultimately fate of microplastics from open waters to the benthic zone has shown to be a very complex process. However, findings of low-density plastic polymers detected all the way down to 508 meters depth are evidence of density modifying processes that transport microplastics downward in the water column. Based on these data, it is

reasonable to suspecting an omnipresence of microplastics on the entire Norwegian Continental Shelf.

References

Alldredge, A. L. & Silver, M. W. (1988). Characteristics, dynamics and significance of marine snow. doi: https://doi.org/10.1016/0079-6611(88)90053-5.

Andrady, A. L. (2011). Microplastics in the marine environment. *Marine Pollution Bulletin*, 62 (8): 1596-1605. doi: https://doi.org/10.1016/j.marpolbul.2011.05.030.

Baztan, J., Bergmann, M., Booth, A., Broglio, E., Carrasco, A., Chouinard, O., Clüsener-Godt, M., Cordier, M., Cózar, A., Devriese, L., et al. (2017). Breaking Down the Plastic Age. 177-181. doi: https://doi.org/10.1016/B978-0-12-812271-6.00170-8.

Bergmann, M., Wirzberger, V., Krumpen, T., Lorenz, C., Primpke, S., Tekman, M. B. & Gerdts, G. (2017). High Quantities of Microplastic in Arctic Deep-Sea Sediments from the HAUSGARTEN Observatory. *Environ Sci Technol*, 51 (19): 11000-11010. doi: https://doi.org/10.1021/acs.est.7b03331.

Britannica, T. E. o. E. (2009). *Bakelite*. Encyclopædia Britannica: Encyclopædia Britannica, inc. Available at: https://www.britannica.com/science/Bakelite (accessed: 12. of May).

Browne, M. A., Crump, P., Niven, S. J., Teuten, E., Tonkin, A., Galloway, T. & Thompson, R. (2011). Accumulation of Microplastic on Shorelines Woldwide: Sources and Sinks. *Environmental Science & Technology*, 45 (21): 9175-9179. doi: https://doi.org/10.1021/es201811s.

Claessens, M., De Meester, S., Van Landuyt, L., De Clerck, K. & Janssen, C. R. (2011). Occurrence and distribution of microplastics in marine sediments along the Belgian coast. *Mar Pollut Bull*, 62 (10): 2199-204. doi: https://doi.org/10.1016/j.marpolbul.2011.06.030.

Colantonio, A. & B. Potter, R. (2006). City profile - Havana. *Elsevier*, 23: 63-78. doi: https://doi.org/10.1016/j.cities.2005.10.001.

Cole, M., Lindeque, P., Halsband, C. & Galloway, T. S. (2011). Microplastics as contaminants in the marine environment: A review. *Marine Pollution Bulletin*, 62 (12): 2588-2597. doi: https://doi.org/10.1016/j.marpolbul.2011.09.025.

Cole, M., Lindeque, P. K., Fileman, E., Clark, J., Lewis, C., Halsband, C. & Galloway, T. S. (2016). Microplastics Alter the Properties and Sinking Rates of Zooplankton Faecal Pellets. *Environmental Science & Technology*, 50 (6): 3239-3246. doi: https://doi.org/10.1021/acs.est.5b05905.

Cózar, A., Echevarría, F., González-Gordillo, J. I., Irigoien, X., Úbeda, B., Hernández-León, S., Palma, Á. T., Navarro, S., García-de-Lomas, J., Ruiz, A., et al. (2014). Plastic debris in the open ocean. *Proceedings of the National Academy of Sciences*, 111 (28): 10239-10244. doi: https://doi.org/10.1073/pnas.1314705111.

Department of Climate and Industry. (2011). *Guidelines for offshore environmental monitoring - The petroleum sector on the Norwegian Continental Shelf*. The Norwegian Environment Agency. Available at: http://www.miljodirektoratet.no/old/klif/publikasjoner/2849/ta2849.pdf.

Derraik, J. G. B. (2002). The pollution of the marine environment by plastic debris: a review. *Marine Pollution Bulletin*, 44 (9): 842-852. doi: https://doi.org/10.1016/S0025-326X(02)00220-5.

Ellen MacArthur Foundation. (2016). *The New Plastic Economy - Rethinking the Future of Plastic*. Ellen MacArthur Foundation. Available at: https://www.ellenmacarthurfoundation.org/assets/downloads/EllenMacArthurFoundation_NewPlasticsEconomy_21-1-2016.pdf.

Eriksen, M., Mason, S., Wilson, S., Box, C., Zellers, A., Edwards, W., Farley, H. & Amato, S. (2013). Microplastic pollution in the surface waters of the Laurentian Great Lakes. *Marine Pollution Bulletin*, 77 (1): 177-182. doi: https://doi.org/10.1016/j.marpolbul.2013.10.007.

Eriksen, M., Lebreton, L. C. M., Carson, H. S., Thiel, M., Moore, C. J., Borerro, J. C., Galgani, F., Ryan, P. G. & Reisser, J. (2014). Plastic Pollution in the World's Oceans: More than 5 Trillion Plastic Pieces Weighing over 250,000 Tons Afloat at Sea. *PLOS ONE*, 9 (12): e111913. doi: https://doi.org/10.1371/journal.pone.0111913.

Filella, M. (2015). Questions of size and numbers in environmental research on microplastics: methodological and conceptual aspects. *Environmental Chemistry*, 12 (5): 527-538. doi: https://doi.org/10.1071/EN15012.

Fischer, V., Elsner, N. O., Brenke, N., Schwabe, E. & Brandt, A. (2015). Plastic pollution of the Kuril–Kamchatka Trench area (NW pacific). *Deep Sea Research Part II: Topical Studies in Oceanography*, 111: 399-405. doi: https://doi.org/10.1016/j.dsr2.2014.08.012.

Fok, L. & Cheung, P. K. (2015). Hong Kong at the Pearl River Estuary: A hotspot of microplastic pollution. *Mar Pollut Bull*, 99 (1-2): 112-8. doi: https://doi.org/10.1016/j.marpolbul.2015.07.050.

Free, C. M., Jensen, O. P., Mason, S. A., Eriksen, M., Williamson, N. J. & Boldgiv, B. (2014). High-levels of microplastic pollution in a large, remote, mountain lake. *Marine Pollution Bulletin*, 85 (1): 156-163. doi: https://doi.org/10.1016/j.marpolbul.2014.06.001.

Geyer, R., Jambeck, J. R. & Law, K. L. (2017). Production, use, and fate of all plastics ever made. *Science Advances*, 3 (7). doi: https://doi.org/10.1126/sciadv.1700782.

Gilfillan, L. R., Ohman, M. D., Doyle, M. J. & Watson, W. (2009). *Occurrence of plastic micro-debris in the Southern California Current System*. Article. California Cooperative Oceanic Fisheries Investigations Reports. Available at: https://escholarship.org/uc/item/34w4g0s0.

Goldstein, M. C., Rosenberg, M. & Cheng, L. (2012). Increased oceanic microplastic debris enhances oviposition in an endemic pelagic insect. *Biology Letters*, 8 (5): 817-820. doi: https://doi.org/10.1098/rsbl.2012.0298.

Gorry, C. (2017). Making Travel to Cuba Work for Health and Sustainable Development. *MEDICC Rev*, 19 (1): 48.

Gray, A. D., Wertz, H., Leads, R. R. & Weinstein, J. E. (2018). Microplastic in two South Carolina Estuaries: Occurrence, distribution, and composition. *Marine Pollution Bulletin*, 128: 223-233. doi: https://doi.org/10.1016/j.marpolbul.2018.01.030.

Gregory, M. R. (2009). Environmental implications of plastic debris in marine settings—entanglement, ingestion, smothering, hangers-on, hitch-hiking and alien invasions. *Philosophical Transactions of the Royal Society B: Biological Sciences*, 364 (1526): 2013-2025. doi: https://doi.org/10.1098/rstb.2008.0265.

Hidalgo-Ruz, V. & Thiel, M. (2013). Distribution and abundance of small plastic debris on beaches in the SE Pacific (Chile): a study supported by a citizen science project. *Mar Environ Res*, 87-88: 12-8. doi: https://doi.org/10.1016/j.marenvres.2013.02.015.

Holmes, L. A., Turner, A. & Thompson, R. C. (2012). Adsorption of trace metals to plastic resin pellets in the marine environment. *Environmental Pollution*, 160: 42-48. doi: https://doi.org/10.1016/j.envpol.2011.08.052.

Hudgins, C. M. (1964). Solubility and Density Studies of the CaCl2-ZnCl2-H2O System at 0 and 25 C. *Journal of Chemical & Engineering Data*, 9 (3): 434-436. doi: https://doi.org/10.1021/je60022a045.

Hurley, R., Woodward, J. & Rothwell, J. J. (2018). Microplastic contamination of river beds significantly reduced by catchment-wide flooding. *Nature Geoscience*, 11 (4): 251-257. doi: https://doi.org/10.1038/s41561-018-0080-1.

Imhof Hannes, K., Schmid, J., Niessner, R., Ivleva Natalia, P. & Laforsch, C. (2012). A novel, highly efficient method for the separation and quantification of plastic particles in sediments of aquatic environments. *Limnology and Oceanography: Methods*, 10 (7): 524-537. doi: https://doi.org/10.4319/lom.2012.10.524.

Imhof, H. K., Laforsch, C., Wiesheu, A. C., Schmid, J., Anger, P. M., Niessner, R. & Ivleva, N. P. (2016). Pigments and plastic in limnetic ecosystems: A qualitative and quantitative study on microparticles of different size classes. *Water Research*, 98: 64-74. doi: https://doi.org/10.1016/j.watres.2016.03.015.

Jahnke, A., Arp, H. P. H., Escher, B. I., Gewert, B., Gorokhova, E., Kühnel, D., Ogonowski, M., Potthoff, A., Rummel, C., Schmitt-Jansen, M., et al. (2017). Reducing Uncertainty and Confronting Ignorance about the Possible Impacts of Weathering Plastic in the Marine Environment.

Environmental Science & Technology Letters, 4 (3): 85-90. doi:
https://doi.org/10.1021/acs.estlett.7b00008.

Jambeck, J. R., Geyer, R., Wilcox, C., Siegler, T. R., Perryman, M., Andrady, A., Narayan, R. & Law, K. L. (2015). Plastic waste inputs from land into the ocean. *Science*, 347 (6223): 768-771. doi: https://doi.org/10.1126/science.1260352.

Jayasiri, H. B., Purushothaman, C. S. & Vennila, A. (2013). Quantitative analysis of plastic debris on recreational beaches in Mumbai, India. *Mar Pollut Bull*, 77 (1-2): 107-12. doi: https://doi.org/10.1016/j.marpolbul.2013.10.024.

Jensen, K. B. J. & Cramer, J. (2017). *MAREANOs pilotprosjekt på mikroplast - resultater og forslag til videre arbeid.* Norges Geologiske Undersøkelse (NGU). Available at: http://www.ngu.no/upload/Publikasjoner/Rapporter/2017/2017_043.pdf.

Jung, M. R., Horgen, F. D., Orski, S. V., Rodriguez C, V., Beers, K. L., Balazs, G. H., Jones, T. T., Work, T. M., Brignac, K. C., Royer, S.-J., et al. (2018). Validation of ATR FT-IR to identify polymers of plastic marine debris, including those ingested by marine organisms. *Marine Pollution Bulletin*, 127: 704-716. doi: https://doi.org/10.1016/j.marpolbul.2017.12.061.

Kim, I. S., Chae, D. H., Kim, S. K., Choi, S. & Woo, S. B. (2015). Factors Influencing the Spatial Variation of Microplastics on High-Tidal Coastal Beaches in Korea. *Arch Environ Contam Toxicol*, 69 (3): 299-309. doi: https://doi.org/10.1007/s00244-015-0155-6.

Koelmans, A. A., Bakir, A., Burton, G. A. & Janssen, C. R. (2016). Microplastic as a Vector for Chemicals in the Aquatic Environment: Critical Review and Model-Supported Reinterpretation of Empirical Studies. *Environmental Science & Technology*, 50 (7): 3315-3326. doi: https://doi.org/10.1021/acs.est.5b06069.

Laglbauer, B. J. L., Franco-Santos, R. M., Andreu-Cazenave, M., Brunelli, L., Papadatou, M., Palatinus, A., Grego, M. & Deprez, T. (2014). Macrodebris and microplastics from beaches in Slovenia. *Marine Pollution Bulletin*, 89 (1): 356-366. doi: https://doi.org/10.1016/j.marpolbul.2014.09.036.

Lattin, G. L., Moore, C. J., Zellers, A. F., Moore, S. L. & Weisberg, S. B. (2004). A comparison of neustonic plastic and zooplankton at different depths near the southern California shore. *Marine Pollution Bulletin*, 49 (4): 291-294. doi: https://doi.org/10.1016/j.marpolbul.2004.01.020.

Law, K. L., Moret-Ferguson, S., Maximenko, N. A., Proskurowski, G., Peacock, E. E., Hafner, J. & Reddy, C. M. (2010). Plastic accumulation in the North Atlantic subtropical gyre. *Science*, 329 (5996): 1185-8. doi: https://doi.org/10.1126/science.1192321.

Lebreton, L. C. M., Greer, S. D. & Borrero, J. C. (2012). Numerical modelling of floating debris in the world's oceans. *Marine Pollution Bulletin*, 64 (3): 653-661. doi: https://doi.org/10.1016/j.marpolbul.2011.10.027.

Lebreton, L. C. M., van der Zwet, J., Damsteeg, J.-W., Slat, B., Andrady, A. & Reisser, J. (2017). River plastic emissions to the world's oceans. *Nature Communications*, 8: 15611. doi: https://doi.org/10.1038/ncomms15611.

Lenz, R., Enders, K., Stedmon, C. A., Mackenzie, D. M. A. & Nielsen, T. G. (2015). A critical assessment of visual identification of marine microplastic using Raman spectroscopy for analysis improvement. *Marine Pollution Bulletin*, 100 (1): 82-91. doi: https://doi.org/10.1016/j.marpolbul.2015.09.026.

Liebezeit, G. & Dubaish, F. (2012). Microplastics in beaches of the East Frisian islands Spiekeroog and Kachelotplate. *Bull Environ Contam Toxicol*, 89 (1): 213-7. doi: https://doi.org/10.1007/s00128-012-0642-7.

Lorenze, C. (2014). Detection of microplastics in marine sediments of the German Coast via FT-IR spectroscopy (Master thesis). doi: https://doi.org/10013/epic.43880.

Mahat, S. (2017). *Separation and quantification of Microplastics from Beach and Sediments samples using the Bauta microplastic-sediment separator (Master thesis).* Brage: Norwegian Univeristy of Life Science Available at: https://brage.bibsys.no/xmlui/handle/11250/2459114.

MEPEX. (2014). *Sources of microplasticpollution to the marine environment* Miljødirektoratet. Available at: http://www.miljodirektoratet.no/Documents/publikasjoner/M321/M321.pdf.

MERI. (2015). *Guide to Microplastic Identification*. Available at: http://sfyl.ifas.ufl.edu/media/sfylifasufledu/flagler/sea-grant/pdf-files/sea-turtle-curriculum/microplastics/MERI_Guide-to-Microplastic-Identification.pdf.

Møskeland, T., Knutsen, H., Arp, H. P. & Lilleeng, Ø. (2018). *Microplastics in sediments on the Norwegian Continental Shelf*. Miljødirektoratet / Norwegian Environment Agency. Available at: http://www.miljodirektoratet.no/Documents/publikasjoner/M976/M976.pdf.

Nor, N. H. & Obbard, J. P. (2014). Microplastics in Singapore's coastal mangrove ecosystems. *Mar Pollut Bull*, 79 (1-2): 278-83. doi: https://doi.org/10.1016/j.marpolbul.2013.11.025.

Nuelle, M.-T., Dekiff, J. H., Remy, D. & Fries, E. (2014). A new analytical approach for monitoring microplastics in marine sediments. *Environmental Pollution*, 184: 161-169. doi: https://doi.org/10.1016/j.envpol.2013.07.027.

Obbard, R. W., Sadri, S., Wong, Y. Q., Khitun, A. A., Baker, I. & Thompson, R. C. (2014). Global warming releases microplastic legacy frozen in Arctic Sea ice. *Earth's Future*, 2 (6): 315-320. doi: https://doi.org/10.1002/2014EF000240.

Olivares-Rieumont, S., De La Rosa, D., Lima, L., Graham, D., D' Alessandro, K., Borroto, J., Martínez, F. & Sánchez, J. (2005). *Assessment of heavy metal levels in Almendares River sediments - Havana City, Cuba*, vol. 39.

Olsen, L. M., Mahat, S. & Arp, H. P. (*In preparation*). A solvation-digestion method for the isolation of microplastics from organic matter collected from surface-water trawls, coastlines and sediments.

Peeken, I., Primpke, S., Beyer, B., Gütermann, J., Katlein, C., Krumpen, T., Bergmann, M., Hehemann, L. & Gerdts, G. (2018). Arctic sea ice is an important temporal sink and means of transport for microplastic. *Nature Communications*, 9 (1): 1505. doi: https://doi.org/10.1038/s41467-018-03825-5.

PlasticsEurope. (2017). *Plastics - The Facts 2017 - An Analysis of European Plastics Production, Demand and Waste Data*. Available at: https://www.plasticseurope.org/application/files/5715/1717/4180/Plastics_the_facts_2017_FINAL_for_website_one_page.pdf.

Reddy, M. S., Shaik, B., Adimurthy, S. & Ramachandraiah, G. (2006). Description of the small plastics fragments in marine sediments along the Alang-Sosiya ship-breaking yard, India. *Estuarine, Coastal and Shelf Science*, 68 (3): 656-660. doi: https://doi.org/10.1016/j.ecss.2006.03.018.

Rochman, C. M., Browne, M. A., Halpern, B., T Hentschel, B., Hoh, E., Karapanagioti, H., Rios, L., Takada, H., Teh, S. & C Thompson, R. (2013). Policy: Classify plastic waste as hazardous. 494: 169-71. doi: https://doi.org/10.1038/494169a.

Ryan, P. G., Moore, C. J., van Franeker, J. A. & Moloney, C. L. (2009). Monitoring the abundance of plastic debris in the marine environment. *Philosophical Transactions of the Royal Society B: Biological Sciences*, 364 (1526): 1999-2012. doi: https://doi.org/10.1098/rstb.2008.0207.

Ryggvik, H. & Smith-Solbakken, M. (2018). *Petroleumsfeltene På Norsk Kontinentalsokkel*. I Store norske leksikon. Available at: https://snl.no/Petroleumsfeltene_p%C3%A5_norsk_kontinentalsokkel (accessed: 7. May).

Santos, I. R., Friedrich, A. C. & Ivar do Sul, J. A. (2009). Marine debris contamination along undeveloped tropical beaches from northeast Brazil. *Environ Monit Assess*, 148 (1-4): 455-62. doi: https://doi.org/10.1007/s10661-008-0175-z.

Sarkissian, G., Keegan, J., Du Pasquier, E., Depriester, J. P. & Rousselot, P. (2004). *The analysis of tires and tire traces using FTIR and Py-GC/MS*, vol. 37.

Scheurer, M. & Bigalke, M. (2018). Microplastics in Swiss Floodplain Soils. *Environmental Science & Technology*, 52 (6): 3591-3598. doi: https://doi.org/10.1021/acs.est.7b06003.

Schmidt, C., Krauth, T. & Wagner, S. (2017). Export of Plastic Debris by Rivers into the Sea. *Environmental Science & Technology*, 51 (21): 12246-12253. doi: https://doi.org/10.1021/acs.est.7b02368.

Scientific Polymer Inc. (2013). *Density of Polymers (by density).* Scientific Polymer Products, Inc (Website). Available at: http://scientificpolymer.com/density-of-polymers-by-density/ (accessed: 7th of May).

Siegfried, M., Koelmans, A. A., Besseling, E. & Kroeze, C. (2017). Export of microplastics from land to sea. A modelling approach. *Water Res*, 127: 249-257. doi: https://doi.org/10.1016/j.watres.2017.10.011.

Singh, B. & Nisha Sharma, N. (2008). Mechanistic implications of plastic degradation. 93: 561-584. doi: https://doi.org/10.1016/j.polymdegradstab.2007.11.008.

Statista. (2016). *Density of selected plastic materials that float or sink in relation to seawater density (in grams per cubic centimeter)*. Available at: https://www.statista.com/statistics/595434/plastic-materials-density/.

Su, L., Xue, Y., Li, L., Yang, D., Kolandhasamy, P., Li, D. & Shi, H. (2016). Microplastics in Taihu Lake, China. *Environmental Pollution*, 216: 711-719. doi: https://doi.org/10.1016/j.envpol.2016.06.036.

Suaria, G., Avio, C. G., Mineo, A., Lattin, G. L., Magaldi, M. G., Belmonte, G., Moore, C. J., Regoli, F. & Aliani, S. (2016). The Mediterranean Plastic Soup: synthetic polymers in Mediterranean surface waters. *Scientific Reports*, 6: 10. doi: https://doi.org/10.1038/srep37551.

The Norwegian Petroleum Directorate. (2018a). *Licensing position for the Norwegian continental shelf*. Norskpetroleum (Website): Norwegian Petroleum,. Available at: https://www.norskpetroleum.no/en/exploration/licensing-position-for-the-norwegian-continental-shelf/ (accessed: 7th of May).

The Norwegian Petroleum Directorate. (2018b). *Norway's petroleum history*. Norskpetroleum (Website): Norwegian Petroleum,. Available at: https://www.norskpetroleum.no/en/framework/norways-petroleum-history/ (accessed: 2018).

Van Cauwenberghe, L., Vanreusel, A., Mees, J. & Janssen, C. R. (2013). Microplastic pollution in deep-sea sediments. *Environ Pollut*, 182: 495-9. doi: https://doi.org/10.1016/j.envpol.2013.08.013.

Vianello, A., Boldrin, A., Guerriero, P., Moschino, V., Rella, R., Sturaro, A. & Da Ros, L. (2013). Microplastic particles in sediments of Lagoon of Venice, Italy: First observations on occurrence, spatial patterns and identification. *Estuarine, Coastal and Shelf Science*, 130: 54-61. doi: https://doi.org/10.1016/j.ecss.2013.03.022.

Villarrubia-Gómez, P., Cornell, S. E. & Fabres, J. (2017). Marine plastic pollution as a planetary boundary threat – The drifting piece in the sustainability puzzle. *Marine Policy*. doi: https://doi.org/10.1016/j.marpol.2017.11.035.

Vollertsen, J. (n.d.). *Overview of methods and challenges for microplastic analysis*. Available at: http://www.svensktvatten.se/globalassets/utbildning/konferenser-och-seminarier/microplastics/03_vollertsen_microplastic-intro.pdf.

Waller, C. L., Griffiths, H. J., Waluda, C. M., Thorpe, S. E., Loaiza, I., Moreno, B., Pacherres, C. O. & Hughes, K. A. (2017). Microplastics in the Antarctic marine system: An emerging area of research. *Science of The Total Environment*, 598: 220-227. doi: https://doi.org/10.1016/j.scitotenv.2017.03.283.

Willis, K., Maureaud, C., Wilcox, C. & Hardesty, B. D. (2017). How successful are waste abatement campaigns and government policies at reducing plastic waste into the marine environment? *Marine Policy*. doi: https://doi.org/10.1016/j.marpol.2017.11.037.

Woodall, L. C., Sanchez-Vidal, A., Canals, M., Paterson, G. L. J., Coppock, R., Sleight, V., Calafat, A., Rogers, A. D., Narayanaswamy, B. E. & Thompson, R. C. (2014). The deep sea is a major sink for microplastic debris. *Royal Society Open Science*, 1 (4). doi: https://doi.org/10.1098/rsos.140317.

World Population Review. (2018). *Havana Population 2018*. Available at: http://worldpopulationreview.com/world-cities/havana-population/ (accessed: 9th of May).

Yang, D., Shi, H., Li, L., Li, J., Jabeen, K. & Kolandhasamy, P. (2015). Microplastic Pollution in Table Salts from China. *Environmental Science & Technology*, 49 (22): 13622-13627. doi: https://doi.org/10.1021/acs.est.5b03163.

Ye, S. & Andrady, A. L. (1991). Fouling of floating plastic debris under Biscayne Bay exposure conditions. *Marine Pollution Bulletin*, 22 (12): 608-613. doi: https://doi.org/10.1016/0025-326X(91)90249-R.

Zarfl, C. & Matthies, M. (2010). Are marine plastic particles transport vectors for organic pollutants to the Arctic? *Mar Pollut Bull*, 60 (10): 1810-4. doi: https://doi.org/10.1016/j.marpolbul.2010.05.026.

Zhang, H. (2017). Transport of microplastics in coastal seas. *Estuarine, Coastal and Shelf Science*, 199: 74-86. doi: https://doi.org/10.1016/j.ecss.2017.09.032.

Appendix - A1 – Sampling, separation, digestion and data correction (NCS)

Appendix A1-1
Sampling information – Norwegian Continental Shelf

| Station ID | Oil field | Coordinates | | TOC | Direction from Oil & Gas installation | Distance from Oil & Gas installation |
| | | Lat | Long | | | |
		(x)	(y)	(%)	(°)	(m)
Reg-01	Regional	57.14843	2.774225	0.30	n.r.	n.r.
Reg-02	Regional	56.91602	3.331869	0.30	n.r.	n.r.
Reg-03	Regional	56.54823	3.455098	0.37	n.r.	n.r.
Reg-04	Regional	56.24933	3.831911	0.32	n.r.	n.r.
Reg-06	Regional	56.74934	2.665193	0.33	n.r.	n.r.
Reg-07	Regional	56.49933	2.748539	0.36	n.r.	n.r.
Reg-08	Regional	56.04123	3.456675	0.32	n.r.	n.r.
Reg-09	Regional	57.12435	3.180022	0.19	n.r.	n.r.
Reg-11	Regional	56.24149	3.159982	0.29	n.r.	n.r.
Reg-14	Regional	57.54343	2.394618	0.24	n.r.	n.r.
EKO-12	Ekofisk	56.5298	3.232563	n.d.	2500	78
EKO-14	Ekofisk	56.54302	3.219975	0.48	850	76
EKO-21	Ekofisk	56.55947	3.148956	n.d.	4000	71
ULA-06	Ula	57.11202	2.847409	0.28	250	71
GYDA-18	Gyda	56.90272	3.086334	0.88	250	67
GYDA-21	Gyda	56.89159	3.106612	n.d.	2000	67
VAL-02	Valhall	56.27933	3.400768	n.d.	500	76
VAL-04	Valhall	56.28297	3.424097	n.d.	2000	72
VAL-05	Valhall	56.28781	3.455216	n.d.	5000	70
VAL-15	Valhall	56.2769	3.385223	0.42	500	76
Reg-12	Regional	61.85751	2.579576	n.d.	n.r	n.r
SNB-16R	Snorre B ref/regional	61.58758	2.074973	n.d.	315	10000
VI-RB	Visund ref/regional	61.44553	2.362113	n.d.	330	10000
STC-06R	Statjord C / regional	61.23829	2.043409	n.d.	130	10000
KV-02	Kvitebjørn	60.99432	2.451635	n.d.	140	500
KV-14	Kvitebjørn	61.12257	2.397238	n.d.	316	7224
VegaR	Vega	61.26151	3.208005	n.d.	n.d.	n.d.
VI-01	Visund	61.36625	2.459592	n.d.	150	500
VI-03	Visund	61.36122	2.466823	n.d.	150	1000
VI-30	Visund	61.37012	2.454849	n.d.	330	250
KRT-14	Kråketind	72.82409	20.82844	1.93	n.r.	n.r.
SC3-4	Scarecrow3	73.40998	20.01403	1.56	270	100
GRS2	Gråspett	73.73573	21.14572	2.09	90	250
KF2-6	Korpefjell	73.98689	35.83393	1.76	85	900
STT2	Stangnestind	72.64857	34.85362	1.93	90	250

n.d: No data

n.r: Not relevant

Appendix A1-2

Calculation of dry matter content (NCS)

	Wet weight (g)			Dry weight (g)			
Sample-ID	Date	Al.tray	Al.tray + sample	Date	Al.tray + sample	Calculated dry matter of sample (- al.tray)	Calculated dry matter (%)
20171006-Reg-01	06.10.2017	2.19	120.71	09.10.2017	94.88	93	78
20171211-Reg-02	06.10.2017	2.19	151.30	09.10.2017	117.99	116	78
20171004-Reg-03	04.10.2017	2.19	109.40	06.10.2017	86.11	84	78
20171005-Reg04	05.10.2017	2.1	127.85	09.10.2017	99.74	98	78
20170926-Reg-06	26.09.2017	2.17	134.19	28.09.2017	102.33	100.16	75
20170929-Reg-07	29.09.2017	2.18	136.18	02.10.2017	105.10	103	77
20171206-Reg-08	04.10.2017	2.17	134.21	06.10.2017	101.90	100	76
20171005-Reg-09	05.10.2017	2.18	178.87	09.10.2019	94.78	93	52
20171002-Reg-11	02.10.2017	2.18	135.34	04.10.2017	102.73	101	76
20171002-Reg-14	02.10.2017	2.19	130.51	04.10.2017	104.87	103	80
20171019-ULA-06	19.10.2017	2.17	118.86	23.10.2017	94.38	92	79
20171103-GYDA-18	03.11.2017	2.16	123.32	07.10.2017	87.80	86	71
20171106-GYDA-21	06.11.2017	2.16	110.11	13.10.2017	87.05	85	79
20171027-VAL-02	27.10.2017	2.17	134.37	30.10.2017	102.82	101	76
20171030-VAL-04	30.10.2017	2.17	126.9	07.10.2017	99.44	97	78
20171102-VAL-05	02.11.2017	2.18	128.75	07.11.2017	102.1	100	79
20171102-VAL-15	02.11.2017	2.19	131.81	07.10.2017	101.20	99	76
20171026-EKO-12	26.10.2017	2.15	127.11	30.10.2017	98.41	96.26	77
20171206-EKO-14	20.10.2017	2.16	150.17	23.10.2017	115.48	113	77
20171026-EKO-21	26.10.2017	2.17	115.93	30.10.2017	90.34	88.17	77
20171117-Reg-12	17.11.2017	2.19	113.09	23.11.2017	53.26	51.07	46
20171113-SNB-16R	13.11.2017	2.19	121.7	23.11.2017	77.75	75.5676	63
20171117-VI-RB	17.11.2017	2.17	119.65	23.11.2017	74.46	72.2996	62
20171121-STC-06R	21.11.2017	2.18	116.49	27.11.2017	86.05	84	73
20171120-KV-02	20.11.2017	2.18	120.28	23.11.2017	91.22	89.0489	75
20171121-KV-14	21.11.2017	2.15	109.30	27.11.2017	84.39	82	77
20171213-VI-01	09.11.2017	2.16	123.95	23.11.2017	73.69	71.5399	59
20171120-VI-03	20.11.2017	2.17	122.43	23.11.2017	75.71	73.5426	61
20171120-VI-30	20.11.2017	2.17	122.92	23.11.2017	74.34	72.17	60
20171116-Vega-R	16.11.2017	2.17	99.60	23.11.2017	36.9	34.73	36
20171127-KRT-14	30.11.2017	2.18	84.96	06.12.2017	39.75	37.57	45
20171122-SC3-4	22.11.2017	2.16	113.45	27.11.2017	50.24	48	43
20171124-GRS-2	24.11.2017	2.17	84.83	27.11.2017	32.5	30.33	37
20171122-KF2-6	22.11.2017	2.18	124.14	27.11.2017	68.12	66	54
20171122-STT-2	22.11.2017	2.16	106.41	27.11.2017	44.49	42	41

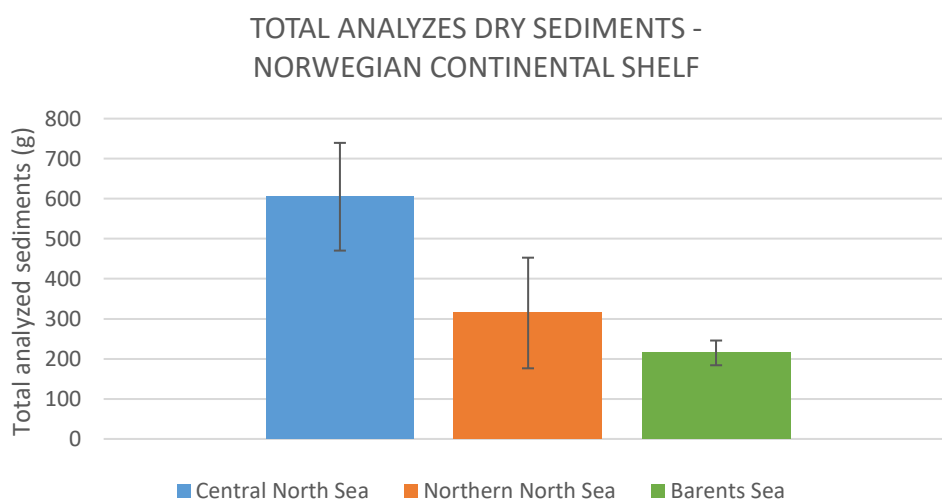DRY MATTER CONTENT -
NORWEGIAN CONTINETAL SHELF
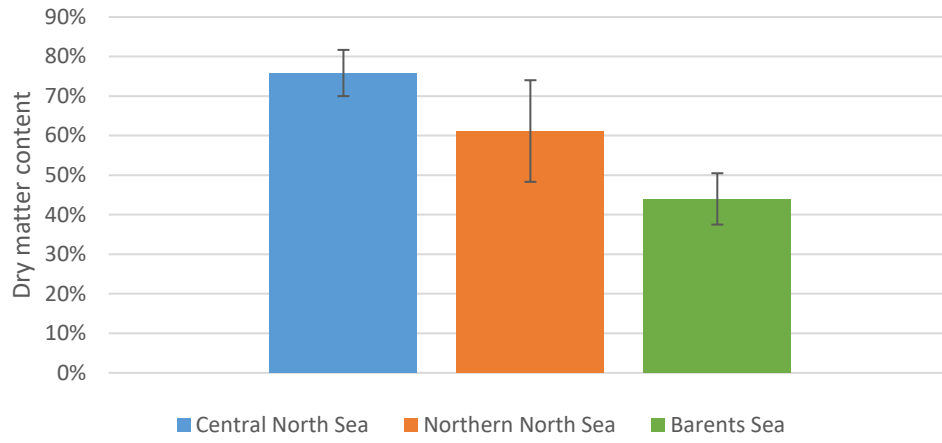
Appendix A1-3
Sediment preparation and weight-correction (NCS)

Sample-ID	Date	Density of ZnCl2: CaCl2 (g/mL)	Al.tray (g)	Al.tray + weight of sediments (g)	Wet sediments to bauta (g)	Al.tray + sediment + ZnCl2:CaCl2 (g)	Al.tray after added to bauta (g)	Wet sediment + ZnCl2 to bauta (g)	Corrected amount of dry sediments added to bauta (g)
20171006-Reg-01	06.10.2017	1.52	30.63	1603.1	918.3	992.4	99.92	892.48	644
20171211-Reg-02	11.12.2017	1.52	28.79	1692.4	612.9	764	45.89	718.11	443
20171004-Reg-03	04.10.2017	1.54	30.48	1609.3	943.1	1095.8	47.27	1048.53	703
20171005-Reg04	05.10.2017	1.52	30.54	1704.2	962.5	1035.1	91.84	943.26	679
20170926-Reg-06	26.09.2017	1.55	29.35	1627.3	737.7	969.9	173.145	796.755	455
20170929-Reg-07	29.09.2017	1.55	30.51	1752.1	1008.4	1111.8	70.78	1041.02	723
20171206-Reg-08	06.12.2017	1.52	28.95	1828.0	687.4	838.1	45.61	792.49	487
20171005-Reg-09	05.10.2017	1.53	30.49	1362.1	907.8	1059.1	109.92	949.18	424
20171002-Reg-11	02.10.2017	1.54	30.39	1572.2	780	916.5	40.62	875.88	560
20171002-Reg-14	02.10.2017	1.53	30.47	1592.9	725.2	875	145.32	729.68	480
20171019-ULA-06	19.10.2017	1.51	30.93	1527.1	958.9	1108.4	54.92	1053.48	717
20171103-GYDA-18	03.11.2017	1.51	29.31	1464.3	905.3	1053.8	119.49	934.31	565
20171106-GYDA-21	06.11.2017	1.52	29.27	1501.3	963.3	1112.8	39.6	1073.2	728
20171027-VAL-02	27.10.2017	1.59	29.42	1520.2	926	1026.2	50.53	975.67	668
20171030-VAL-04	30.10.2017	1.56	29.52	1486.8	976.7	1129.7	35.81	1093.89	734
20171102-VAL-05	02.11.2017	1.55	29.28	1524.3	950.9	1098.5	35.69	1062.81	723
20171102-VAL-15	02.11.2017	1.51	29.46	1571.1	938.1	1095.5	37.98	1057.52	689
20171026-EKO-12	24.10.2017	1.57	30.86	1561.7	973.4	1125.3	37.68	1087.62	721
20171206-EKO-14	06.12.2017	1.52	28.98	1564.2	406.94	487.02	54.89	432.13	273
20171026-EKO-21	26.10.2017	1.51	30.86	1699.4	916.9	1064	40.65	1023.35	680

Graph continue below.

64

20171117-Reg-12	17.11.2017	1.52	29.33	1311.7	461.03	620.9	43.48	577.42	194
20171113-SNB-16R	13.11.2017	1.56	6.575	915.71	457.855	466.78	12.195	454.585	281
20171113-SNB-16R #1	13.11.2017	1.55	6.57	915.71	456.38	464.2	13.08	451.12	280
20171113-SNB-16R #2	13.11.2017	1.57	6.58	915.71	459.33	469.36	11.31	458.05	283
20171117-VI-RB	17.11.2017	1.52	29.26	522.12	459.86	616.5	57.35	559.15	252
20171121-STC-06R	21.11.2017	1.54	29.29	2092.6	730.4	881.1	33.11	847.99	512
20171120-KV-02	20.11.2017	1.52	29.1	2067.8	595.92	745.3	37.25	708.05	423
20171121-KV-14	21.11.2017	1.54	29.31	2512.2	752.3	913.7	35.01	868.59	544
20171213-VI-01	13.12.2017	1.53	28.97	1332.2	333.75	493.71	55.84	437.87	168
20171120-VI-03	20.11.2017	1.52	29.23	1452.6	583.59	733.2	54.93	678.27	327
20171120-VI-30	20.11.2017	1.57	29.08	862.5	533.29	682.4	51.56	630.84	291
20171116-Vega-R	16.11.2017	1.51	29.32	1201.2	433.5	593.56	n.d.	593.56	151
20171127-KRT-14	23.11.2017	1.51	30.09	1235.6	531.61	689.7	n.d.	689.7	238
20171122-SC3-4	22.11.2017	1.51	28.93	1082.7	565.8	714.3	112.23	602.07	204
20171124-GRS-2	23.11.2017	1.51	29.23	1077	537.36	696.2	n.d.	696.2	194
20171122-KF2-6	22.11.2017	1.51	28.91	1291.4	574.8	645.5	110.85	534.65	256
20171122-STT-2	22.11.2017	1.53	28.87	963.2	520.33	622	80.02	541.98	182

*n.d. – no data available.

TOTAL ANALYZES DRY SEDIMENTS -
NORWEGIAN CONTINENTAL SHELF

Central North Sea   Northern North Sea   Barents Sea

Filtration – before digestion (NCS)

		Weight before separation (g)			Weight after separation (g)	
Sample-ID	**Date**	**Steel filter**	**Steel wire**	**Total weight**	**Date**	**Total weight**
20171006-Reg-01	09.10.2017	1.696	0.3169	2.0131	12.10.2017	2.1524
20171211-Reg-02	12.12.2017	1.3007	0.2867	1.5878	18.12.2017	1.5942
20171004-Reg-03	05.10.2017	1.4296	0.3268	1.7564	06.10.2017	1.7846
20171005-Reg04	06.10.2017	1.6703	0.2805	1.9508	09.10.2017	2.0828
20170926-Reg-06	29.09.2017	1.4615	0.3015	1.7473	02.10.2017	1.8472
20170929-Reg-07	02.10.2017	1.7111	0.2125	1.9239	04.10.2017	2.1030
20171206-Reg-08	11.12.2017	1.6202	0.3281	1.9481	12.12.2017	1.9622
20171005-Reg-09	06.10.2017	1.7196	0.2977	2.0177	09.10.2017	2.0389
20171002-Reg-11	03.10.2017	1.7062	0.2485	1.9550	04.10.2017	1.9744
20171002-Reg-14	03.10.2017	1.7067	0.2121	1.9189	04.10.2017	1.9377
20171019-ULA-06	20.10.2017	1.4279	0.2556	1.6835	23.10.2017	2.0508
20171103-GYDA-18	06.11.2017	1.5492	0.2977	1.8463	07.11.2017	1.8839
20171106-GYDA-21	07.11.2017	1.5522	0.2557	1.8075	07.11.2017	2.0588
20171027-VAL-02	02.11.2017	1.4210	0.3160	1.7371	07.11.2017	1.8548
20171030-VAL-04	02.11.2017	1.5013	0.3020	1.7823	07.11.2017	2.0938
20171102-VAL-05	03.11.2017	1.7238	0.2892	2.0128	07.11.2017	2.0588
20171102-VAL-15	03.11.2017	1.4303	0.2041	1.6347	07.11.2017	1.7577
20171026-EKO-12	26.10.2017	3.0105	0.4275	3.4382	30.10.2017	4.0015
20171206-EKO-14	11.12.2017	1.5335	0.2369	1.7704	12.12.2017	1.7791
20171026-EKO-21	27.10.2017	3.2649	0.5478	3.8127	07.11.2017	4.1237
20171117-Reg-12	20.11.2017	1.3226	0.2431	1.565	30.11.2017	1.5655
20171113-SNB-16R (Mean)	14.11.207	1.3451	0.27985	1.6247	23.11.2017	1.63845
20171113-SNB-16R #1	14.11.2017	1.2848	0.2729	1.5573	30.11.2017	1.5552
20171113-SNB-16R #2	14.11.2017	1.4054	0.2868	1.6921	23.11.2017	1.7217
20171117-VI-RB	20.11.2017	1.3029	0.2495	1.5524	30.11.2017	1.5532
20171121-STC-06R	22.11.2017	1.1362	0.2509	1.3870	24.10.2017	1.3974
20171120-KV-02	21.11.2017	1.1447	0.3155	1.4603	30.11.2017	1.4876
20171121-KV-14	22.11.2017	1.1811	0.1874	1.3686	24.10.2017	1.4229
20171213-VI-01	14.12.2017	2.0496	0.2828	2.3322	19.12.2017	2.3428
20171120-VI-03	21.11.2017	1.1053	0.2958	1.4011	30.11.2017	1.4107
20171120-VI-30	21.11.2017	1.3574	0.2515	1.6089	23.11.2017	1.6687
20171116-Vega-R	17.11.2017	1.5426	0.2962	1.8391	23.11.2017	1.8899
20171127-KRT-14	27.11.2017	1.5826	0.2493	1.8319	30.11.2017	1.8711
20171122-SC3-4	23.11.2017	1.5110	0.2742	1.7852	24.10.2017	1.8245
20171124-GRS-2	27.11.2017	1.6412	0.2778	1.9190	30.11.2017	1.9576
20171122-KF2-6	23.11.2017	1.5419	0.2744	1.8163	24.10.2017	1.9055
20171122-STT-2	23.11.2017	1.5136	0.2541	1.7677	24.10.2017	1.8442

Appendix A1-5
Digestion and correction of sample (NCS)

Sample-ID	Calculated weight of sample prior digestion	After digestion	Rounds of digestions	Corrected for method blanks	Correction for recovery	Correct for sediments and mg/kg
20171006-Reg-01	0.1393	0.0312	2	0.0302	0.0392	60.8
20171211-Reg-02	0.0064	0.0031	1	0.0021	0.0027	6.1
20171004-Reg-03	0.0282	0.0098	2	0.0088	0.0114	16.2
20171005-Reg04	0.132	0.0639	2	0.0629	0.0816	120.0
20170926-Reg-06	0.0998	0.0537	1	0.0528	0.0684	150.3
20170929-Reg-07	0.1791	0.0368	2	0.0358	0.0464	64.2
20171206-Reg-08	0.0141	0.0034	1	0.0024	0.0031	6.4
20171005-Reg-09	0.0212	0.0025	2	0.0015	0.0019	4.6
20171002-Reg-11	0.0194	0.0066	2	0.0056	0.0073	13.0
20171002-Reg-14	0.0188	0.001	2	0.0000	0.0000	< LOD
20171019-ULA-06	0.3673	0.2287	3	0.2277	0.2953	411.8
20171103-GYDA-18	0.0376	0.0037	1	0.0027	0.0035	6.2
20171106-GYDA-21	0.2513	0.1289	1	0.1279	0.1659	228.0
20171027-VAL-02	0.1177	0.0662	1	0.0652	0.0845	126.5
20171030-VAL-04	0.3115	0.0835	1	0.0825	0.1070	145.7
20171102-VAL-05	0.046	0.0534	1	0.0524	0.0679	94.0
20171102-VAL-15	0.123	0.0374	1	0.0364	0.0472	68.6
20171026-EKO-12	0.5633	0.0515	1	0.0505	0.0655	90.8
20171206-EKO-14	0.0087	0.0056	1	0.0046	0.0060	21.9
20171026-EKO-21	0.311	0.0704	1	0.0694	0.0900	132.3
20171117-Reg-12	0.0005	0	1	-0.0010	-0.0013	< LOD
20171113-SNB-16R*	0.01375	-0.00205	1	-0.0030	-0.0040	< LOD
20171117-VI-RB	0.0008	0.0003	1	-0.0007	-0.0009	< LOD
20171121-STC-06R	0.0104	0.0052	1	0.0042	0.0054	10.6
20171120-KV-02	0.0273	0.0218	1	0.0208	0.0270	63.8
20171121-KV-14	0.0543	0.018	1	0.0170	0.0220	40.5
20171213-VI-01	0.0106	0.0092	1	0.0082	0.0106	63.0
20171120-VI-03	0.0096	0.0057	1	0.0047	0.0061	18.7
20171120-VI-30	0.0598	0.0269	1	0.0259	0.0336	115.4
20171116-Vega-R	0.0508	-0.0004	1	-0.0014	-0.0018	< LOD
20171127-KRT-14	0.0392	0.0036	1	0.0026	0.0034	14.2
20171122-SC3-4	0.0393	0.0075	1	0.0065	0.0084	41.4
20171124-GRS-2	0.0386	0.0086	1	0.0076	0.0099	50.6
20171122-KF2-6	0.0892	0.0046	1	0.0036	0.0047	18.2
20171122-STT-2	0.0765	0.006	1	0.0050	0.0065	35.6

*mean

Appendix - A2 – Sampling, separation, digestion and data correction (Rio Almendares)

Appendix A2-1

Sampling information – Rio Almendares, Cuba

			Coordinates	
Sample ID	**Location**	**Date**	**Lat (x)**	**Long (y)**
20170803-LOC-10A	Location 10	03.08.2017	23.1383333°	-82.4100333°
20170803-LOC-10B-1	Location 10	03.08.2017	23.1383333°	-82.4100333°
20170803-LOC-10B-2	Location 10	03.08.2017	23.1361167°	-82.4103500°
20170803-LOC-10B-3	Location 10	03.08.2017	23.1361167°	-82.4103500°
20170803-LOC-10C	Location 10	03.08.2017	23.1361167°	-82.4103500°
20170806-ALM-BOS	Location 10	03.08.2017	23.1367500°	-82.4098833°
20170806-ALM-PAR #1	Bosque de la Habana	06.08.2017	23.109287°	-82.406681°
20170806-ALM-PAR #2	Parque Almendares	06.08.2017	23.118606°	-82.409327°
20170806-LOC-1	Cruise Terminal	06.08.2017	23.137333°	-82.346778°

Appendix A2-2

Calculation of dry matter content

| Sample ID | Date | Wet weight (g) | | Date | Dry weight (g) | Calculated dry matter of sample (- al.tray) | Calculated dry matter (*100%) |
		Al.tray	Al.tray + sample		Al.tray + sample		
20170803-LOC-10A	02.02.2018	2.19	31.29	05.02.2017	26.81	24.62	0.846
20170803-LOC-10B-1	06.02.2018	2.19	33.88	08.02.2018	19.36	17.17	0.541
20170803-LOC-10B-2	08.02.2018	2.22	34.96	08.02.2018	19.81	17.59	0.537
20170803-LOC-10B-3	02.02.2018	2.22	33.77	05.02.2017	19.27	17.05	0.540
20170803-LOC-10C	06.02.2018	2.2	18.72	08.02.2018	9.02	6.82	0.412
20170806-ALM-BOS	05.02.2018	2.2	37.13	06.02.2018	26.94	24.74	0.708
20170806-ALM-PAR #1	05.02.2018	2.19	34.35	06.02.2018	18.81	16.62	0.516
20170806-ALM-PAR #2	-	-	-	-	-	-	-
20170806-LOC-1	02.02.2018	2.18	23.78	05.02.2017	10.22	8.04	0.372

*

Dry matter content (%)
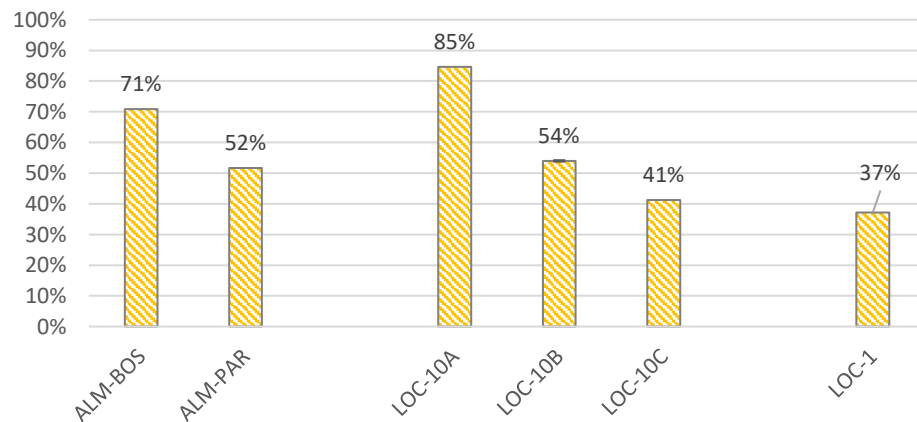
Sediment preparation and weight-correction

Sample ID	Date	Density of ZnCl2:CaCl 2 (g/mL)	Al.tray (g)	Al.tray + weight of sediments (g)	Al.tray + sediment + ZnCl2:CaCl 2 (g)	Al.tray after added to bauta (g)	Wet sediments to bauta (g)	Wet sediment + ZnCl2 to bauta (g)	Corrected amount of dry sediments added to bauta (g)
20170803-LOC-10A	02.02.2018	1.504	29.14	334.25	482.86	30.65	303.6	452.21	172.45
20170803-LOC-10B-1	06.02.2018	1.493	29.21	367.67	514.87	31.72	335.95	483.15	126.57
20170803-LOC-10B-2	08.02.2018	1.491	28.85	362.33	509.11	32.15	330.18	476.96	122.80
20170803-LOC-10B-3	01.02.2018	1.513	28.96	338.56	487.24	31.99	306.57	455.25	111.57
20170803-LOC-10C	06.02.2018	1.501	29.11	82.05	229.81	30.85	51.2	198.96	5.44
20170806-ALM-BOS	05.02.2018	1.502	29.11	323.71	471.55	31.06	292.65	440.49	137.71
20170806-ALM-PAR #1	05.02.2018	1.495	29.38	305.55	453.45	31.23	274.32	422.22	92.11
20170806-ALM-PAR #2	-	-	-	-	-	-	-	-	0.00
20170806-LOC-1	01.02.2018	1.505	29.07	431.65	581.08	31.97	399.68	549.11	108.28

DRY WEIGHT OF TOTAL ANALYZES SEDIMENTS - RIO ALMENDARES
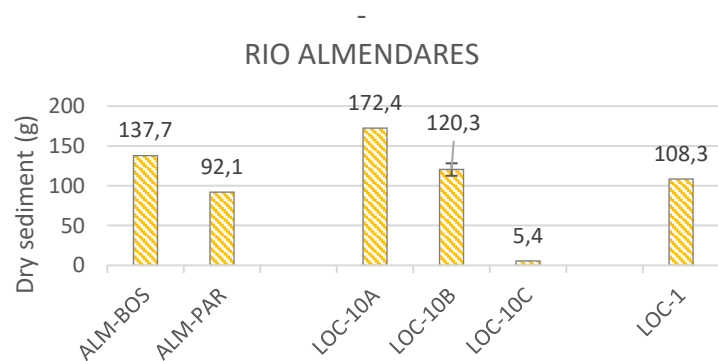
Appendix A2- 4

Filtration – before digestion

Sample ID	Weight before separation (g)				Weight after separation (g) (drying over-night at 60 oC)		
	Date	Steel mesh filter	Steel wire	Total weight (mesh filter + wire)	Date	Total weight	Weight of sample
20170803-LOC-10A	05.02.2018	1.7025	0.2580	1.9605	05.02.2018	1.9885	0.028
20170803-LOC-10B-1	08.02.2018	1.7013	0.2928	1.9941	09.02.2018	2.2532	0.2591
20170803-LOC-10B-2	09.02.2018	1.7637	0.3211	2.0848	12.02.2018	2.2584	0.1736
20170803-LOC-10B-3	02.02.2018	1.5691	0.3148	1.8838	08.02.2018	2.1396	0.2558
20170803-LOC-10C	08.02.2018	1.7973	0.2878	2.0851	09.02.2018	2.1318	0.0467
20170806-ALM-BOS	06.02.2018	1.7214	0.2945	2.0159	08.02.2018	2.5485	0.5326
20170806-ALM-PAR #1	06.02.2018	1.6937	0.2801	1.9738	08.02.2018	3.5246	1.5508
20170806-ALM-PAR #2	06.02.2018	1.7219	0.2923	2.0143	08.02.2018	3.0436	1.0293
20170806-LOC-1	02.02.2018	1.5775	0.3427	1.9202	05.02.2018	3.4495	1.5293

*

Appendix A2- 5

Digestion and corrections of MP sample

SampleID	Weight of sample prior digestion	After digestion	Reduction in %	Rounds of digestions	Calculated amount of sample after digestion (≤4%)	Corrected for method blanks	Correction for recovery	Correction for sediments (g/kg)	Convert to mg (mg/kg)
20170803-LOC-10A	0.0280	0.0117	58 %	4	0.0117	0.01095	0.01386	0.08038	80.376
20170803-LOC-10B-1	0.2591	0.1554	40 %	4	0.1554	0.15465	0.19576	1.54670	1546.704
20170803-LOC-10B-2	0.1736	0.0981	43 %	3	0.0894	0.08868	0.11226	0.91413	914.134
20170803-LOC-10B-3	0.2558	0.1109	57 %	4	0.1104	0.10970	0.13886	1.24460	1244.601
20170803-LOC-10C	0.0467	0.0205	56 %	4	0.0205	0.01975	0.02500	4.59612	4596.121
20170806-ALM-BOS	0.5326	0.1611	70 %	5	0.1611	0.16035	0.20297	1.47394	1473.939
20170806-ALM-PAR #1	1.5508	0.4698	70 %	6	0.5521	0.55140	1.3474	12.31990	12319.895
20170806-ALM-PAR #2	1.0293	0.3458	66 %	6	0.3458	0.34505			
20170806-LOC-1	1.5293	1.196	22 %	3	1.1348	1.13404	1.43549	13.25665	13256.649

REDUCTION IN MASS BETWEEN DIGESTION STEPS
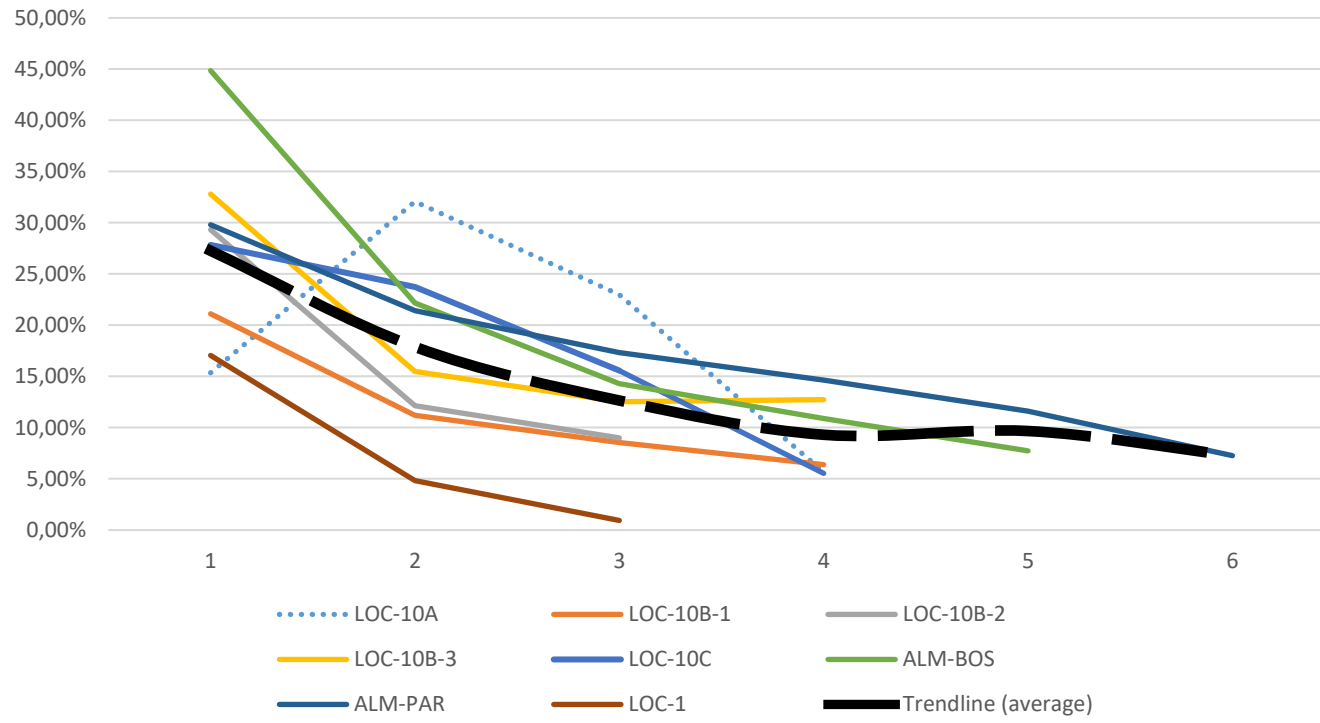
Appendix A2- 6

Final weighing

Date	Weight of steel mesh filter	Original weight of steel wire	Weight of steel wire	Total weight after digestion (filter + wire)	Actual total weight	Match of steel wires	Match of total
20170803-LOC-10A	1.7144	0.2580	0.2578	1.9722	1.9722	99.922 %	100.000 %
20170803-LOC-10B-1	1.8564	0.2928	0.2928	2.1492	2.1495	100.000 %	99.986 %
20170803-LOC-10B-2	1.8618	0.3211	0.3209	2.1827	2.1829	99.938 %	99.991 %
20170803-LOC-10B-3	1.6792	0.3148	0.3147	1.9939	1.9947	99.968 %	99.960 %
20170803-LOC-10C	1.8179	0.2878	0.2877	2.1056	2.1056	99.965 %	100.000 %
20170806-ALM-BOS	1.8825	0.2945	0.2944	2.1769	2.1770	99.966 %	99.995 %
20170806-ALM-PAR #1	2.1632	0.2801	0.2801	2.4433	2.4436	100.000 %	99.988 %
20170806-ALM-PAR #2	2.0674	0.2923	0.2923	2.3597	2.3601	100.000 %	99.983 %
20170806-LOC-1	2.7729	0.3427	0.3427	3.1156	3.1162	100.000 %	99.981 %
20180131-Blank	1.5804	0.3075	0.3072	1.8876	1.8878	99.902 %	99.989 %
20180201-Blank	1.6136	0.3106	0.3103	1.9239	1.9238	99.903 %	100.005 %
20180202-LOC10B-3	1.9108	0.3134	0.3133	2.2241	2.2245	99.968 %	99.982 %
20180208-LOC10B-1	1.8628	0.3646	0.3646	2.2274	2.2276	100.000 %	99.991 %
MEAN ±SD						99.964 ± 0.04%	

Appendix - A3 - Quality control -Method and Recovery Blanks (NCS + RA)

Appendix A3-1

Weight of Method blanks. before and after digestion

Weight of collected impurities (g)

Method Blank-ID	Date	Total weight - Before filtrations	Total weight - Before digestion	Sample weight - Before digstion	Total weight - After digestion	Sample weight - after digestion
20170922-Blank1	22.09.2017	1.66501	1.6709	0.00589	1.6651	0.0001
20170922-Blank2	23.09.2017	1.6531	1.6554	0.0023	1.6533	0.0002
20170922-Blank3	24.09.2017	1.6689	1.6735	0.0046	1.6704	0.0015
20171019-Blank	19.10.2017	1.8426	1.8552	0.0126	1.8424	-0.0002
20171109-blank 5:1	09.11.2017	1.5976	1.6172	0.0196	1.6002	0.0026
20171121-Blank	22.11.2017	1.3098	1.3217	0.0119	1.3103	0.0005
20171123-blank*	23.11.2017	-	-		-	-
20171129-Blank1	29.11.2017	1.6423	1.6461	0.0038	1.6431	0.0008
20171129-Blank2	29.11.2017	1.7062	1.7089	0.0027	1.7063	0.0001
20171206-Test1	06.12.2017	1.9549	1.9657	0.0108	1.9562	0.0013
20171312-Test2	13.12.2017	1.6128	1.6264	0.0136	1.6159	0.0031
20180131-Blank (RA)	31.01.2018	1.8882	1.8885	0.0003	1.8878	-0.0004
20180201-Blank (RA)	01.02.2018	1.9244	1.9246	0.0002	1.9238	-0.0006
Average				0.0074		0.0007
Standard deviation				0.0062		0.0012

*No weights recorded. Sample is only listed due to visual analysis.

Recovery rates including weight of added spiking material

Recovery Blank-ID	Weight of added MP powder	Weight of added MP fibres	Weight of *five* granulates	Weight of sample prior digestion	Weight of sample after digestion
20171004-Reg-03-Blank	0.2	-	-	0.1949	0.139801
20171002-Reg-11-Blank	0.4298	-	-	0.2316	0.184801
20171005-Reg-09-Blank	-	0.1318	0.1007	0.2388	0.226001
20171114-SNB-16R-Blank 1	-	0.0527	-	0.0634	0.043501
20171114-SNB-16R-Blank 2	0.1074	-	-	0.0969	0.060501
20171009-Reg-01 Blank	-	0.1308	0.094	0.2698	0.220301
20171130-KRT-14-Blank - 1	-	0.0532	-	0.0524	0.047401
20171130-KRT-14-Blank - 2	0.1022	-	-	0.1019	0.086301
20180202-LOC10B-3	0.2003	-	-	0.1653	0.1474
20180208-LOC10B-1	-	0.0524	-	0.0626	0.0523

RECOVERY RATES AND DEVIATION
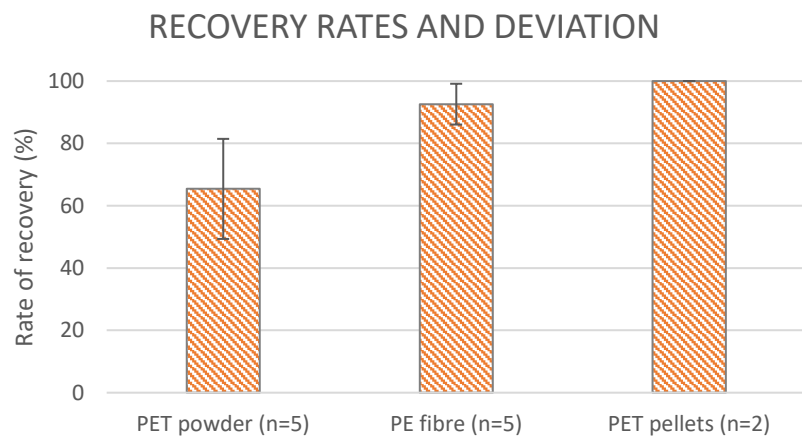
Appendix A3-3

Densities for all samples tested for microplastics on NCS

Sample ID	Density (g/ml)
20171006-Reg-01	1.52
20171211-Reg-02	1.52
20171004-Reg-03	1.54
20171005-Reg04	1.52
20170926-Reg-06	1.55
20170929-Reg-07	1.55
20171206-Reg-08	1.52
20171005-Reg-09	1.53
20171002-Reg-11	1.54
20171002-Reg-14	1.53
20171026-EKO-12	1.57
20171206-EKO-14	1.52
20171026-EKO-21	1.50
20171103-GYDA-18	1.51
20171106-GYDA-21	1.52
20171027-VAL-02	1.59
20171030-VAL-04	1.56
20171102-VAL-05	1.55
20171102-VAL-15	1.51
20171019-ULA-06	1.51
20171117-Reg-12	1.52
20171113-SNB-16R	1.56
20171117-VI-RB	1.52
20171121-STC-06R	1.54
20171121-KV-14	1.54
20171120-KV-02	1.52
20171213-VI-01	1.53
20171120-VI-03	1.52
20171120-VI-30	1.57
20171116-Vega-R	1.51
20171122-STT-2	1.53
20171122-KF2-6	1.51
20171122-SC3-4	1.51
20171127-KRT-14	1.51
20171124-GRS-2	1.51
Mean	1.53
Deviation	0.02

Appendix A3-4
Densities for all samples tested for microplastics in RA

Sample ID	Density (g/ml)
20170803-LOC-10A	1.504
20170803-LOC-10B-1	1.493
20170803-LOC-10B-2	1.491
20170803-LOC-10B-3	1.513
20170803-LOC-10C	1.501
20170806-ALM-BOS	1.502
20170806-ALM-PAR	1.495
20170806-LOC-1	1.505
MEAN	1.501
DEVIATION	0.007

Appendix A3-5
Densities for all recovery blanks tested for microplastics

Sample ID	Density (g/mL)
20171004-Reg-03-Blank	1.505
20171002-Reg-11-Blank	1.505
20171005-Reg-09-Blank	1.511
20171114-SNB-16R-Blank 1	1.55
20171114-SNB-16R-Blank 2	1.57
20171009-Reg-01 Blank	1.515
20171130-KRT-14-Blank - 1	1.48
20171130-KRT-14-Blank - 2	1.47
20180202-LOC10B-3	1.511
20180208-LOC10B-1	1.491
MEAN	1.51
DEVIATION	0.03

Appendix A3-6

Densities for all method blanks tested for microplastics

Sample ID	Density (g/ml)
20170922-Blank 1 (NCS)	1.54
20170922-Blank 2 (NCS)	1.57
20170922-Blank 3 (NCS)	1.55
20171019-Blank (NCS)	1.51
20171109-blank 5:1 (NCS)	1.51
20171123-blank* (NCS)	1.52
20171121-Blank (NCS)	1.50
20171129-Blank 1 (NCS)	1.48
20171129-Blank 2 (NCS)	1.47
20171206-Test 1 (NCS)	1.52
20171213-Test 2 (NCS)	1.53
20180102–Blank 1(Cuba)	1.51
20180102–Blank 2 (Cuba)	1.5
MEAN	1.52
DEVIATION	0.03

Appendix - B1 – Final results – (NCS)

MP$_{max}$ concentrations for the central North Sea

Appendix-B1-1

Sample-ID	Max. mg/kg	Max.mg/m2	Items/kg	Items/area
20171006-Reg-01	61	500	4 600	57 000
20171211-Reg-02	6	53	470	6 100
20171004-Reg-03	16	130	1 200	15 000
20171005-Reg04	120	1 000	9 200	120 000
20170926-Reg-06	150	1 200	11 000	140 000
20170929-Reg-07	64	570	4 900	65 000
20171206-Reg-08	6	58	490	6 600
20171005-Reg-09	5	21	730	5 100
20171002-Reg-11	13	100	990	12 000
20171002-Reg-14	< LOD	< LOD	490	6 100
20171019-ULA-06	410	3 200	31 000	370 000
20171103-GYDA-18	6	42	370	3 700
20171106-GYDA-21	220	1 800	17 000	200 000
20171027-VAL-02	130	960	9 700	110 000
20171030-VAL-04	150	1 100	11 000	130 000
20171102-VAL-05	94	740	7 200	85 000
20171102-VAL-15	69	540	5 200	62 000
20171026-EKO-12	91	710	6900	82 000
20171206-EKO-14	22	260	1 700	20 000
20171026-EKO-21	130	1 100	10 000	130 000
Mean ± SD	88 ± 8	704 ± 773	6707 ± 7431	81280 ± 89108
Range	< LOD -410	< LOD -3200	370 – 31 000	3700 - 370 000

Appendix-B1-2

MP_{max} concentrations for the northern North Sea

Sample-ID	Max. mg/kg	Max.mg/m2	Items/kg	Items/area
20171117-Reg-12	< LOD	< LOD	180	700
20171113-SNB-16R	< LOD	< LOD	580	2 200
20171117-VI-RB	< LOD	< LOD	640	1 300
20171121-STC-06R	11	110	810	8 200
20171120-KV-02	64	650	4 900	50 000
20171121-KV-14	40	510	3 100	39 000
20171213-VI-01	63	320	4 800	25 000
20171120-VI-03	19	110	550	3 200
20171120-VI-30	120	380	8 800	29 000
20171116-Vega-R	< LOD	< LOD	280	780
Mean ± SD Range	32 ± 40 <LOD – 120	208 ± 240 < LOD - 650	2464 ± 2891 180 - 8800	15938 ± 18354 780-50000

Appendix-B1-3

MP_{max} concentrations for the Barents Sea

Sample-ID	Max. mg/kg	Max.mg/m2	Items/kg	Items/area
20171127-KRT-14	14	52	830	3 000
20171122-SC3-4	41	130	3 200	9 600
20171124-GRS-2	51	130	3 900	9 900
20171122-KF2-6	18	83	1 400	6 300
20171122-STT-2	36	90	2 700	6 900
Mean ± SD Range	32 ± 16 < LOD - 51	97 ± 33 < LOD–130	2406 ± 1269 830-3900	7140 ± 2809 3000-9900

Average mg $_{max}$ MP/kg based on region
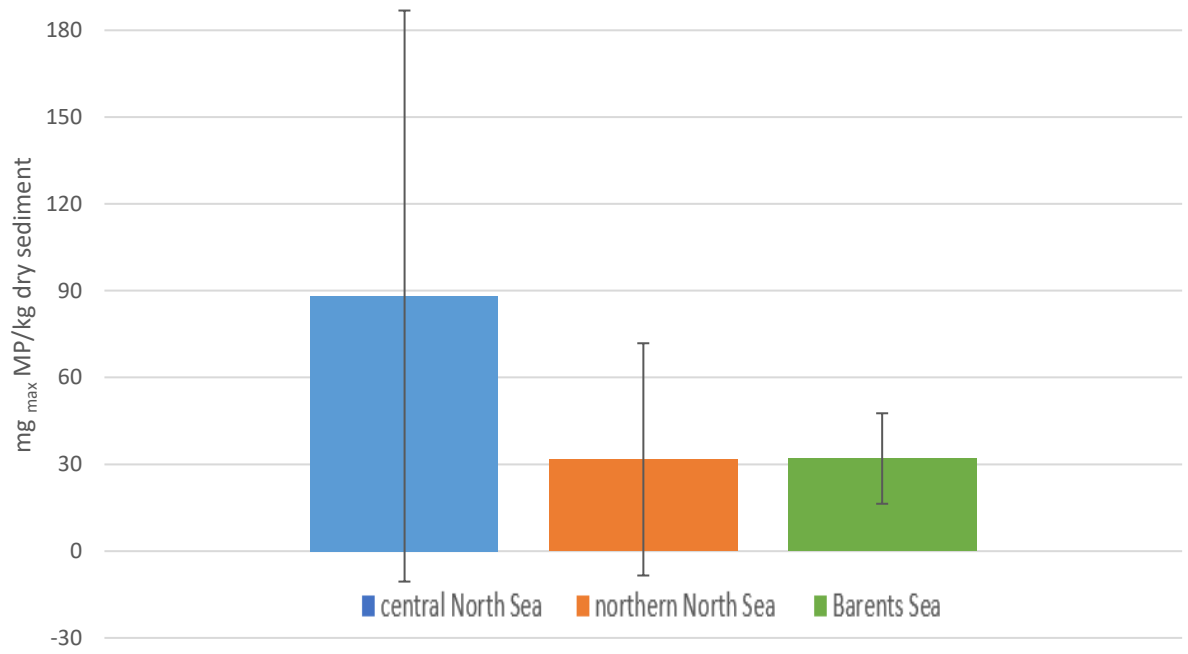
Appendix - B2 – Final Data – (Rio Almendares)

Appendix-B2-1

Microplastic concentration for all sediment samples in Rio Almendares. Cuba + Cruise Terminal (LOC-1)
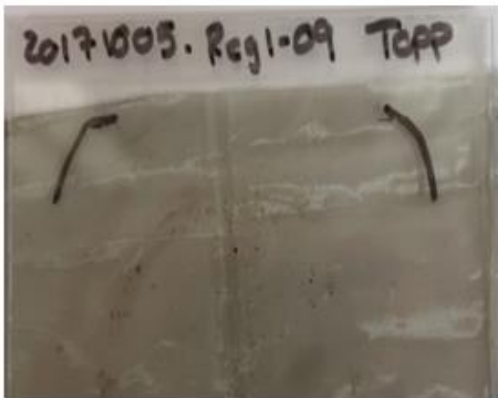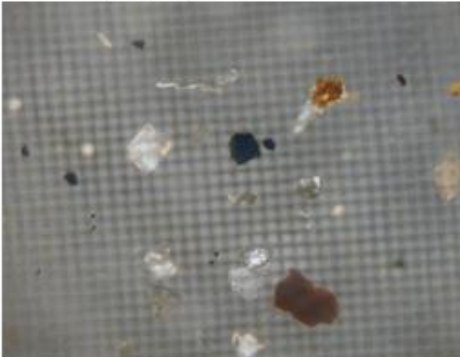
Sample ID	max. mg / kg	Items / kg	MEAN max. mg / kg	MEAN Items / kg
20170803-LOC-10A	80	193		
20170803-LOC-10B-1	1547	3281		
20170803-LOC-10B-2	914	1576	1235 ± 316	2750 ± 1019
20170803-LOC-10B-3	1245	3394		
20170803-LOC-10C	4596	31564		
20170806-ALM-BOS	1474	2571	6896 ± 7669	17182 ± 20663
20170806-ALM-PAR	12320	31793		
20170806-LOC-1	13257	9172		
	4429	10443		
MEAN ± SD	5327	13364		

NGI

B1 20171005-Reg-09

| Overview | Clear layer (µm) |
| White fibre (> 500 µm) | Heterogenous distribution of particles |

NGI
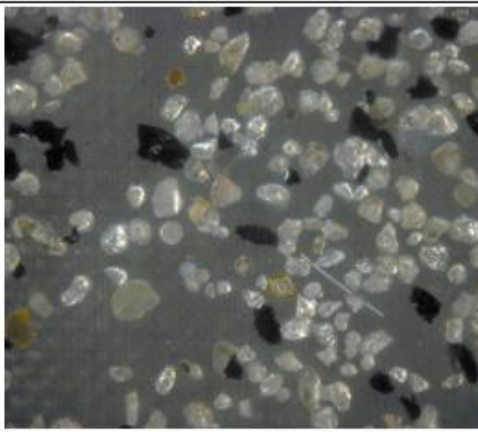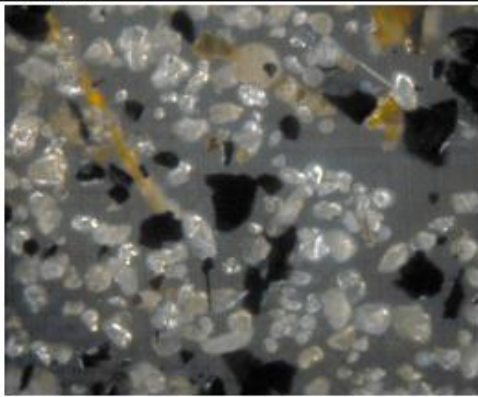
B2   20171002-Reg-14

Overview	Blue fibre
Red fibre	Mostly black particles

B3   20171026-EKO-12

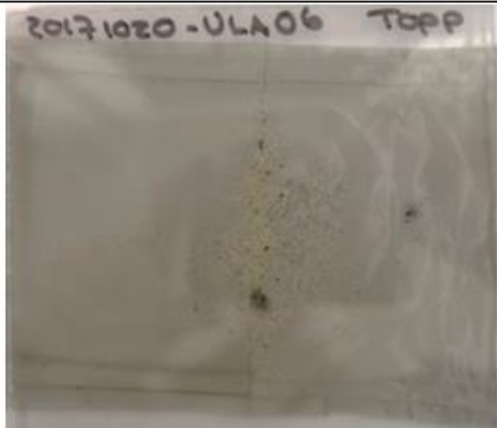|	
Overview	Spherical and irregularly shaped granules
Red, spherical granule	Spherical and irregularly shaped granules

Relatively homogenous composition of white/clear granules of approximately the same size (100-300 μm).

NGI
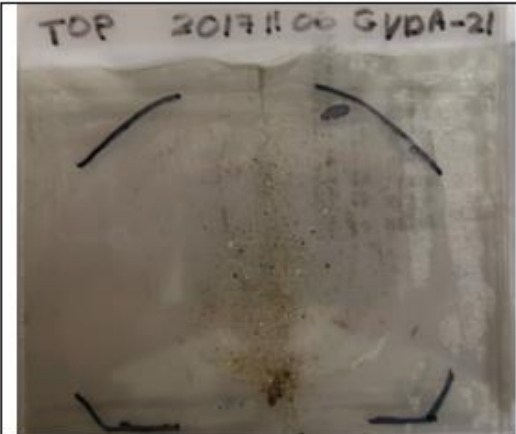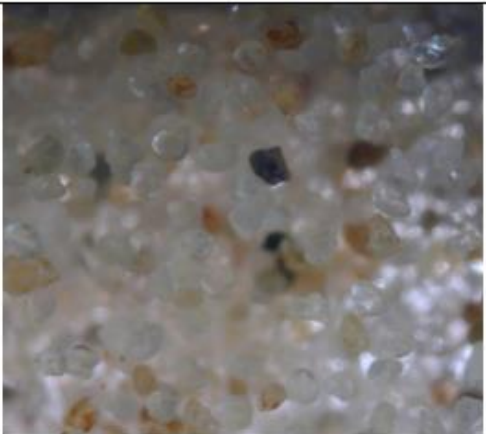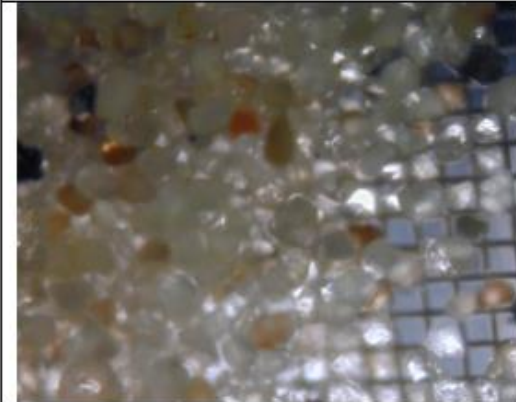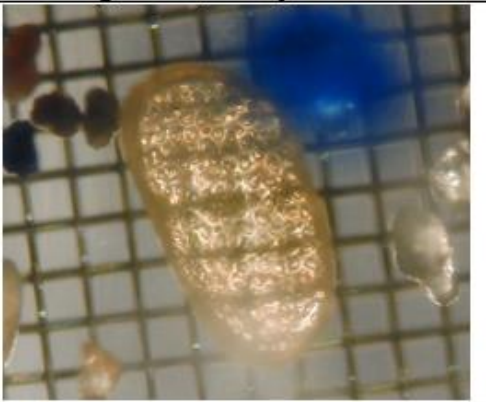
B4   20171103-GYDA-18
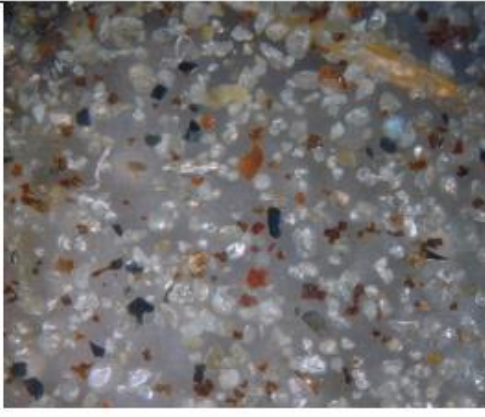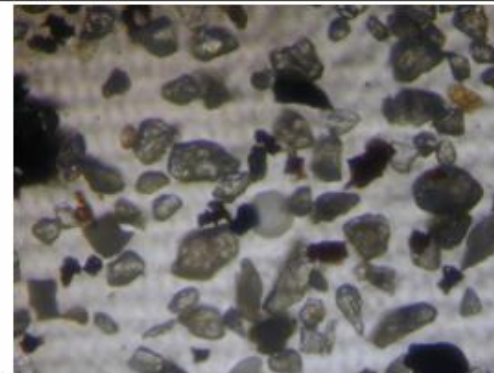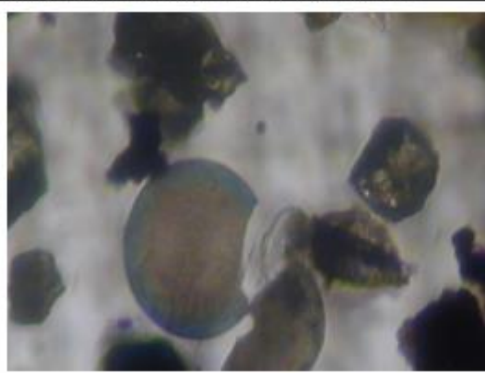
Overview	Mostly clear and brown granules (100-300 μm)
Blue fibre	Brown granule with sharp edges

NGI

B5   20171106-GYDA-21

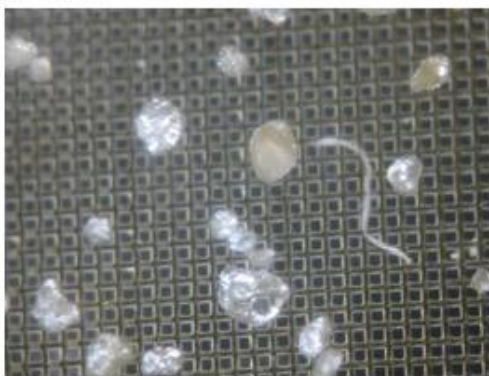|	
Overview	Several granules, mostly white/clear.
Several granules, mostly white/clear.	Probably organic matter due to cellular structure
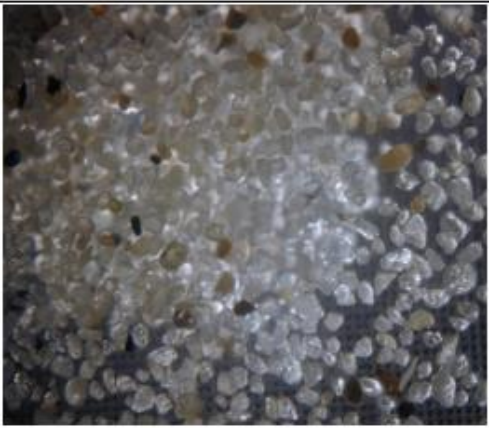
Relatively homogenous composition of white/clear granules of approximately the same size (100-300 μm).

NGI

B6   20171102-VAL-05

|	
Overview	Heterogeneous particle distribution
Several grey/black particles – charcoal?	Example of granule with sharp edges

Relatively homogenous composition of white/clear granules of approximately the same size (100-300 μm).
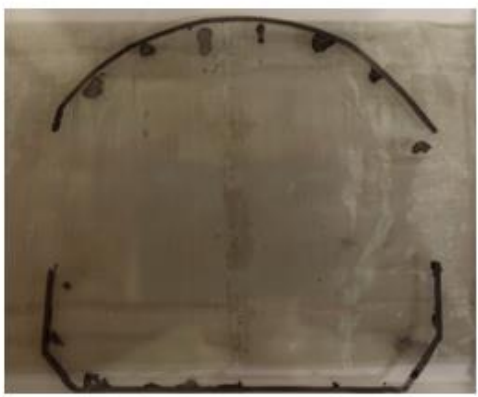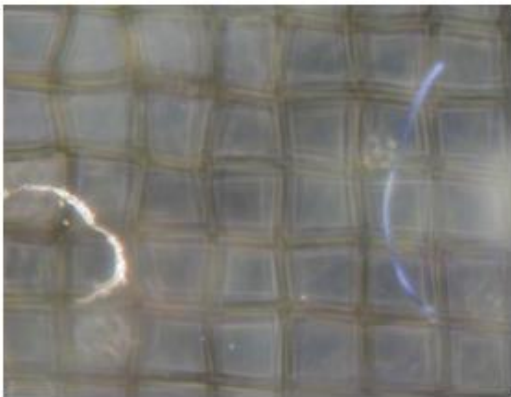
B7   20171019-ULA-06
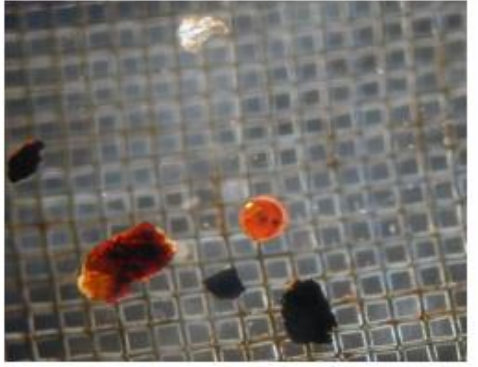

Overview	Homogenous distribution of white/clear granules
Mostly white/clear granules	White fibre

Relatively homogenous composition of white/clear granules of approximately the same size (100-300 µm).

B8   20171117-Reg-12

| Overview | Heterogeneous distribution of particles |

NGI
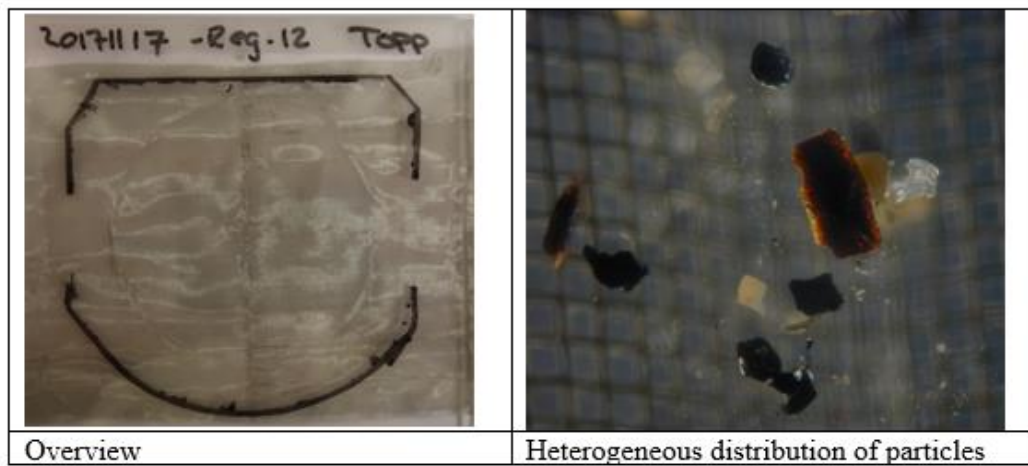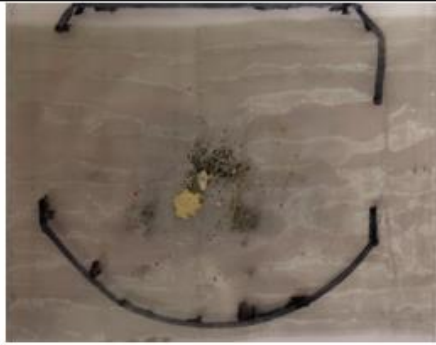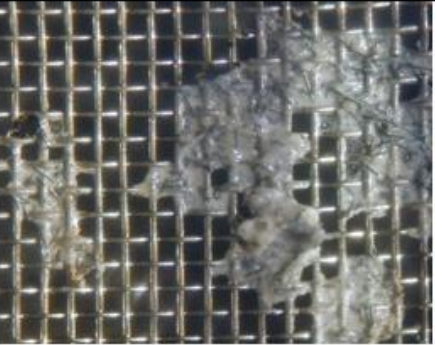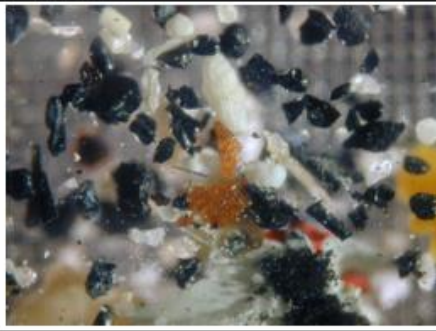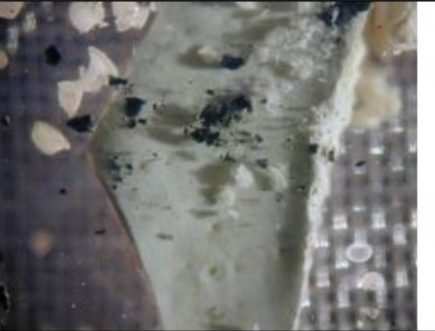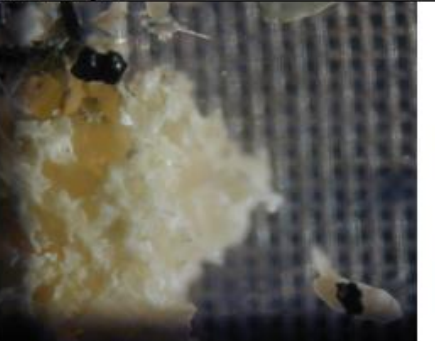
B9   20171113-SNB-16R

Overview	White and blue fibre
Some black, clear and red/orange granules, one spherical.	White fibre

NGI

B10   20171121-KV-14

Overview	Heterogeneous composition
Mostly white and clear granules	White layer

NGI
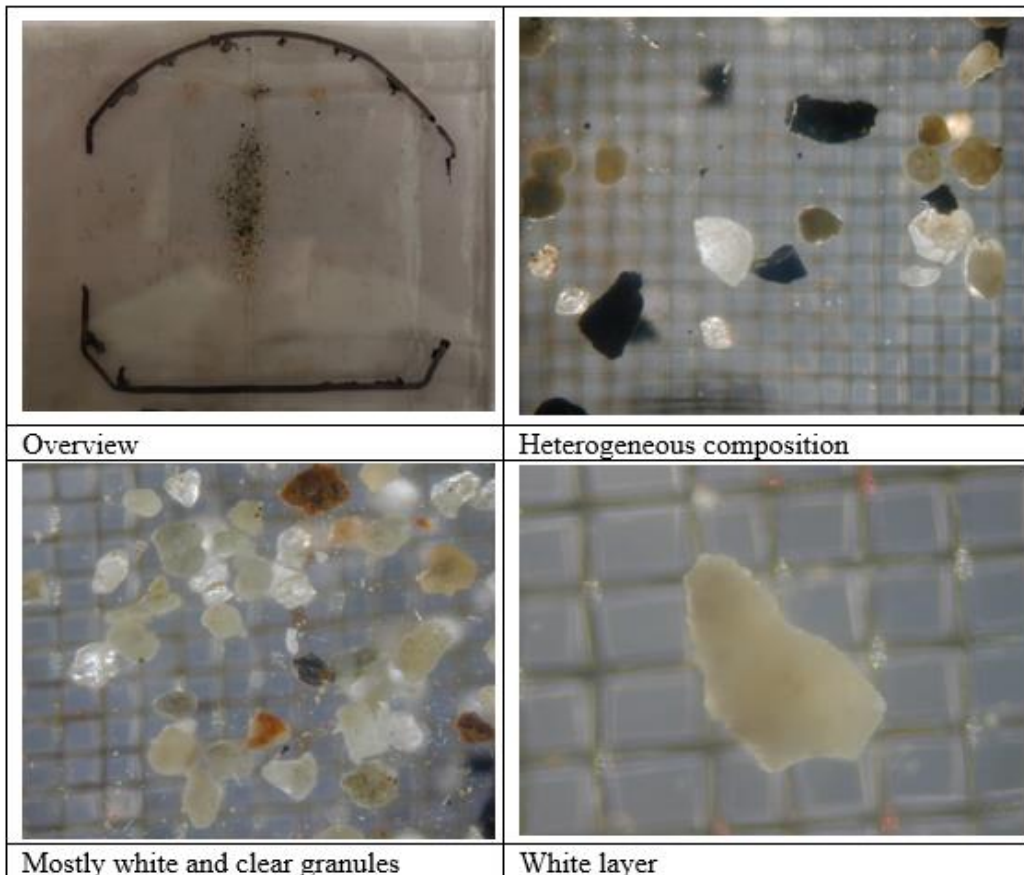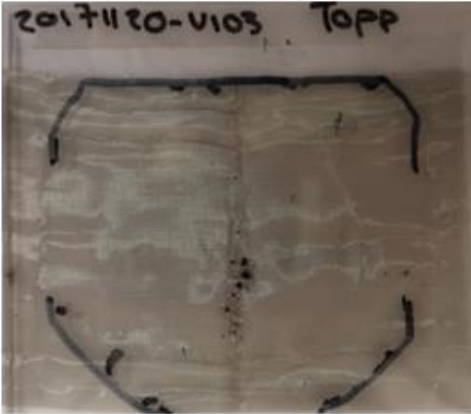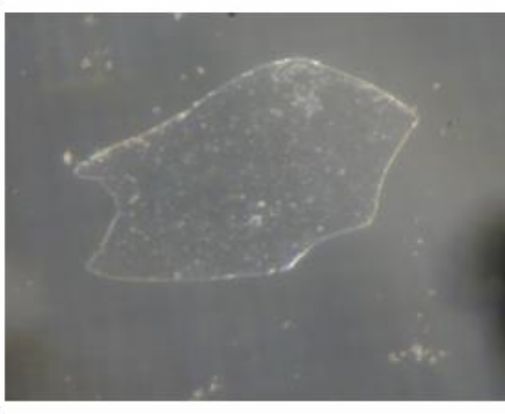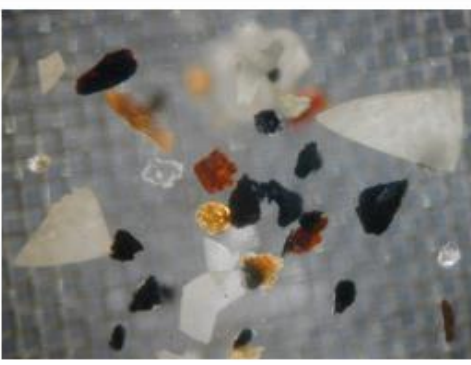
B11   20171120-KV-02

Overview	Unknown structure
Several black granules and other particles	White layer
Cluster of white fibres	Yellow/white foam?
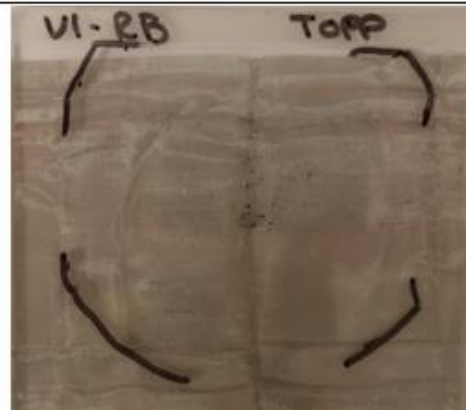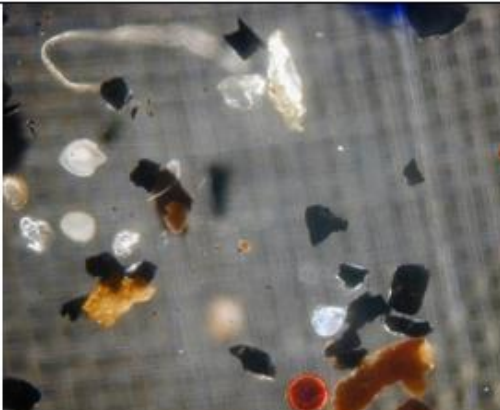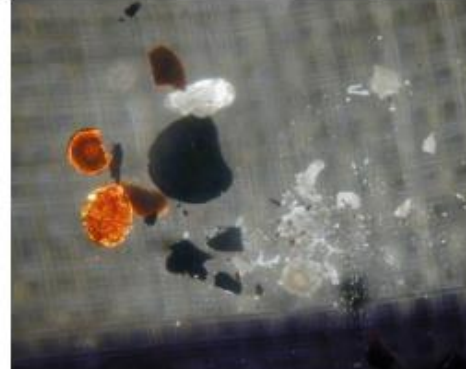
This sample contained several particles not found in any other of the sediment samples, as shown in the photos above. The uppermost right pictures shows several black fibres clustered together with something that looks like glue or slime. Layers of different colours (white, blue and red) were also found, as well as white clusters of white fibres and a foam-looking particle. In agreement with other samples, a heterogeneous composition of granules was identified.

B12   20171120-VI-03

Overview	Clear layer
Heterogeneous composition of particles. A substantial amount of white layers	White layers, black and clear granules

NGI
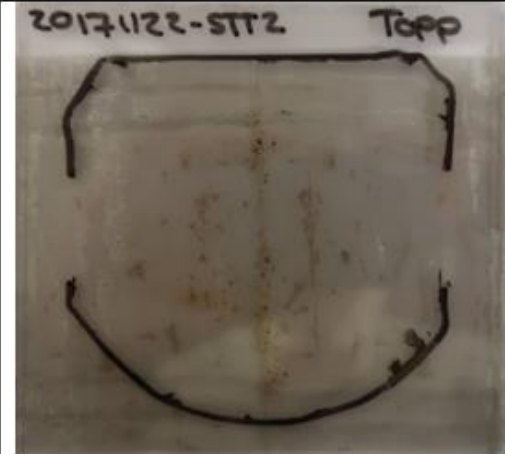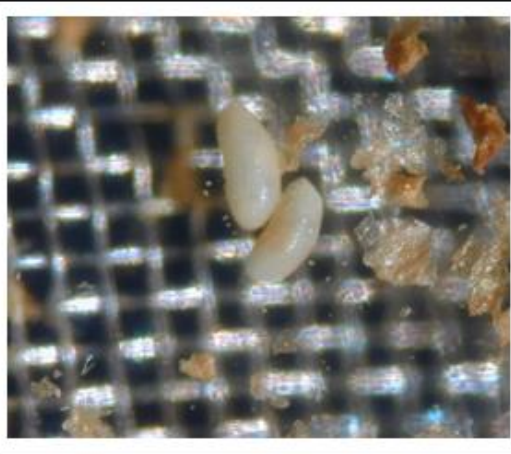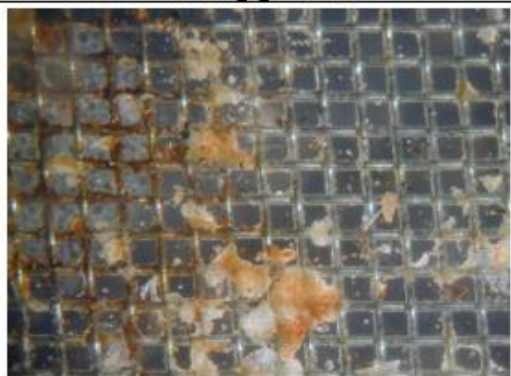
B13   20171117-VI-RB

Overview	Heterogeneous distribution of particles – one spherical, red granule
Heterogeneous distribution of particles	Clear layer

B14   2017116-Vega-R

Overview	Orange, spherical granula
Some white granules	Black granule < 500 μm

NGI
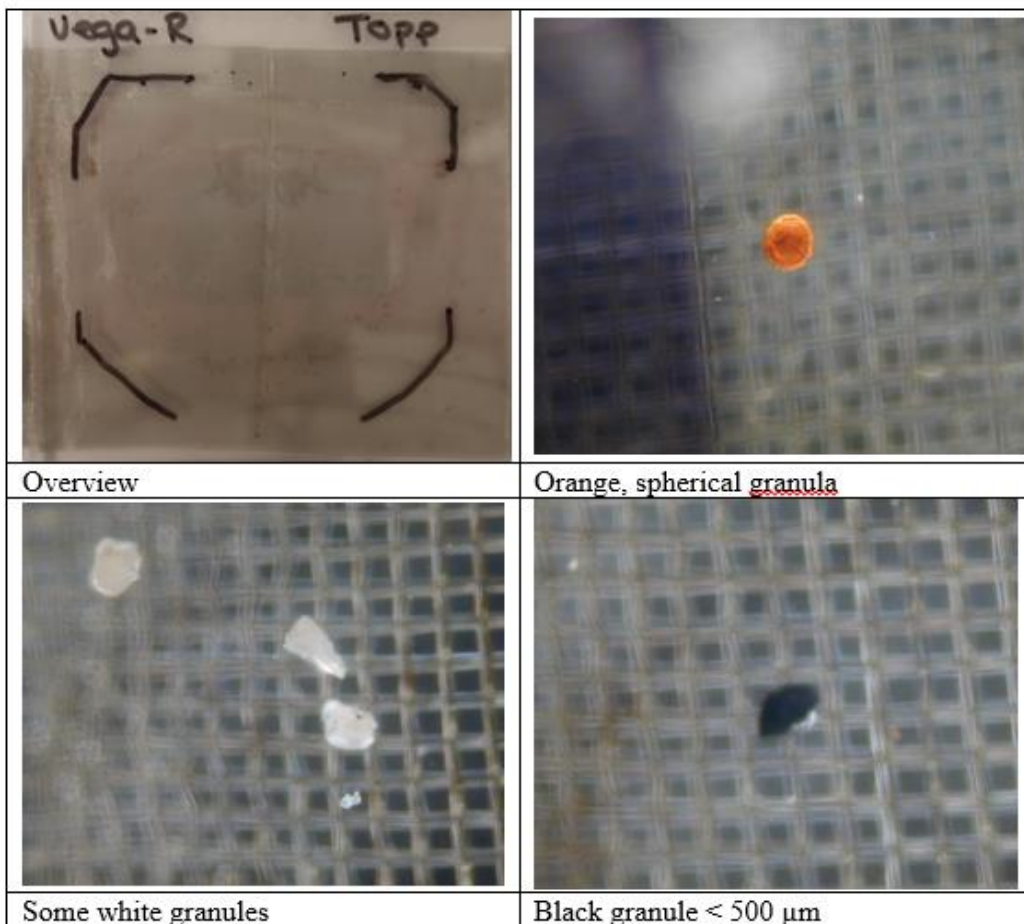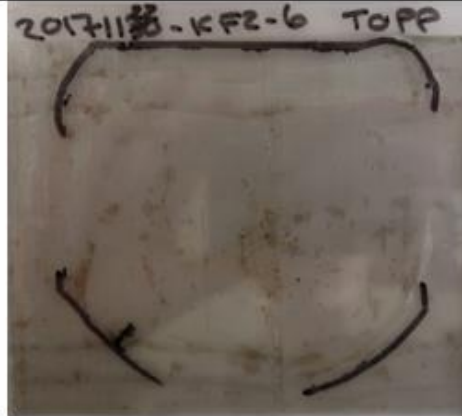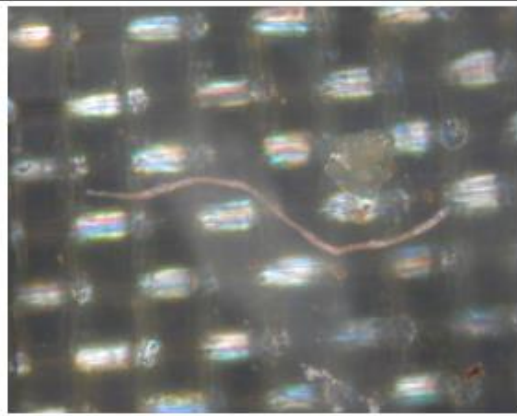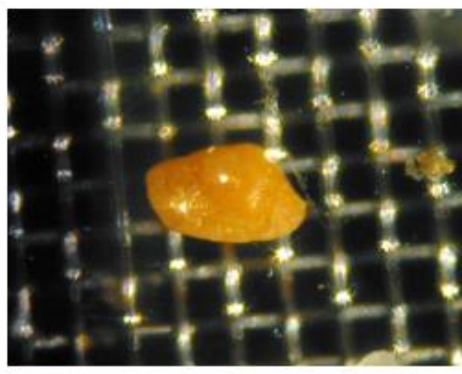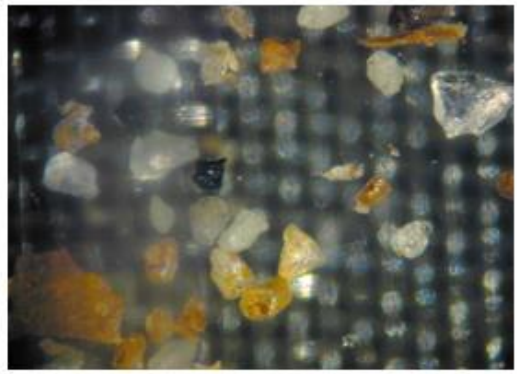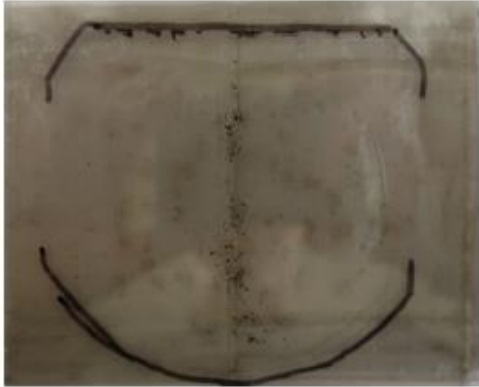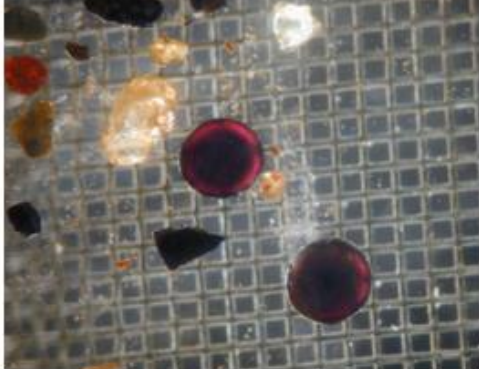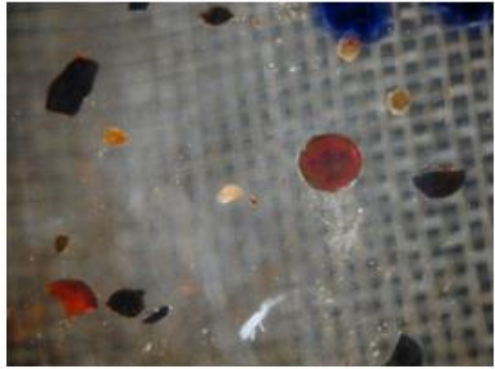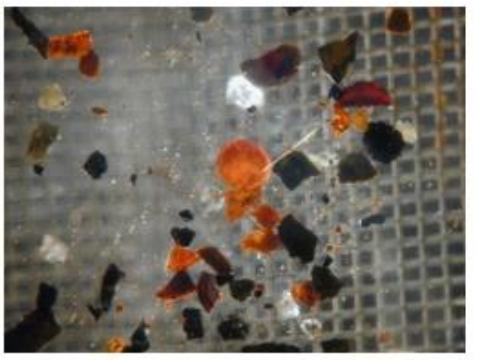
B15   20171122-STT-2

Overview	White, bean-looking granules
White fibre	Area with rust and ZnCl$_2$-crystals
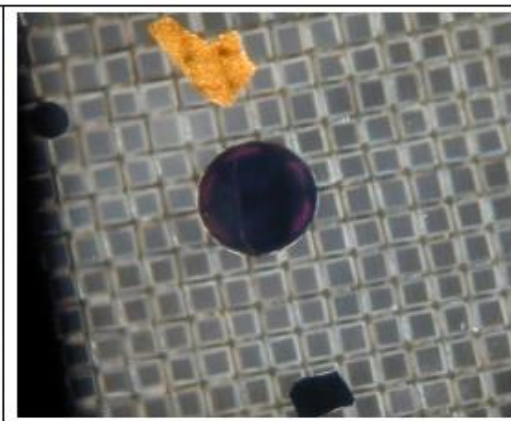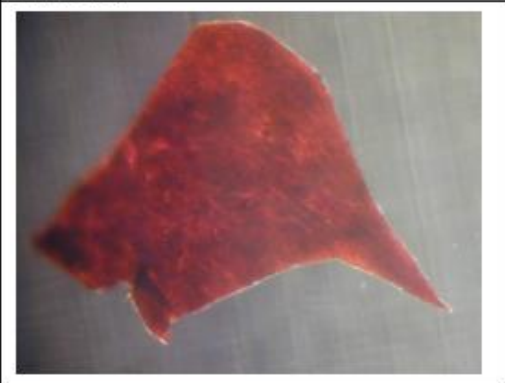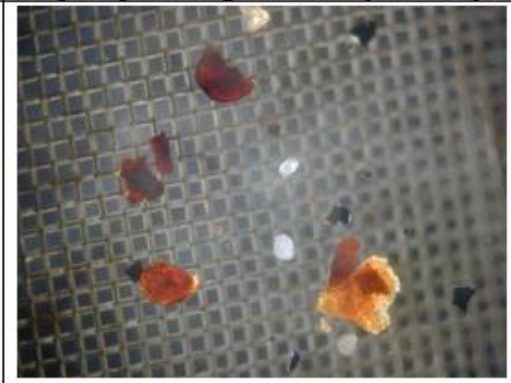
B16   20171122-KF2-6

Overview	Red fibre
Orange granule	Clear, white, black and orange granules

B17   20171122-SC3-4

Overview

Red fibre

Spherical, purple granules

Spherical orange to red granule and red granule with sharp edges

Heterogeneous composition of particles. NB! Orange, spherical granule

White fibre

B18   20171127-KRT-14

Overview	Purple, spherical granule and yellow layer
Red layer with sharp edges	Heterogeneous composition of particles, some with sharp edges
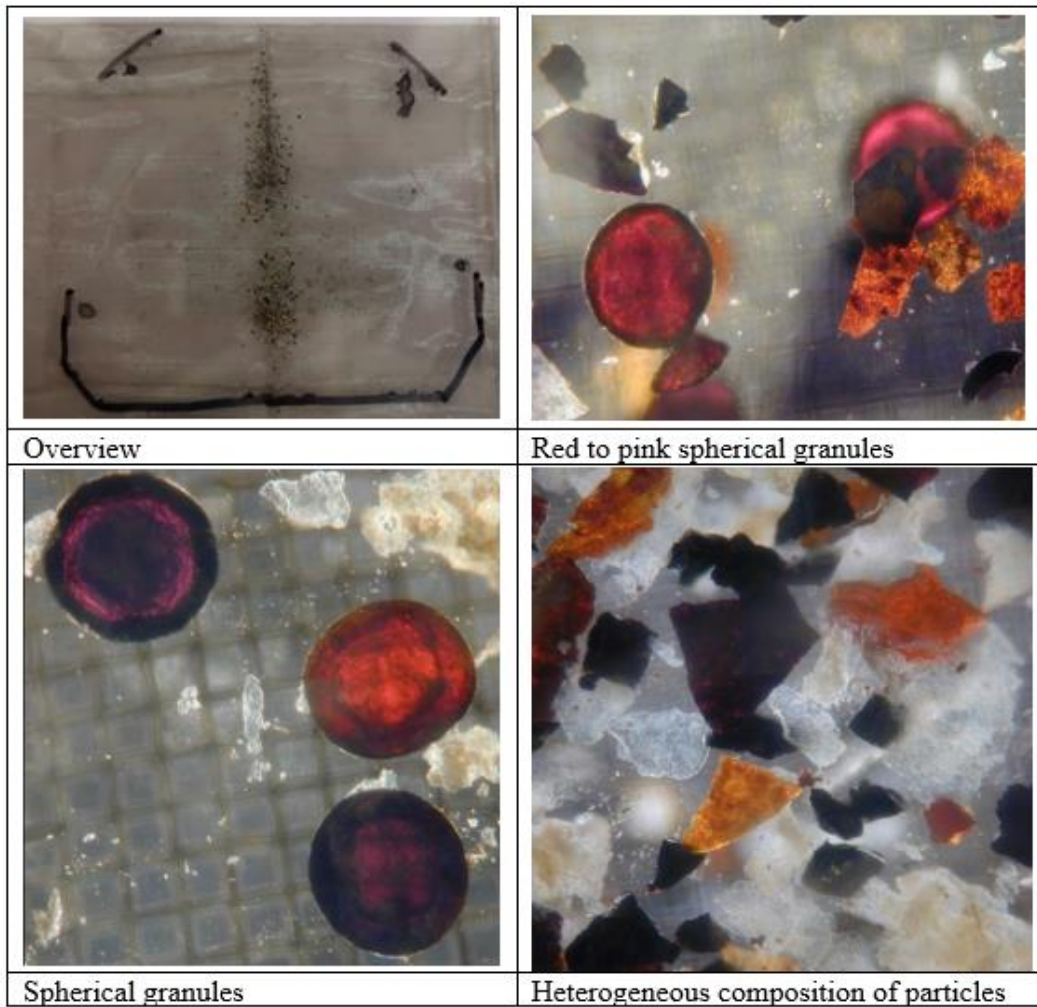
NGI

B19   20171124-GRS-2

Overview	Red to pink spherical granules
Spherical granules	Heterogeneous composition of particles
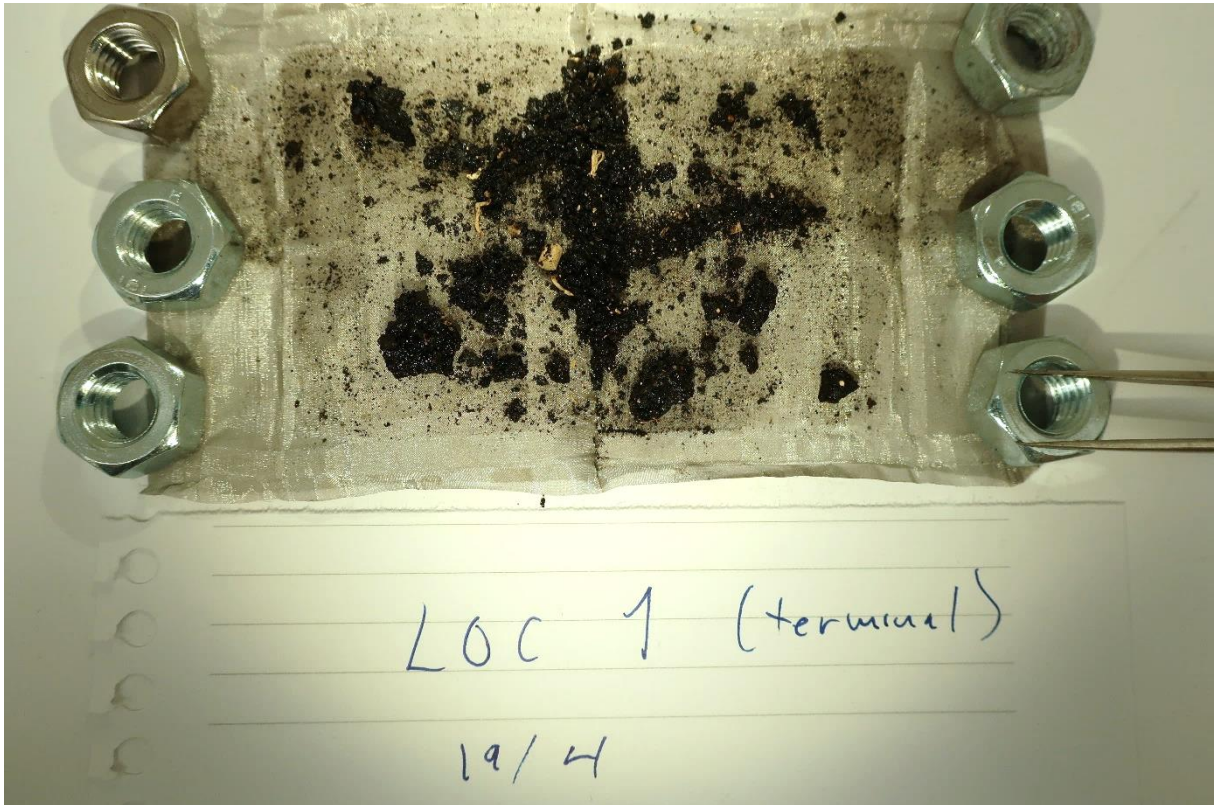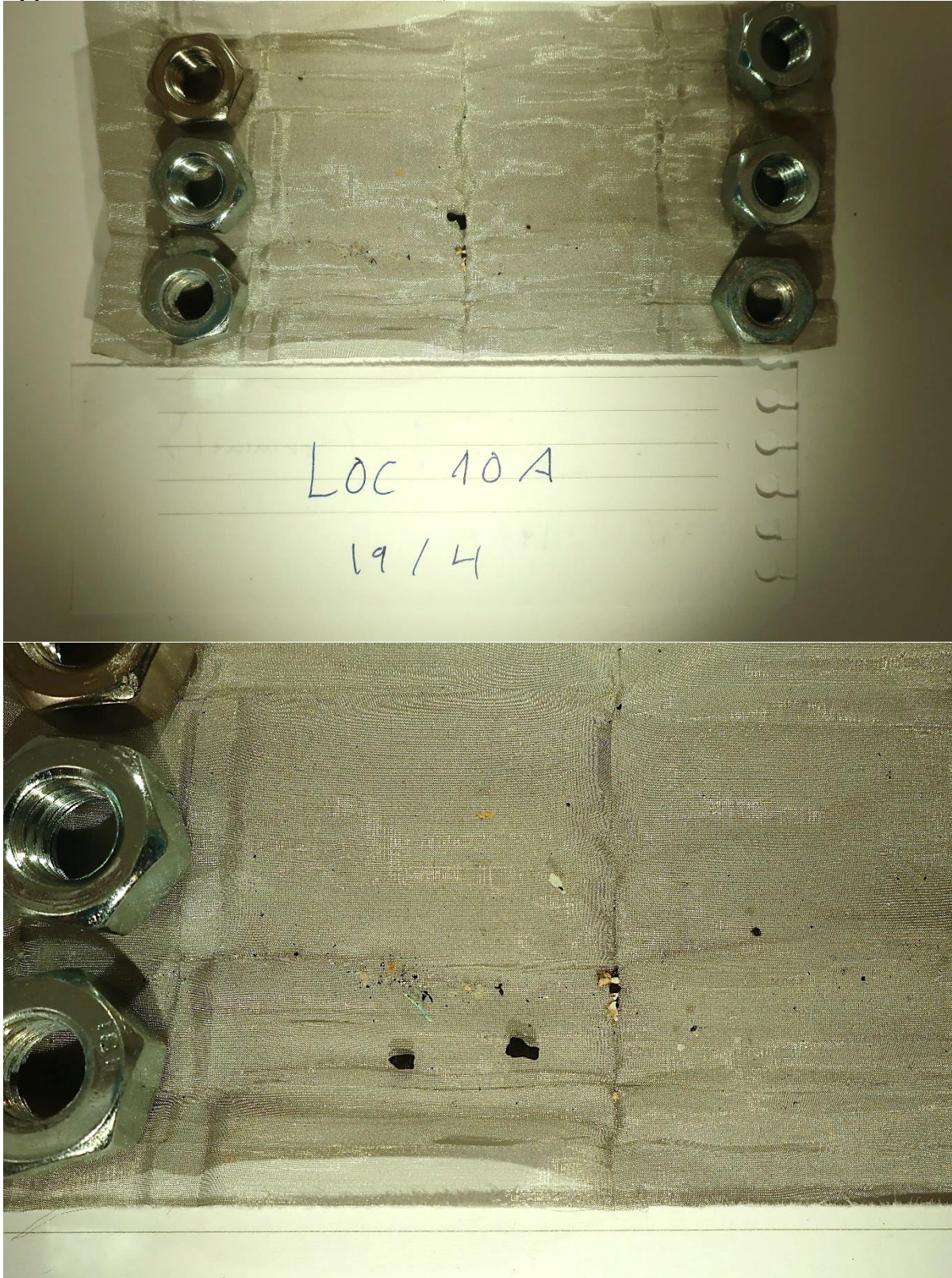
Appendix C2-3 (20170803-LOC-10B-1)
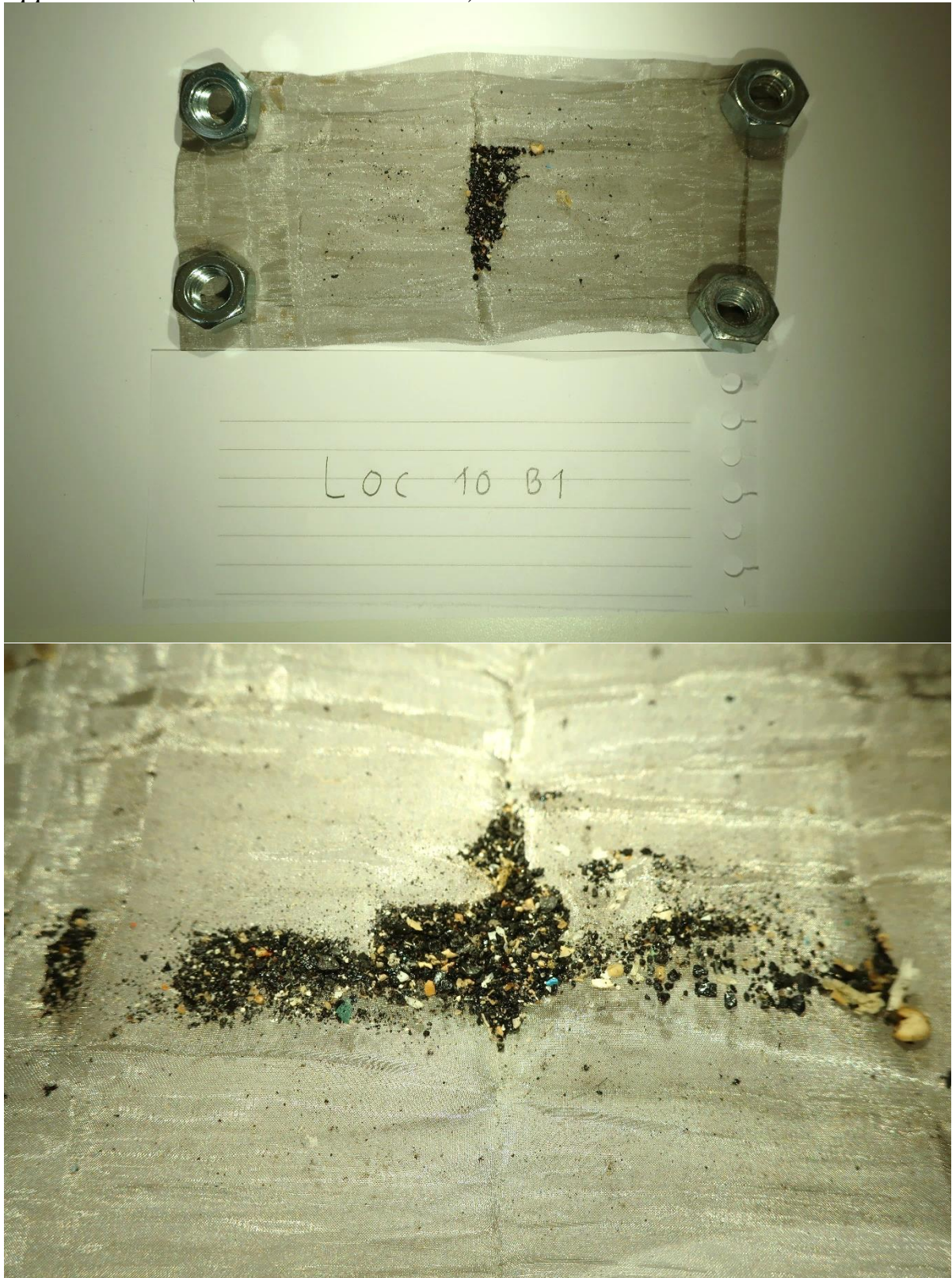
Appendix C2-4 (20170803-LOC-10B-2)
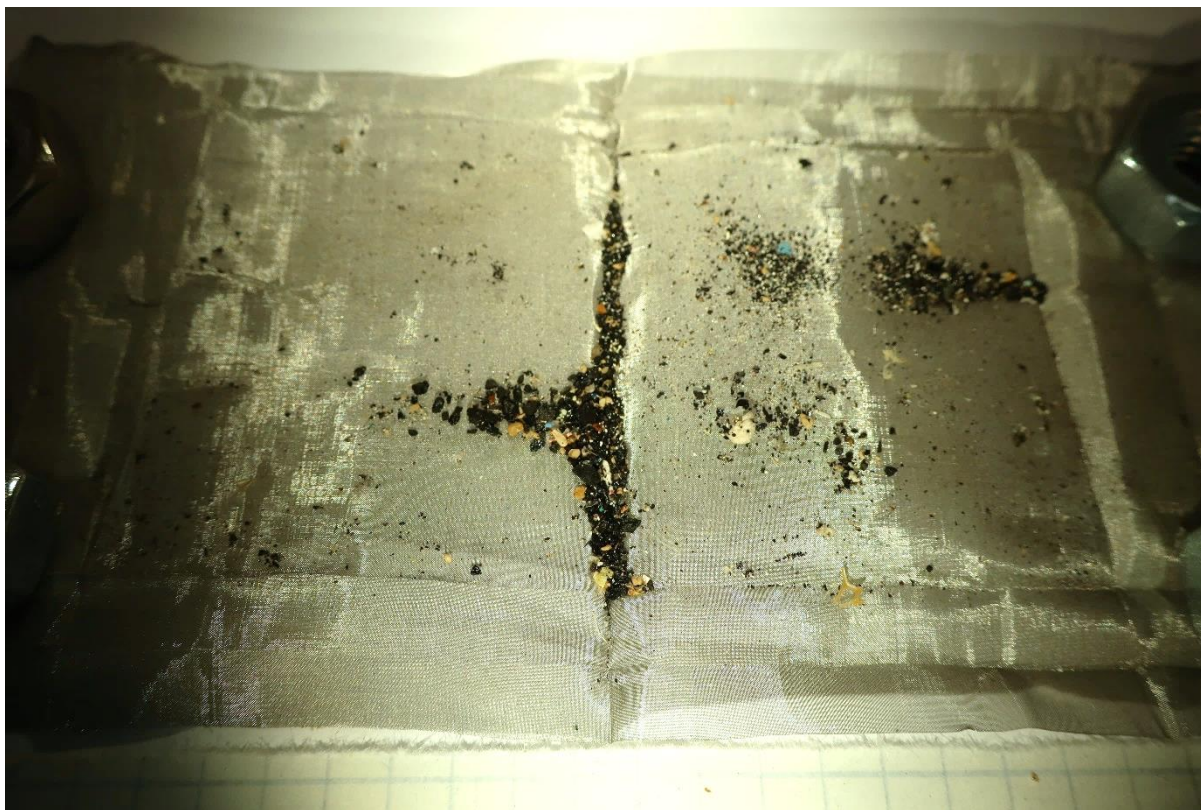
Appendix C2-6 (20170803-LOC-10C)
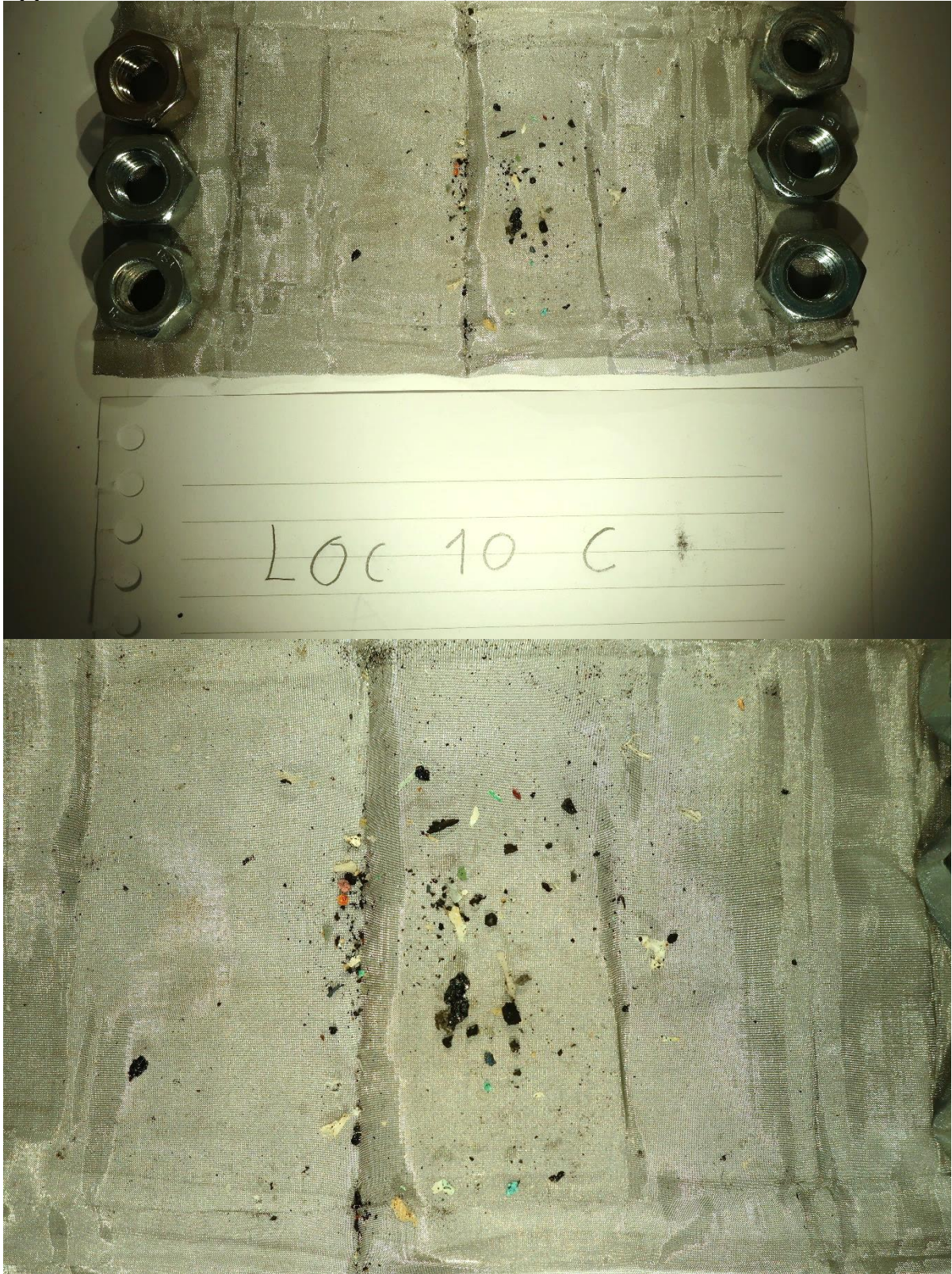
Appendix C2-7 (20170806-ALM-PAR #1 and #2)
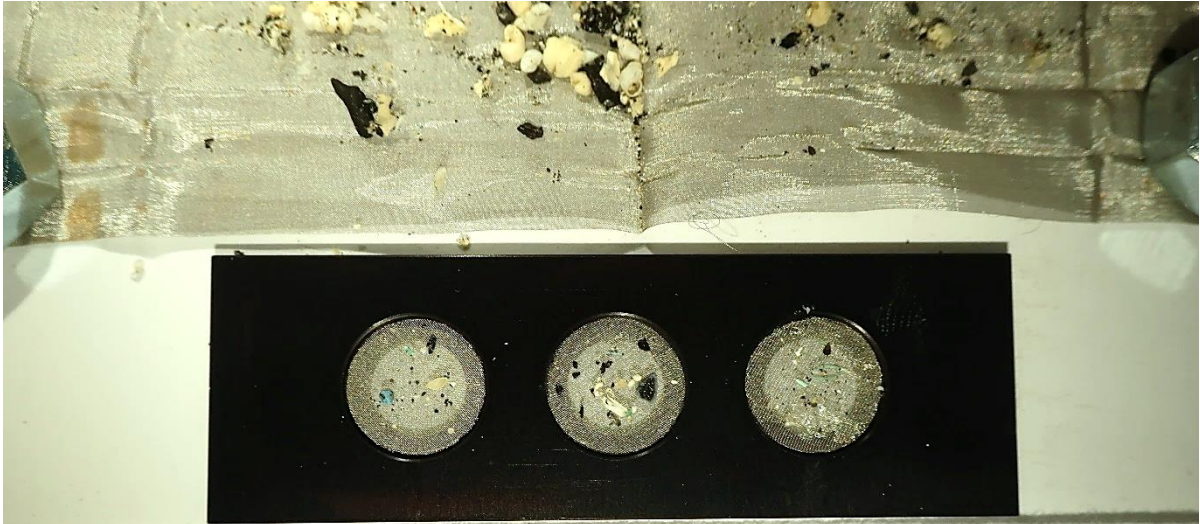
ALM - PAR #1
19/ 4
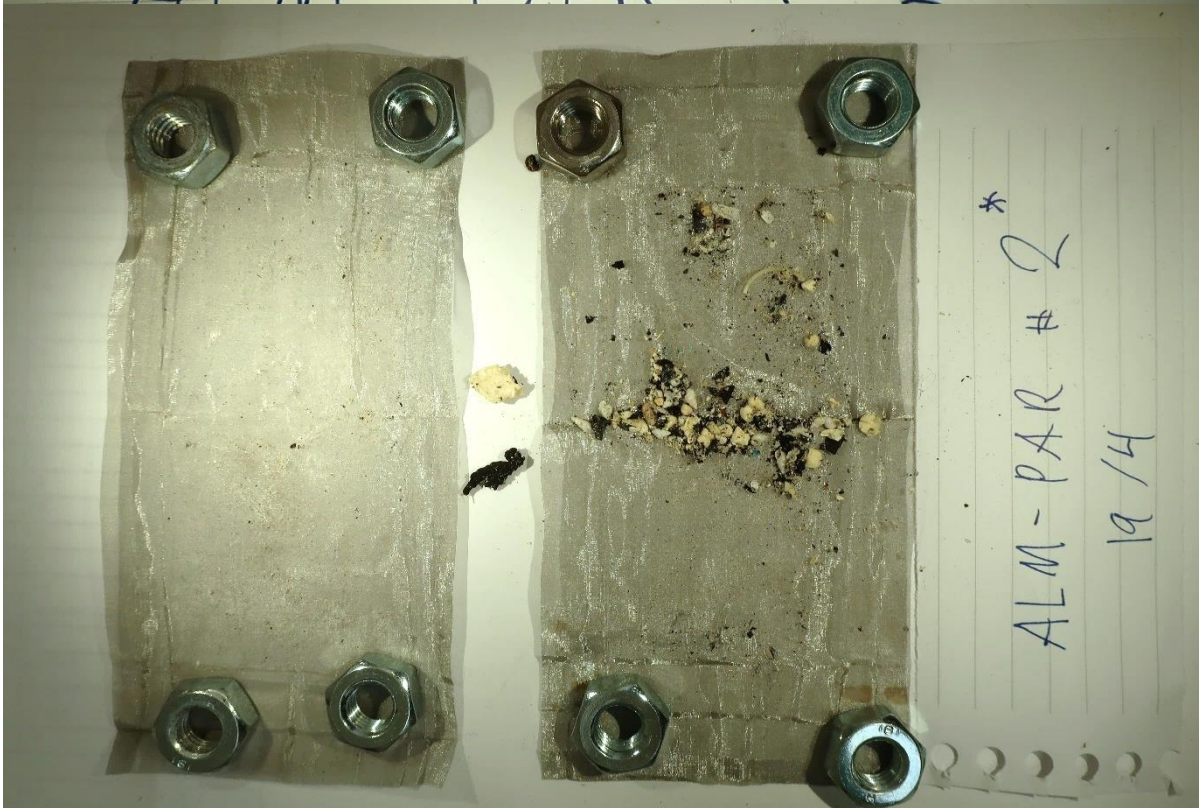
ALM - PAR #2
19 /4

ALM - PAR # 2 *

ALM - PAR # 2 *
19/4

PAR-BOS

18/4 - 18

PAR-BOS

114
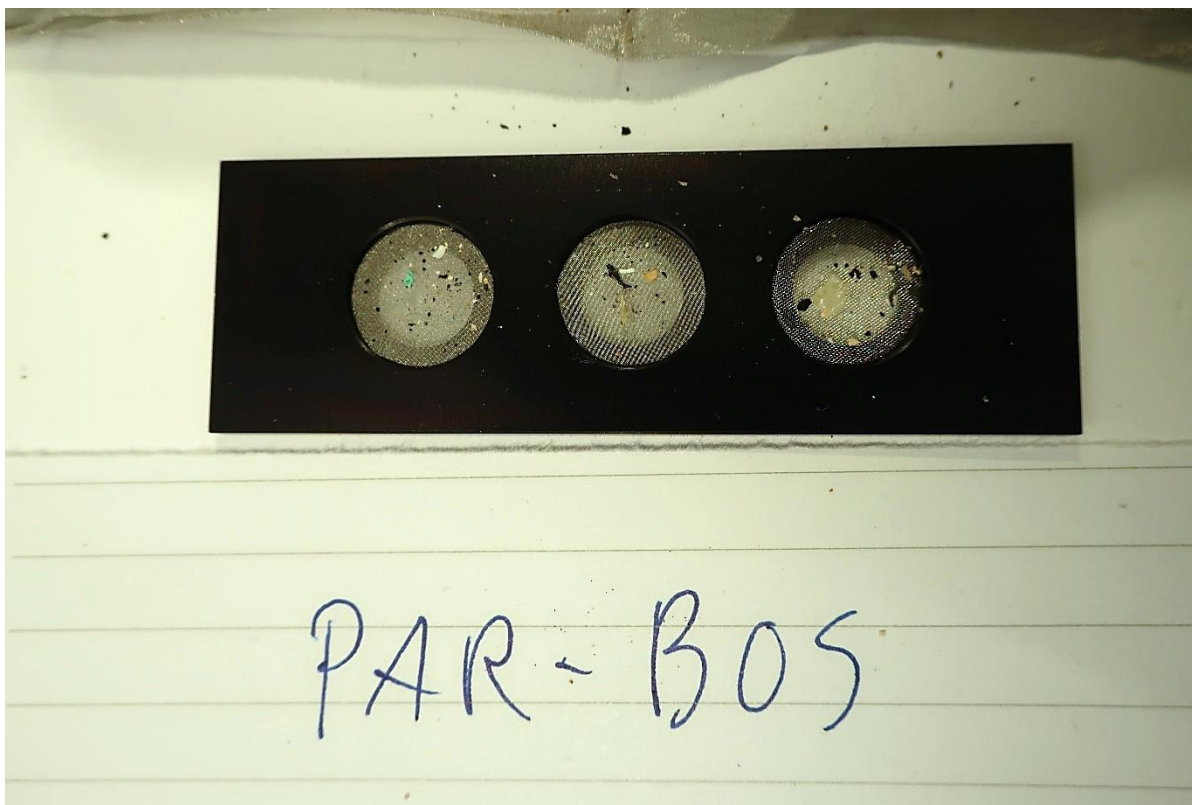
Appendix D1-1

Mean abundance of microplastics detected on the method blanks

	Colour	Fibre 1D				Layer 2D				Granulat 3D			
		A	B	C	D	A	B	C	D	A	B	C	D
	Clear/white	3.5	5.9	4.5	1.9	1.8	0.4	0.8	0.1	19.0	3.6	0.0	0.0
	Light brown	0.0	0.3	0.0	0.0	1.8	1.1	0.6	0.3	2.3	2.0	0.1	0.0
	Dark brown	0.0	0.1	0.0	0.0	0.3	0.0	0.0	0.0	0.9	0.3	0.3	0.0
	Black	0.1	0.0	0.0	0.0	0.0	0.0	0.0	0.0	0.4	0.0	0.0	0.0
	Blue	0.1	0.6	0.5	0.6	0.0	0.1	0.0	0.0	0.0	0.0	0.0	0.0
Average (n=8)	Red	0.0	0.0	0.1	0.0	0.3	0.0	0.0	0.0	0.8	0.0	0.0	0.0
	Green	0.0	0.0	0.0	0.0	0.0	0.0	0.0	0.0	0.0	0.0	0.0	0.0
	Orange	0.0	0.0	0.0	0.0	0.0	0.0	0.0	0.0	0.3	0.1	0.0	0.0
	Yellow	0.0	0.0	0.0	0.0	0.0	0.0	0.0	0.0	0.0	0.0	0.0	0.0
	Sum	3.8	6.9	5.1	2.5	4.0	1.6	1.4	0.4	23.5	6.0	0.4	0.0
	Fraction of total	18.3		32.9 %		7.4		13.3 %		29.9		53.8 %	
	SUM										55.5		

Appendix D1-2

Visually identifed samples used in to estimate items /m^2 and items /kg

Sample ID	Number of items (counted)	g MP/filter	Items/g MP	Items/mg MP
VI-03	180	0.0061	29446	29
KRT-14	197	0.0034	58298	58
Reg-09	308	0.0019	158244	158
GYDA-18	208	0.0035	59316	59
Items /mg/kg MEAN ± SD	223 ± 58		76326 ± 56340	76 ± 56

Visual analysis for method blanks

Dato examined: 04.12.2017 **Sample ID:** Blank 1 (20170922)

Colour	Fibre 1D A	B	C	D	Layer 2D A	B	C	D	Granulat 3D A	B	C	D	No further comment
Clear/white	6	9	1	1	2	1			12	1			
Light brown		1			2				3	9			
Dark brown					2				7	2			
Black		1							1				
Blue													
Red													
Green													
Orange													
Yellow													
Total	6	11	1	1	6	1	0	0	23	12	0	0	61
Fraction	19		31,1 %		7		11,5 %		35		57,4 %		

Dato examined: 05.12.2017 **Sample ID:** Blank 2 (20170922)

Colour	Fibre 1D A	B	C	D	Layer 2D A	B	C	D	Granulat 3D A	B	C	D	Damage on filter.
Clear/white	1	2	2		2				1	1			
Light brown													
Dark brown													
Black	1												
Blue		2	1	3									
Red					1				2				
Green													
Orange													
Yellow													
Total	2	4	3	3	3	0	0	0	3	1	0	0	19
Fraction	12		63,2 %		3		15,8 %		4		21,1 %		

Visual analysis for method blanks

Blank 3 (20170922) — Dato examined 05.12.2017

Colour	Fibre 1D A	B	C	D	Layer 2D A	B	C	D	Granulat 3D A	B	C	D	Comment
Clear/white	2	2											No further comment
Light brown									1				
Dark brown													
Black													
Blue	1												
Red									3				
Green													
Orange													
Yellow													
	3	2	0	0	0	0	0	0	4	0	0	0	9
	5			55,6 %	0			0,0 %	4			44,4 %	

Blank (20171019) — Dato examined 05.12.2017

Colour	Fibre 1D A	B	C	D	Layer 2D A	B	C	D	Granulat 3D A	B	C	D	Comment
Clear/white	15	7	12	1	2				3				Rust and damage on filter. Holes observed.
Light brown									4				
Dark brown		1					3						
Black													
Blue			1	1									
Red					1				1				
Green													
Orange													
Yellow													
	15	8	13	2	3	0	3	1	8	0	0	0	53
	38			71,7 %	7			13,2 %	8			15,1 %	

Visual analysis for method blanks

Dato examined: 05.12.2017 **Sample ID:** Blank (20171123)

Colour	Fibre 1D A	B	C	D	Layer 2D A	B	C	D	Granulat 3D A	B	C	D	Notes
Clear/white					10								
Light brown													
Dark brown		3	1						3	1			Possible cross-contamination of micropowder detected.
Black													
Blue													
Red													
Green													
Orange													
Yellow													
Total	0	3	1	0	10	0	0	0	3	1	0	0	
	4 (22,2 %)				10 (55,6 %)				4 (22,2 %)				18

Dato examined: 05.12.2017 **Sample ID:** Blank (20171121)

Colour	Fibre 1D A	B	C	D	Layer 2D A	B	C	D	Granulat 3D A	B	C	D	Notes
Clear/white	2	13							21	4			
Light brown													
Dark brown			3	1		2	5						Damage to filter, but no holes.
Black													
Blue			1			1							
Red													
Green													
Orange													
Yellow													
Total	2	13	4	1	0	3	5	0	21	4	0	0	
	20 (37,7 %)				8 (15,1 %)				25 (47,2 %)				53

Visual analysis for method blanks

Dato examined	Sample ID	Colour	Fibre 1D A	B	C	D	Layer 2D A	B	C	D	Granulat 3D A	B	C	D	No further comment
05.12.2017	Blank 2 (20171129)	Clear/white	2	4	12	7	10	9	1	2	108	9			
		Light brown									11		1		
		Dark brown											2		
		Black									2				
		Blue		2	1	1									
		Red			1										
		Green													
		Orange									2				
		Yellow													
			2	6	14	8	10	9	1	2	123	9	3	0	187
			30			16,0 %	22			11,8 %	135			72,2 %	

Dato examined	Sample ID	Colour	Fibre 1D A	B	C	D	Layer 2D A	B	C	D	Granulat 3D A	B	C	D	No further comment
22.12.2017	Blank 5:1 (20171109)	Clear/white		7	5	5			2		3	13			
		Light brown		1								7			
		Dark brown													
		Black													
		Blue													
		Red													
		Green													
		Orange										1			
		Yellow													
			0	8	5	5	0	0	2	0	3	21	0	0	44
			18			40,9 %	2			4,5 %	24			54,5 %	

Appendix D1-6

Visual analysis for method blanks

Colour	Fibre 1D				Layer 2D				Granulat 3D				% based on color
	A	B	C	D	A	B	C	D	A	B	C	D	
Clear/white	3,5	5,9	4,5	1,9	1,8	0,4	0,8	0,1	19,0	3,6	0,0	0,0	73,9 %
Light brown	0,0	0,3	0,0	0,0	1,8	1,1	0,6	0,3	2,3	2,0	0,1	0,0	15,0 %
Dark brown	0,0	0,1	0,0	0,0	0,3	0,0	0,0	0,0	0,9	0,3	0,3	0,0	3,1 %
Black	0,1	0,0	0,0	0,0	0,0	0,0	0,0	0,0	0,4	0,0	0,0	0,0	0,9 %
Blue	0,1	0,6	0,5	0,6	0,0	0,1	0,0	0,0	0,0	0,0	0,0	0,0	3,6 %
Red	0,0	0,0	0,1	0,0	0,3	0,0	0,0	0,0	0,8	0,0	0,0	0,0	2,0 %
Green	0,0	0,0	0,0	0,0	0,0	0,0	0,0	0,0	0,0	0,0	0,0	0,0	0,0 %
Orange	0,0	0,0	0,0	0,0	0,0	0,0	0,0	0,0	0,3	0,1	0,0	0,0	0,7 %
Yellow	0,0	0,0	0,0	0,0	0,0	0,0	0,0	0,0	0,0	0,0	0,0	0,0	0,0 %
Sum	3,8	6,9	5,1	2,5	4,0	1,6	1,4	0,4	23,5	6,0	0,4	0,0	
Fraction of total	18,3		32,9 %		7,4		13,3 %		29,9		53,8 %		55,5

Average (n=8)

SUM

Visual analysis of MP-samples (not corrected)

Dato examined	Sample ID	Colour	Fibre 1D A	B	C	D	Layer 2D A	B	C	D	Granulat 3D A	B	C	D
22.12.2017	VI-03 (20171120)	Clear/white	1	7	10	3			23	17		25		
		Light brown							1			3		
		Dark brown										12		
		Black				1					2	27	36	14
		Blue												
		Red										6	1	
		Green												
		Orange										5		
		Yellow										8		
		Total	1	7	10	4	0	0	24	17	2	86	37	14
		Fraction			10,9 %				20,3 %				68,8 %		202

Dato examined	Sample ID	Colour	Fibre 1D A	B	C	D	Layer 2D A	B	C	D	Granulat 3D A	B	C	D
03.01.2018	KRT-14 (20171130)	Clear/white	1	5	10	4			2			28		
		Light brown										1		
		Dark brown			1							30	9	
		Black									4	55	13	4
		Blue			2									
		Red								1		14	3	3
		Green												
		Orange										8	2	
		Yellow							2	1	1	11	2	
		Total	1	5	13	4	0	0	4	2	5	147	29	7
		Fraction			10,6 %				2,8 %				86,6 %		217

Visual analysis of MP-samples (not corrected)

Dato examined	Sample ID	Colour	Fibre 1D A	B	C	D	Layer 2D A	B	C	D	Granulat 3D A	B	C	D	
18.12.2017	SNB-16R (AVG)	Clear/white	14,5	40,0	9,5	2,5	13,0	14,0			12,5	30,0			See SNB-16R #1 and SNB-16R #2 for separate tables
		Light brown					2,5	3,5			1,5	3,0			
		Dark brown					1,5	2,0				2,5			
		Black		2,0			18,0	9,0			2,5	14,5	1,0		
		Blue													
		Red						1,5			1,0	5,5	1,0		
		Green													
		Orange													
		Yellow													
		Total	14,5	42,5	10	2,5	35	30	0	0	18	56	2	0	210,5
		Fraction	69,5		33,0 %		65		30,9 %		76		36,1 %		0

Dato examined	Sample ID	Colour	Fibre 1D A	B	C	D	Layer 2D A	B	C	D	Granulat 3D A	B	C	D	
12.12.2017	VAL-5 (20171103)	Clear/white		23	13	8		9	2		TMC	TMC	1		TMC = Too Many to Count
		Light brown													
		Dark brown			1			1	5				1		
		Black	1								TMC	73			
		Blue	1		1	2		1	1		3	3			
		Red									3				
		Green													
		Orange									2				
		Yellow													
		Total	1	23	15	10	0	11	8	0	8	77	1	0	154
		Fraction	49		31,8 %		19		12,3 %		86		55,8 %		0

Visual analysis of MP-samples (not corrected)

Appendix D1-9

Dato examined: 20.12.2017 — Sample ID: Reg-12 (20171117)

Colour	Fibre 1D A	B	C	D	Layer 2D A	B	C	D	Granulat 3D A	B	C	D	
Clear/white	1	14	2			7			5	9			
Light brown					2	2			3	2			
Dark brown						1							
Black	1		2						5	5	2		
Blue													
Red													
Green													
Orange													
Yellow													
Total	2	14	4	0	2	10	0	0	13	16	2	0	63
Fraction			31,7 %				19,0 %				49,2 %		

Dato examined: 19.12.2017 — Sample ID: Reg1-09 (20171005)

Colour	Fibre 1D A	B	C	D	Layer 2D A	B	C	D	Granulat 3D A	B	C	D	
Clear/white		2	5	3	13	11	1	1	19	124	11		
Light brown			1			11		2		18			
Dark brown										2		1	
Black						5			10	70	17	8	
Blue										1			
Red										3			
Green													
Orange													
Yellow									2	3	2	1	
Total	0	2	6	3	13	27	1	3	31	221	30	10	347
Fraction			3,2 %				12,7 %				84,1 %		

123

Visual analysis of MP-samples (not corrected)

Dato examined	Sample ID	Colour	Fibre 1D				Layer 2D				Granulat 3D				
			A	B	C	D	A	B	C	D	A	B	C	D	
10.01.2018	Reg-14 (20171002)	Clear/white		10	16	10	6	24	7		77	55	2		
		Light brown													
		Dark brown						5	1		1				
		Black		2		1	6	3			21	19	3		
		Blue			1							3	1		
		Red					3				3				
		Green													
		Orange													
		Yellow													
		Total	0	12	17	11	15	32	8	0	102	77	6	0	280
		Fraction		14,3 %			19,6 %				66,1 %				

Dato examined	Sample ID	Colour	Fibre 1D				Layer 2D				Granulat 3D				
			A	B	C	D	A	B	C	D	A	B	C	D	
10.01.2018	Vega-R (20171116)	Clear/white	1	6	8	2					4	34			
		Light brown										2			
		Dark brown													
		Black									1	7			
		Blue													
		Red													
		Green													
		Orange										1			
		Yellow													
		Total	1	6	8	2	0	0	0	0	5	44	0	0	66
		Fraction		25,8 %			0,0 %				74,2 %				

Visual analysis of MP-samples (not corrected)

Appendix D1-11

Dato examined: 10.01.2018 **Sample ID:** VI-RB (20171117)

Colour	Fibre 1D A	B	C	D	Layer 2D A	B	C	D	Granulat 3D A	B	C	D	Total
Clear/white	1	3	3	2		5			6	39	2		
Light brown									1	5	2		
Dark brown									6	2			
Black									17	75	7		
Blue													
Red										1			
Green													
Orange										8			
Yellow							1						
Total	1	3	3	2	0	5	1	0	30	130	11	0	186
Fraction			4,8 %				3,2 %				91,9 %		

Dato examined: 10.01.2018 **Sample ID:** GYDA-18 (20171103)

Colour	Fibre 1D A	B	C	D	Layer 2D A	B	C	D	Granulat 3D A	B	C	D	Total
Clear/white		4	5			1	1		3	92			
Light brown										101			
Dark brown										8			
Black										6			
Blue				1									
Red													
Green													
Orange									1	1			
Yellow									2	3			
Total	0	4	5	1	0	1	1	0	6	211	0	0	229
Fraction			4,4 %				0,9 %				94,8 %		

Visual analysis of MP-samples (not corrected)

SNB-16R #1 — Dato examined: 18.12.2017

Colour	Fibre 1D A	B	C	D	Layer 2D A	B	C	D	Granulat 3D A	B	C	D
Clear/white	29	67	11		26	28			20	21		
Light brown					5	7			3	6		
Dark brown					3	4						
Black		1			36	18				1		
Blue		4							1			
Red						1						
Green												
Orange												
Yellow												
	29	72	11	0	70	58	0	0	24	28	0	0
	112				128				52			
Fraction	38,4 %				43,8 %				17,8 %			

Total: 292

SNB-16R #2 — Dato examined: 09.01.2018

Colour	Fibre 1D A	B	C	D	Layer 2D A	B	C	D	Granulat 3D A	B	C	D
Clear/white		13	8	5					5	39		
Light brown												
Dark brown										5		
Black			1						5	28	2	
Blue												
Red						2			2	11	2	
Green												
Orange										1		
Yellow												
	0	13	9	5	0	2	0	0	12	84	4	0
	27				2				100			
Fraction	20,9 %				1,6 %				77,5 %			

Total: 129

Visual analysis of MP-samples (corrected)

Dato examined	Sample ID	Colour	Fibre 1D A	B	C	D	Layer 2D A	B	C	D	Granulat 3D A	B	C	D	Comment
22.12.2017	VI-03 (20171120)	Clear/white		1	6	1			22	17		21			Sample contained unusual amounts of crystal formation
		Light brown										1			
		Dark brown										12			
		Black									2	27	36	14	
		Blue													
		Red										6	1		
		Green													
		Orange										5			
		Yellow										8			
														sum	180

Dato examined	Sample ID	Colour	Fibre 1D A	B	C	D	Layer 2D A	B	C	D	Granulat 3D A	B	C	D	Comment
03.01.2018	KRT-14 (20171130)	Clear/white			6	2			1			24			No further comment
		Light brown													
		Dark brown			1							30	9		
		Black			2						4	55	13	4	
		Blue			2										
		Red								1		14	3	3	
		Green													
		Orange										8	2		
		Yellow							2	1		11	2		
														sum	197

127

Visual analysis of MP-samples (corrected)

Appendix D1-14

Visual analysis of MP-samples (corrected)

Table 1 — SNB-16R (AVG), Dato examined 18.12.2017

Colour	Fibre 1D A	B	C	D	Layer 2D A	B	C	D	Granulat 3D A	B	C	D	Notes	sum
Clear/white	11	34	5		11	14				26				
Light brown						2				1				
Dark brown					1	2				2				
Black		1			18	9			2	15	1			
Blue														
Red						2				6	1			
Green														
Orange													An average of SNB-16R#1 og SNB-16R#2	
Yellow														164

Table 2 — VAL-5 (20171103), Dato examined 12.12.2017

Colour	Fibre 1D A	B	C	D	Layer 2D A	B	C	D	Granulat 3D A	B	C	D	Notes	sum
Clear/white	17		9	6		9	1		TMC	TMC	1			
Light brown			1											
Dark brown						1	5							
Black							1		TMC	73				
Blue				1					3	3			An underestimate. Rust around crystal formation. Round transparent particles observed: (278 pcs A-B). Damage to filter observed.	
Red									2					
Green														
Orange									2					
Yellow														135

Visual analysis of MP-samples (corrected)

Dato examined	Sample ID	Colour	Fibre 1D A	B	C	D	Layer 2D A	B	C	D	Granulat 3D A	B	C	D	
20.12.2017	Reg-12 (20171117)	Clear/white		8				7				5			One round transparent particles observed. Masse is mainly crystals.
		Light brown													
		Dark brown						1							
		Black			2						5	5	2		
		Blue													
		Red													
		Green													
		Orange													
		Yellow													
															sum 34

Dato examined	Sample ID	Colour	Fibre 1D A	B	C	D	Layer 2D A	B	C	D	Granulat 3D A	B	C	D	
19.12.2017	Reg1-09 (20171005)	Clear/white				1	11	11		1		120	11	1	5 round transparent particles observed. Relativly large damage to filter (~125um).
		Light brown			1			10		2		16		1	
		Dark brown										2			
		Black						5			10	70	17	8	
		Blue										1			
		Red										3			
		Green													
		Orange													
		Yellow									2	3	2	1	
															sum 308

Visual analysis of MP-samples (corrected)

Dato examined	Sample ID	Colour	Fibre 1D A	Fibre 1D B	Fibre 1D C	Fibre 1D D	Layer 2D A	Layer 2D B	Layer 2D C	Layer 2D D	Granulat 3D A	Granulat 3D B	Granulat 3D C	Granulat 3D D	
10.01.2018	Reg-14 (20171002)	Clear/white		4	12	8	4	24	6		58	51	2		4 round transparent particles observed.
		Light brown						4							
		Dark brown													
		Black		1			6	3			21	19	3		
		Blue										3	1		
		Red					3				2				
		Green													
		Orange													
		Yellow													
														sum	235

Dato examined	Sample ID	Colour	Fibre 1D A	Fibre 1D B	Fibre 1D C	Fibre 1D D	Layer 2D A	Layer 2D B	Layer 2D C	Layer 2D D	Granulat 3D A	Granulat 3D B	Granulat 3D C	Granulat 3D D	
10.01.2018	Vega-R (20171116)	Clear/white										30			No further comment
		Light brown													
		Dark brown													
		Black													
		Blue										7			
		Red													
		Green													
		Orange										1			
		Yellow													
														sum	42

Visual analysis of MP-samples (corrected)

Dato examined	Sample ID	Colour	Fibre 1D				Layer 2D				Granulat 3D				
			A	B	C	D	A	B	C	D	A	B	C	D	
		Clear/white						5				35		2	Multiple orange spheric particles.
		Light brown										3		2	
		Dark brown									5	2			
10.01.2018	VI-RB (20171117)	Black									17	75		7	
		Blue										1			
		Red													
		Green													
		Orange										8			
		Yellow							1						
													sum		162

Dato examined	Sample ID	Colour	Fibre 1D				Layer 2D				Granulat 3D				
			A	B	C	D	A	B	C	D	A	B	C	D	
		Clear/white										88			Most of the light brown particles looks like weathered beads.
		Light brown										99			
		Dark brown										8			
10.01.2018	GYDA-18 (20171103)	Black										6			
		Blue													
		Red													
		Green									1	1			
		Orange									2	3			
		Yellow													
													sum		208

131

Appendix - D2 – FTIR analysis (Rio Almendares)

Appendix D2- 1

Number of detected particles per ~0.0065 gram of selected sample material.

Polymer Compound	LOC-1	LOC-10A	LOC-10B1	LOC-10B2	LOC-10B3	LOC-10C	ALM-PAR	ALM-BOS
PE*		1	1	1	4	2	2	8
PE:PVS		2	2					
PE-Chlorinated							2	1
PE-Oxidized*				1			1	2
PET			1	1		1		1
POLYACRYLAT				1				1
PP*	1	1	1	1	4		9	1
PS	1	1		1	2	4	3	
PS-COPOLYMER	1				2			
PTFE								1
PUF			2	1	1			
PVS	7		1		1	1		
Various		2	6	1		2	1	
SUM	10	5	14	10	14	10	18	15

* Polymers with density lower than 1.03 g/cm^3

FTIR analysis containing data concerning total markers, identified markers and

Sample	Total markers	Total identified markers (>0.60)	Identified as anthropogenic (>0.60)	Identified as plastic (>0.60)	Fraction of plastic	Total sample weight (g)	Correction for sediments (max MP g/kg)	Items / kg dry sediment
LOC 1	268	177	126	9	3 %			
LOC10A	43	12	7	5	12 %			
LOC10B1	238	41	28	14	6 %	0.0066	1.547	3281
LOC10B2	197	36	21	10	5 %	0.0058	0.914	1576
LOC10B3	223	44	22	15	7 %	0.0055	1.245	3394
LOC10C	30	14	14	10	33 %			
ALM-PAR	75	27	21	16	21 %	0.0062	12.320	31793
ALM-BOS	110	30	24	15	14 %	0.0086	1.474	2571
MEAN	148	48	33	12	13 %	0.0065		8523
SD	94	54	38	4	10 %	0.0012		13029

identified plastics

Number of particles identified (above 0.6) sorted by type of compound

					Location				
Type of compound	LOC-1	LOC-10A	LOC-10B1	LOC-10B2	LOC-10B3	LOC-10C	ALM-PAR	ALM-BOS	Sum
Plastic	9	5	14	10	14	10	16	15	93
Paint	1	1	2	3	2	3	4	2	18
Rubber	5	1	7	4	4	1	1	3	26
Petro-pyro	111	0	5	4	1	0	0	4	125
Organic	51	5	13	15	20	0	6	5	115
Inorganic	0	0	0	0	0	0	0	1	1
Unknown	0	0	0	0	2	0	0	0	2
Air	2	0	8	0	5	0	1	1	17
Total (no air)	177	12	41	36	44	14	27	30	381

DISTRIBUTION OF IDENTIFIED PARTICLES

Petro-pyro 33 %
Organic 30 %
Unknown <1%
Inorganic <1%
Plastic 25 %
Paint 5 %
Rubber 7 %
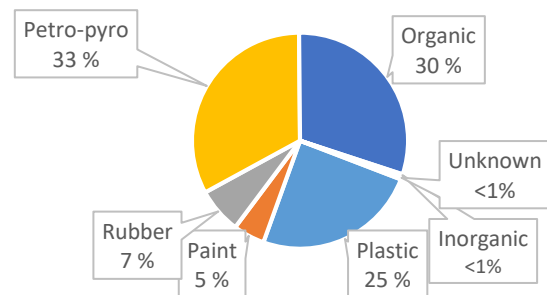
Appendix - E - List of Abbreviations

BMSS	Bauta Microplastic-Sediment Separator
DI	Deionized
DM	Dry matter
FTIR	Fourier transform infrared spectroscopy
GC/C	Glass microfiber filter / grade C
HCl	Hydrogen Chloride
HDPE	High density polyethylene
LDPE	Low density polyethylene
MP	Microplastic
MP $_{max}$	Maximum Microplastic Concentration
MPSS	Munich Plastic-Sediment Separator
NaCl	Sodium Chloride
NaI	Sodium Iodide
NCS	Norwegian Continental Shelf
PE	Polyethylene
PET	Polyethylene terephthalate
POPs	Persistent Organic Pollutants
PP	Polypropylene
PS	Polystyrene
PTFE	Polytetrafluoroethylene
PVC	Polyvinyl chloride
PUR	Polyurethane
RA	Rio Almendares

Symbols

ρ	Density
μ	Micro
m	Mass
V	Volume

Appendix - F - Table of figures